# Multifactorial analyses of the sticking tendency of ibuprofen and ibuprofen sodium dihydrate tablet formulations

**Dissertation**

with the aim of achieving a doctoral degree

at the Faculty of Mathematics, Informatics and Natural Sciences

Department of Chemistry

Universität Hamburg

submitted by

**Claudia Al-Karawi**

Hamburg 2018

*"The spirit becomes memories living in the minds of people"*

*H. Arakawa*

*For Sami the poet and Moubtada the lioness*

## Zusammenfassung

Tabletten zählen zu den bedeutendsten Darreichungsformen auf dem Arzneimittelmarkt. Eines der häufigsten Probleme während des Tablettierens ist das Kleben von Tablettiermasse am Stempelwerkzeug, was Komplikationen verursachen kann. Trotz zahlreicher Forschungsarbeiten zu diesem Thema sind die Ursachen und die vielseitigen Einflussgrößen des Klebens nicht vollständig identifiziert und verstanden. Das nicht-steroidale Antirheumatikum Ibuprofen beispielsweise zeigt eine ausgeprägte Klebeneigung und stellt einen besonders problematisch zu tablettierenden Wirkstoff dar, obwohl Ibuprofen bereits seit Jahren auf dem Markt ist. Die Hauptursache dafür ist möglicherweise, dass das Kleben ein multifaktorielles Phänomen ist, welches sich schwer durch klassische Versuchsmodelle wie dem sogenannten One-Factor-at-a-Time-Ansatz erfassen lässt.

Ziel dieser Arbeit war es daher, die Klebeneigung von Ibuprofen-Formulierungen an den Stempelwerkzeugen zu untersuchen, um diese schließlich, auch im Produktionsmaßstab, zu reduzieren. Mit einem systematischen und multifaktoriell angelegten Herangehensweise sollten der Zusammenhang zwischen dem Kleben und verschiedenen Faktoren, die das Kleben beeinflussen, beurteilt werden. Besonderes Augenmerk lag hierbei auf der Verwendung unterschiedlich beschichteter Stempelwerkzeuge.

Der Einfluss von unterschiedlichen Stempelbeschichtungen auf das Klebeverhalten von Ibuprofen wurde im Zusammenhang mit der Presskraft und der Wahl des Schmiermittels in einer ersten Studie untersucht. Alle Faktoren, sowie deren Wechselwirkungen wurden mithilfe der statistischen Versuchsplanung (DoE) untersucht. Es stellte sich dabei heraus, dass insbesondere die Presskraft, die

Stempelbeschichtung, sowie deren Abnutzungserscheinungen den größten Einfluss auf die Klebeneigung haben.

Die starke Auswirkung von Stempeloberflächen auf die Klebeneigung ist in der Fachliteratur unumstritten; die entsprechenden Untersuchungen sind jedoch aus praktischen Gründen schwierig. In einer zweiten Studie dieser Arbeit wurde daher eine neuartige Methode entwickelt, bei der mithilfe von hochauflösendem Abformmaterial Abdrücke der Stempeloberflächen produziert werden können, um sie anschließend systematisch zu charakterisieren. Diese neuartige Methode eignete sich außerdem zur Untersuchung von klebendem Material direkt auf der Stempeloberfläche, sodass erstmalig eine systematische Charakterisierung des Klebeverhaltens nach aufeinanderfolgenden Tablettierungen ermöglicht wurde.

Da neben der Oberflächenbeschaffenheit auch die chemische Zusammensetzung der Stempelbeschichtungen eine wichtige Rolle bei Adhäsionsphänomenen spielt, wurden in einer weiteren Studie der Arbeit die Auswirkungen beider Faktoren untersucht. Als hydrophiler Vergleichswirkstoff zu Ibuprofen wurde Ibuprofen-Natrium-Dihydrat ausgewählt, um die Auswirkung unterschiedlicher Hydrophilien bzw. Hydrophobien dieser Arzneistoffe auf die Haftneigung der ebenfalls unterschiedlich hydrophoben Stempeloberflächen zu untersuchen. Die polarere und somit hydrophilere Substanz zeigte eine deutlich erhöhte Klebeneigung, unabhängig von der Hydrophobie der Stempeloberfläche. Mittels Bestimmung von Adhäsionskräften auf partikulärer Ebene und von Oberflächenenergien der Stempel konnten tendenziell Stempel mit erhöhter oder verringerter Haftneigung unterschieden werden. Die Oberflächenbeschaffenheit der Stempel konnte diese jedoch stark beeinflussen. Generell neigten glatte und homogene Oberflächen zu verringertem Kleben. In bestimmten Fällen jedoch führte eine sehr feine und

homogene Rauheit der Oberflächentextur zu einer verringerten Haftneigung durch eine reduzierte Kontaktfläche. Jede Stempelbeschichtung muss daher als individuelles System betrachtet und beurteilt werden.

Im Rahmen dieser Arbeit wurden die Ursachen, die zum Kleben von Wirkstoffen wie Ibuprofen führen, näher untersucht. Basierend auf den Ergebnissen der Arbeit konnte in einer letzten Studie die Haftneigung von Ibuprofen, mittels einer geeigneten Kombination aus einer optimaler Presskraft, Stempelbeschichtung und Ibuprofen-Formulierung deutlich verringert werden.

## Abstract

Tablets are one of the most important dosage forms on the pharmaceutical market. A major problem during tableting is the sticking of tableting material to the punch tooling, which may cause serious complications. Despite numerous studies that have been conducted on the subject, the causes and the various influencing factors are not fully identified and understood. The non-steroidal anti-inflammatory drug ibuprofen shows a pronounced sticking tendency and therefore represents a particularly problematic active pharmaceutical ingredient (API), although it has been on the market for years. The main reason for this sticking problem is most likely the fact that sticking is a multifactorial phenomenon, which cannot easily be characterized by classical experimental models such as the so-called One-Factor-at-a-Time approach.

Therefore, the aim of this thesis was to investigate the sticking tendency of ibuprofen formulations to the punch tooling to ultimately reduce sticking even on a production-scale. By application of a systemic and multifactorial approach, the relation between sticking and the various factors leading to sticking were evaluated. Special attention has been given to the application of differently coated punches. In the first study of this work, the influence of the different punch coatings on the sticking behavior of ibuprofen was analyzed with regard to the compaction force and the choice of the lubricant, which is usually added to a tablet formulation to prevent sticking. To analyze these influencing factors as well as their interactions, a design of experiment (DoE) approach was used. It was found, that the compaction force, the punch coating, and the wear of the punches had the strongest influence on sticking ibuprofen to the punches.

The strong influence of the punch surfaces on the sticking tendency is uncontroversial. However, the investigation of these surfaces is difficult to conduct in practice.

In a second study of this thesis, a novel method was developed by the application of high-resolution impression material to produce molds of the punches for a systematic characterization of their surfaces. Furthermore, this method allowed the visualization of material sticking to the punches after successive tableting runs.

Beyond the surface texture, the chemical composition of the punch coating material plays an important role in adhesion events. Therefore, the effect of both factors was investigated in a further study. Ibuprofen sodium dihydrate was chosen as a hydrophilic model API in addition to the hydrophobic ibuprofen, to compare the effect differently hydrophilic or hydrophobic APIs on the anti-sticking performance of the differently hydrophobic punch surfaces. It was observed that sticking was distinctly increased with the more polar and thus more hydrophilic API, independent of the hydrophobicity of the punch surface. The determination of the punch surfaces' adhesive forces on a particulate level as well as their surface free energies allowed a rough differentiation between punches with an increased or decreased sticking tendency. However, the surface texture strongly affected this result. In general, the smooth and homogenous punch surfaces showed reduced sticking. However, it was shown that in certain cases a very fine and homogenous roughness of the surface texture may lead to a decreased sticking tendency because of a reduced contact area. Therefore, each punch coating has to be investigated and evaluated as an individual system.

Within the scope of this work, the causes which may lead to sticking of APIs such as ibuprofen were examined in more detail. Based on the previous results of this work,

in a final study the sticking of ibuprofen could be distinctly reduced with an appropriate combination of a suitable compaction force, punch coating and ibuprofen formulation.

# Conference contributions and publications

In context with this work, the following contributions have been presented at conferences and published journal articles.

### Conference contributions - poster presentations

Influence of chromium nitride punch tip coating and a co-processed self-lubricating excipient on the sticking of ibuprofen tablets, Biopharmaceutics and Pharmaceutical Technology 2014, Lisbon, Portugal

Influence of tooling roughness and ibuprofen particle size on tablet sticking, Symposium on Pharmaceutical Engineering Research, 2015, Braunschweig, Germany

Investigation on the adhesion tendency of ibuprofen and ibuprofen sodium dihydrate on coated tablet tooling, 29th Meeting of the American Association of Pharmaceutical Scientists 2015, Orlando, USA

A new method for visualization of sticking material to tablet punch surfaces, 30th Meeting of the American Association of Pharmaceutical Scientists 2016, Denver, USA

A novel technique for characterization of sticking to tableting punch surfaces, 31st Meeting of the American Association of Pharmaceutical Scientists 2017, San Diego, USA

**Journal articles with authors contributions and reference chapters.**

| Title | Journal | Authors | Contribution to the work | Percentage | Reference chapters |
|---|---|---|---|---|---|
| Novel aspects on the direct compaction of ibuprofen with special focus on sticking | Powder Technology (accepted) | Al-Karawi, C. | Project plan, experiments, data analysis, publication | 95 % | 1.2., 1.2.3.1, 1.2.3.2, 1.2.3.4, 1.4, 3.1, 3.2., 4.1. |
| | | Lukášová, I. | Experiments | 5 % | |
| | | Sakmann. A. | Supervisor | | |
| | | Leopold. C.S. | Supervisor | | |
| A novel technique for the visualization of tablet punch surfaces: characterization of surface modification, wear and sticking | International Journal of Pharmaceutics (accepted) | Al-Karawi, C. | Project plan, experiments, data analysis, publication | 100 % | 1.1.5, 1.2.3.3, 3.1, 3.3, 4.2 |
| | | Kaiser, T. | Supervisor | | |
| | | Leopold, C.S. | Supervisor | | |
| A comparative study on the sticking tendency of ibuprofen and ibuprofen sodium dihydrate to differently coated tablet punches | European Journal of Pharmaceutics and Biopharmaceutics (accepted) | Al-Karawi, C. | Project plan, experiments, data analysis, publication | 100 % | 1.2., 1.2.3.3, 1.2.3.5, 1.4, 3.1, 3.4, 4.3 |
| | | Leopold, C.S. | Supervisor | | |
| Investigation of the tableting behavior of Ibuprofen DC 85 W | Drug Development and Industrial Pharmacy (accepted) | Al-Karawi, C. | Project plan, experiments, data analysis, publication | 95 % | 1.1.4, 1.4, 3.1, 3.5, 4.4 |
| | | Cech, T. | Supervisor | | |
| | | Bang, F. | Experiments | 5 % | |
| | | Leopold, C.S. | Supervisor | | |

## List of Abbreviations

| | |
|---|---|
| **AFM** | Atomic force microscope |
| **ANOVA** | Analysis of variance |
| **API** | Active pharmaceutical ingredient |
| **ASME** | American Society of Mechanical Engineers |
| **CrN** | Chromium nitride |
| **CVD** | Chemical vapor deposition |
| **DLC** | Diamond‑like carbon |
| **DoE** | Design of Experiments |
| **DSC** | Differential scanning calorimetry |
| **EDS** | Energy dispersive X‑ray spectroscopy |
| **Eq.** | Equation |
| **EUR** | European project report EUR 15178 EN |
| **FCG-CR+** | Chromium nitride multilayer-coated punches with an oxide toplayer obtained from FETTE Compacting |
| **FCG‑CRN** | Chromium nitride‑coated punches obtained from FETTE Compacting |
| **FCG‑DLC** | Diamond‑like carbon‑coated punches obtained from FETTE Compacting |
| **FCG‑HCP** | Hard chromium‑coated punches obtained from FETTE Compacting |
| **FCG‑R** | Roughened uncoated punches obtained from FETTE Compacting |
| **FCG-TAN** | Titanium aluminium nitride-coated punches obtained from FETTE Compacting |

| | |
|---|---|
| **FCG‑TIN** | Titanium nitride‑coated punches obtained from FETTE Compacting |
| **FCG‑U** | Uncoated punches obtained from FETTE Compacting |
| **Fig.** | Figure |
| **GMS** | Glyceryl monostearate |
| **HCr** | Hard chromium |
| **HPLC** | High performance liquid chromatography |
| **IBU** | Ibuprofen 50 USP |
| **IBU‑Na** | Ibuprofen sodium dihydrate |
| **ISO** | International Organization for Standardization |
| **LSD** | Least significant differences |
| **Lubritose$^{TM}$** | Lubritose$^{TM}$ MCC, a co-processed excipient produced by spray-drying |
| **MCC** | Microcrystalline cellulose |
| **MS** | Magnesium stearate |
| **NSAID** | Nonsteroidal anti-inflammatory drug |
| **OWRK** | Owens, Wendt, Rabel, and Kaelble method |
| **PC** | Principal component |
| **PCA** | Principal component analysis |
| **Ph. Eur.** | European Pharmacopoeia |
| **PVD** | Physical vapor deposition |
| **RH** | Relative humidity |
| **SD** | Standard deviation |
| **SEM** | Scanning electron microscopy |
| **SSF** | Sodium stearyl fumarate |

**TiN**              Titanium nitride

**UV**               Ultraviolet

**VIS**              Visible

# Contents

# 1. Introduction

## 1.1. Tableting

### 1.1.1. General aspects

With the invention of the first tablet press in 1843 by William Brockedon the commercial production of one of the nowadays most popular dosage forms began [1]. The popularity of tablets quickly grew, especially in the US, where because of the Civil War, the demand and thus the development of this dosage form increased [2]. Although there had been speculations at first that tablets might only be in fashion temporarily and would soon be replaced by other dosage forms, tablets are currently still one of the most widely-used solid dosage forms. This is a result of their numerous advantages. They are convenient to handle and to administer as well as easy to dose, resulting in a high popularity and compliance among the patients. Another reason for their ongoing popularity lies in their cost-efficient manufacture, their chemical, physical, microbial, and thus, storage stability as well as their ease of handling during packaging and distribution [3,4].

Apart from the active pharmaceutical ingredient (API), the tablet is composed of different excipients to either improve the tablet properties and/or the tablet production [5]. The excipients are usually classified according to their functionality in the formulation. Typically, fillers and binders (such as lactose and microcrystalline cellulose), lubricants (such as magnesium stearate), glidants (such as fumed silica) and disintegrants (such as croscarmellose sodium) are common excipients used in a tablet formulation. Suitable excipients have to be selected with care as they are known to strongly influence the manufacturability and the resulting tablet properties [6,7].

*1.1.2.   Preparation of tablet formulations*

Tablet formulations may be prepared in two different ways before tableting. The first and most straightforward way is to mix the different powder components directly in an appropriately sized blender. The process of tableting powder blends has been named direct compaction and has several advantages:

- Possibility to process thermolabile and moisture-sensitive APIs and excipients [8].

- Only few process steps and consequently reduced processing time, less energy consumption and therefore lower production costs [9].

- Increased stability of the resulting tablets [3].

- Fast disintegration of the resulting tablets [3].

However, most pharmaceutical compounds either show a poor compressability and/or insufficient flowability, leading to a portion of only approximately 20 % of all compounds which can be tableted directly [10]. Therefore, to improve these poor powder properties, the granulation of the powder formulation prior to tableting is often necessary. The benefits of tableting granules are mainly caused by the narrow particle size distribution and include following advantages:

- Increased flowability and decreased segregation tendency [11].

- Decreased amount of fine particles during processing and consequently reduced cross-contamination [12].

- Improved tablet content uniformity [12].

The two major granulation techniques are the wet and the dry granulation. Wet granulation is the most commonly used granulation process in the pharmaceutical industry [13,14], by which the agglomerate formation and growth is achieved by the addition of a liquid [11]. However, the major drawbacks of wet granulation are its

unsuitability for moisture-sensitive formulation components as well as its long processing time mainly resulting from the necessary drying step [12,15].

Dry granulation as an alternative granulation method involves the agglomeration of the powder particles with a slugging or roller compaction step without the drawbacks caused by the addition of a granulation liquid [16]. However, during dry granulation processes the amount of fine particles is usually increased. Furthermore, the tabletability of the granules is often limited because of the preceding compaction step [17].

In Figure (Fig. 1 an overview of the different processes involved in tableting via direct compaction as well as via wet and dry granulation is given.
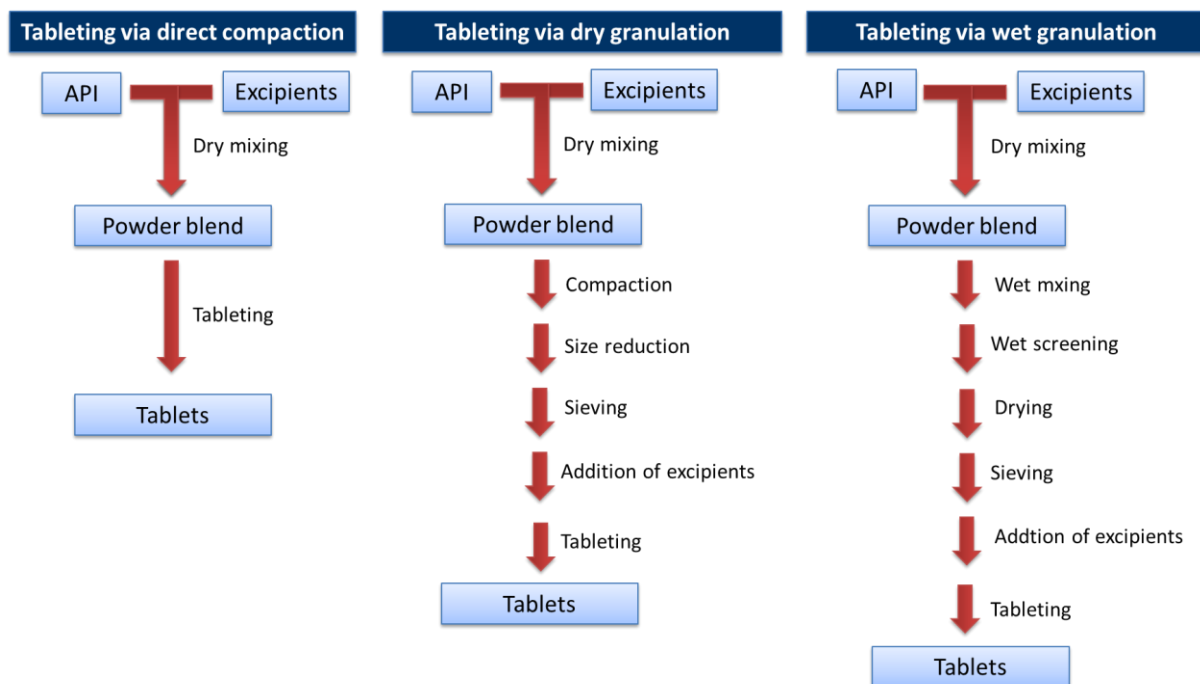


**Fig. 1:** Schematic overview of the major process steps involved in the tableting via direct compaction as well as via dry and wet granulation, modified from [10] and [15].

*1.1.3. The compaction process*

With a production output of over one million tablets per hour, rotary presses are by far the most commonly used tablet presses in the commercial tablet production [18]. In comparison to other tablet presses such as eccentric presses or compaction simulators, which can also be referred to as single station presses, the main reason for the high productivity of the rotary press is the use of numerous punch stations.

The centerpiece of a rotary press is the rotatable die table or turret, which is equipped with the numerous punch stations [19]. Each punch station consists of an upper punch, a die and a lower punch. During operation, the die table rotates and the punch stations pass through different process stations of the tablet production:

1. Fill station: the lower punches are moved downwards by the fill cam when passing the feed frame of the press to fill the dies with tablet formulation.

2. Mass adjustment: the volume and therefore the mass of the tablets is set by a previously adjusted upwards movement of the lower punches and removal of the excess powder with a scraper bar. Immediately after the scraper bar, the lower punches are pulled down again.

3. Pre-compaction and main compaction: both the upper and lower punches pass two successive compaction rolls, where they are moved into the die to exert an adjustable compaction force, which ultimately leads to the formation of the tablets. The pre-compaction force is usually set to be lower than the main compaction force to improve the properties of the resulting tablets by slightly pre-compacting and venting the tablet formulation bed [19,20].

4. Tablet ejection: both the upper and the lower punches are moved upwards by the respective ejection cams. The produced tablets are ejected from the die by the upwards movement of the lower punches and detached by a take-off bar.

For the formation of the tablets the pre- and main compaction events are most important and are therefore described in more detail (Fig. 2).
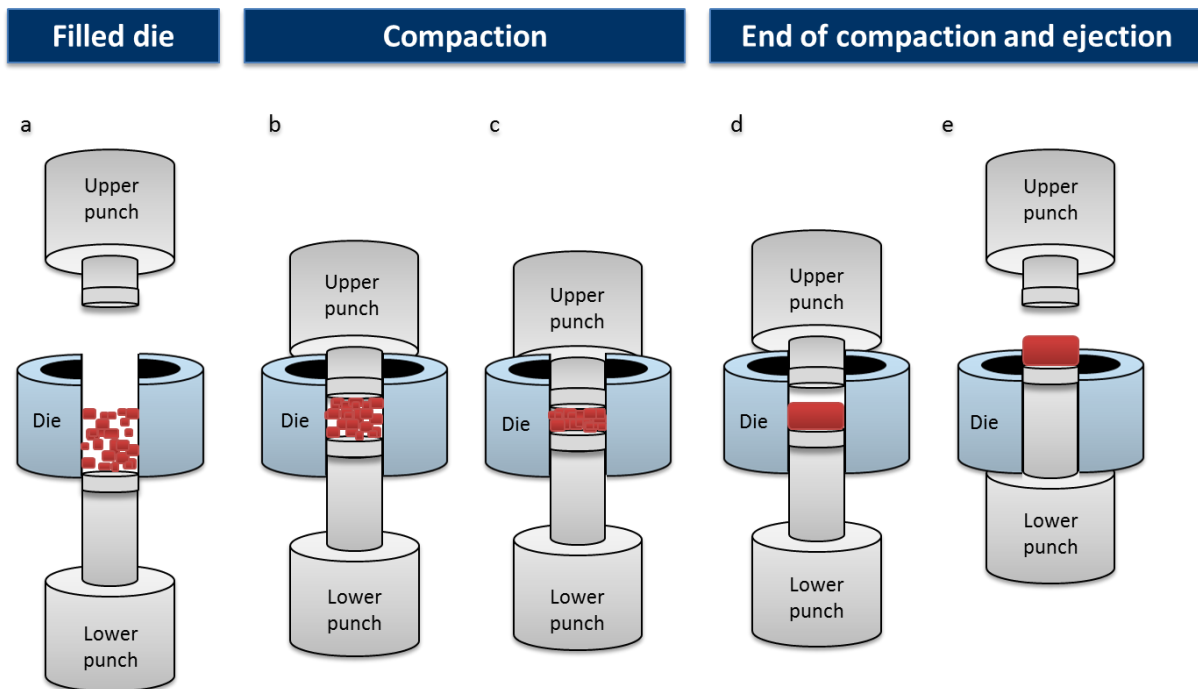


**Fig. 2:** Schematic depiction of the tablet formation process in a rotary tablet press: (a) conditions after die filling, (b, c) particle rearrangement and particle deformation, (d, e) end of compaction and tablet ejection. Modified from [15] and [21].

After filling of the die (Fig. 2 a), the only forces acting between the particles are related to the particle bed characteristics such as the density of the particles and the total mass of the powder material in the die [21].

A higher force is applied to the particle bed when the upper punch enters the die and the lower punch moves towards the upper punch (Fig. 2 b). The particles are rearranged and are exposed to the resulting interparticulate friction.

At a certain degree of density (Fig. 2 c), the particles are immobilized and further compaction leads to particle fragmentation, deformation and subsequently to the formation of bonds. At this stage the particles are forced into contact and the number

of contact points and thus the contact area is increased caused by either the plastic deformation or to the fragmentation of the particles or both [22]. However, a fraction of the energy may be stored as elastic energy. It has to be considered that the extent of the plastic and elastic deformation as well as the fragmentation is different with each material, its preprocessing and its supplier. The tableting material may often be classified as plastically deformable, elastic or brittle, in dependence of their predominating deformation behavior. Viscoelastic deformation behavior describes a combination of elastic and plastic deformation, which is exhibited by almost all materials under certain conditions [23].

With the increase of the number of contact points between the contacting particles, all types of interparticulate and intermolecular bonding forces are increased such as capillary, electrostatic, and secondary valence forces. Furthermore, solid bridges may be formed strongly depending on the chemical properties of the tableting material and may be formed by partial sintering, partial dissolution and recrystallization, or chemical reactions. These processes contribute to a permanent deformation of the tableting material and influence the mechanical strength of the tablet.

With the reduction of the compaction force (Fig. 2 d), the tablet is decompressed and the stored elastic energy is released to a certain extent by elastic recovery of the tablet [24]. This process of stress relaxation manifests itself in a volume expansion because of the elastically deformed particles partially regaining their shape.

In the stage of ejection (Fig. 2 e), the tablet has to overcome frictional and adhesive forces between the tablet and the tablet tooling until it emerges from the die and is removed by the take-off bar [25,26].

The final structure and properties of the tablet are affected by these forces and are a result of a complex combination of the described processes, which to this date need further exploration [27].

## 1.1.4.   Tablet quality attributes

Tablets must meet various requirements to ensure the quality of the product and the safety of the patients. A selection of the essential quality attributes is given in this section.

One essential quality attribute of tablets is their content uniformity. Because tablets are volumetrically dosed, and the volume and the mass of the tablet directly correspond to each other at a given bulk density, the tablet mass can be used as a measure for the content uniformity, after at least one assay to determine the API content of the dosage form has been conducted. The non-conformity of the mass is one of the most common observed complications during tablet manufacture [28]. In most cases, a poor flowability of the tableting material is the cause for an unacceptable tablet mass variation and may be prevented by the addition of glidants to the powder blend or by narrowing the particle size distribution [29].

Furthermore, tablets need to be sufficiently hard to withstand mechanical stress during manufacture and handling [30]. The tablet hardness usually correlates strongly with the tablet disintegration time, which may influence drug release and subsequently the bioavailability [31,32]. Both parameters may give further insight into the tableting process and the compactability of the tableting materials. There are numerous causes for an insufficient tablet hardness and disintegration time such as inadequate deformation properties of the materials, a high lubricant content, or an inappropriate compaction force and compaction speed [33].

Another important quality attribute is the tablet appearance, which includes the tablet dimensions and the tablet surface texture. The dimensions of the tablet may be varied by the tablet mass and the compaction force. The surface texture may be affected by other commonly observed complications during tablet manufacture such

as the sticking of tablet formulations to the punch surfaces [34,35] or a decreased

punch quality [3].

## 1.1.5. Tablet tooling quality

The tooling dimensions have a direct influence on the tablet thickness, hardness and mass [36]. Furthermore, the surface properties of the tablet tooling may significantly affect the surface quality of the produced tablets [37]. An insufficient surface quality of the die walls may cause unacceptable tablet ejection forces or may even lead to an increased risk of damaging primarily the tooling [38]. Moreover, the condition of the tablet punch as well as the die wall surfaces have a direct influence on the appearance of the produced tablets [39].

The quality of the tablet punch decreases over time resulting from abrasive and corrosive wear, which may affect the punch surface and the punch dimensions [36,40,41]. Therefore, tooling inspection should be regularly conducted and performed in the form of in-process inspections and inspections of the incoming punches. Swartz et al. observed that even newly obtained punches may show numerous imperfections regarding the homogeneity of the punch surfaces and thus an improper surface finish. They therefore suggested the introduction of a 100 % inspection program for new punches [42]. However, especially punch tip surfaces are difficult to inspect [36]. Tablet punch surface inspection may be conducted with a mechanical stylus, an optical stylus, or a laser reflectometer. However, it has been reported that these methods have limitations regarding the inspection of concave punches [43]. Therefore, Hyvärinen et al. suggested an inspection of concave punches with a diffractive optical element based sensor, which detects surface quality changes based on the shape and intensity of the resulting signal [44]. However, it is impossible to visualize the surface texture or to quantify it with the common surface parameters such as the arithmetic mean height or the kurtosis. Apart from these publications there appears to be a lack of studies dealing with a systematic characterization of punch surfaces and their changes caused by wear.

## 1.2.    Sticking during tableting

One of the most common and serious complications observed during tablet manufacture is the sticking of tableting material to the punch surfaces [45]. Weak cases of sticking lead to a layer of material adhering to the punch tip surface and are therefore referred to as "filming". As a consequence, tablet production often has to be terminated and the resulting tablets, most of them characterized by rough surfaces and incomplete engravings, have to be discarded. In some extreme cases, the whole tablet may stick to the upper punch resulting in an unwanted second compaction of this tablet together with the next filling of the die. In other extreme cases, sticking of the whole tablet to the lower punch may lead to high take-off forces, which can either destroy the tablet or may push parts of the tablet or even the whole tablet over the sweep-off blade back to the filling station. In either case, serious damages to the tablet tooling and tablet press may be the consequence  [34,35,46].

Current theories dealing with the sticking phenomenon suggest that sticking is caused by an unfavorable balance between the powder-punch adhesive forces and the powder-powder cohesion forces [34,35,47,48]. Sticking occurs if the adhesion force between the tablet and the punch surface exceeds the cohesion force within the tablet powder layers.

It is known that the sticking residue on punch surfaces is usually enriched with the sticky component of a formulation rather than being composed of the original formulation. In most cases, the API is the cause for sticking problems and the sticking residue on the punch surfaces may consist of up to 95 % API [47,49]. In cases where the API is the cause of sticking, the aforementioned theories have to be extended by the API-formulation matrix adhesion force ($F_{API-Formulation}$), the API-punch adhesion force ($F_{API-Punch}$) and the API-API cohesion force ($F_{API-API}$) (Fig. 3). In the cases, where

$F_{API-API} < F_{API-Formulation} < F_{API-Punch}$, sticking occurs and leads to a monolayer of residue on the punch surfaces. More severe multilayer sticking occurs if $F_{API-Formulation} < F_{API-API} < F_{API-Punch}$, because in this case the sticking API layer grows with each compaction run.
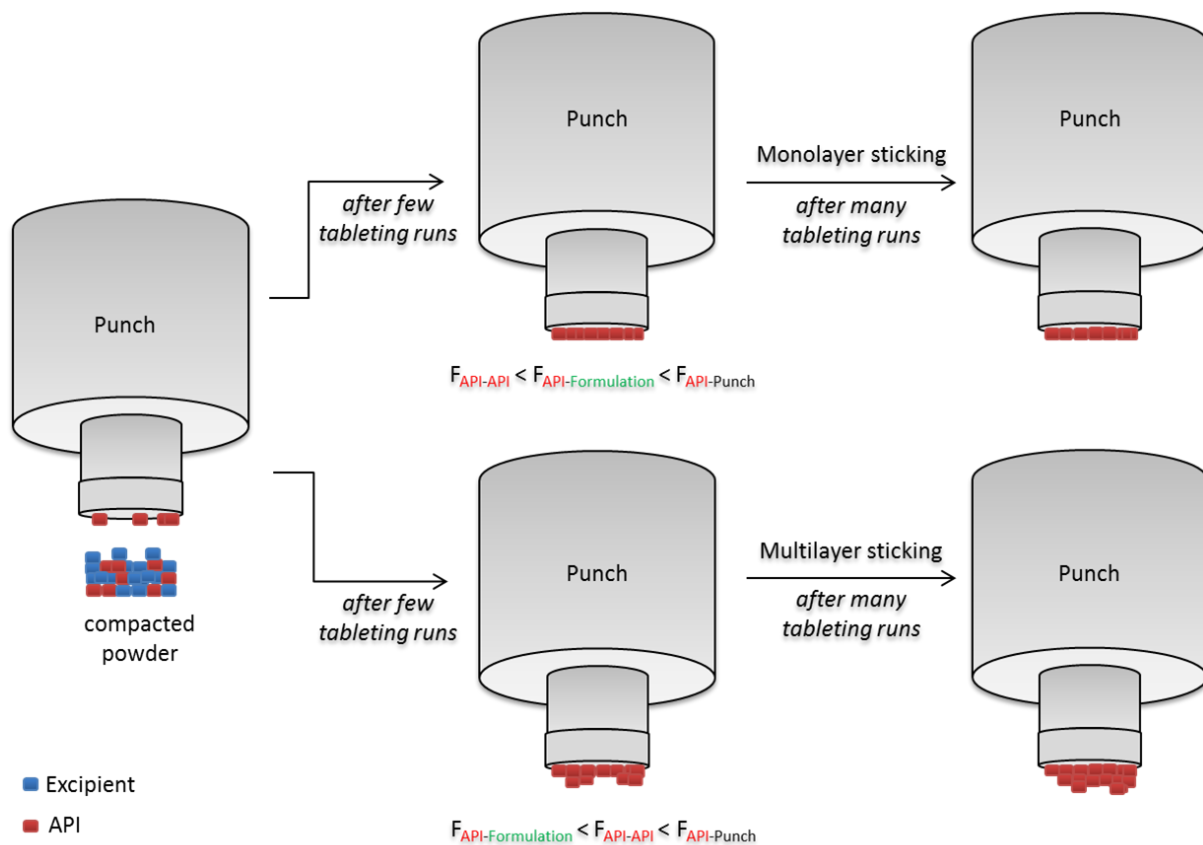


**Fig. 3:** Illustration of mono- and multilayer sticking during tableting, modified from [47].

Frequently, complications in tableting of new APIs become apparent only at the end of the drug development process, when tableting runs are conducted for the first time [45]. Yet, even with drugs that have already been on the market for a long time severe, sticking problems may still be encountered, for example if slight adjustments during tablet manufacturing have to be made.

Changes in the tableting settings may cause the adhesion force between the tablet and the punch surface to exceed the cohesion force within the tablet powder layers which may in turn lead to a sudden sticking occurrence [34,35,47,48]. To avoid sticking it is therefore necessary to keep the cohesion forces higher than the adhesion forces. However, before adjusting these forces it is essential to understand the nature of these forces.

### 1.2.1.   Cohesion forces

The cohesion forces within a tablet result from the same bonding mechanisms responsible for the formation of the tablet [50], which have been outlined in more detail in chapter 1.1.3.

### 1.2.2.   Adhesion forces

Various forces have been discussed as the major causes for powder adhesion to the punch surfaces during tableting [51,52]. The adhesion phenomenon is considered to be caused by the sum of these forces which include Van der Waals, capillary, electric double layer and electrostatic forces [15].

Van der Waals attractive forces act over a relatively short range < 100 nm and are present in all materials. According to the theory, three types of forces contribute to the attraction between two molecules [53]: The "Keesom-orientation force" causes two dipole molecules to orient the negative pole of one molecule towards the positive pole of the other molecule. Furthermore, the "Debye-induction force" may induce an electrical dipole in apolar, polarizable molecules by other, permanent dipolar molecules. However, in most molecules the "London-dispersion force" exceeds the "orientation forces" as well as the "induction forces" and is caused by an instantaneous polarization of the apolar atoms in a molecule, which in turn may polarize nearby atoms. This classical approach explains the attractive force between two atoms or molecules but is insufficient to explain adhesion between two macroscopic solids such as powder particles [54]. The "Liftshitz-van der Waals" theory, also known as the macroscopic approach, provides an explanation of these attractive forces [55]. They are supposed to result from natural density fluctuations in the electron cloud of atoms, which in turn cause the appearance of dipole moments and consequently fluctuations of the electromagnetic field around the atoms. This electromagnetic field may interact with other electromagnetic fields exceeding the

range of the London forces and resulting in attractive forces between macroscopic solids.

In the presence of moisture, capillary forces may cause a liquid bridge within in the gap between a particle and a solid surface causing adhesion in dependence of the geometry of the gap, the surface free energy, the wettability, and the surface roughness of the two adhering materials [51,53]. In moist powders, capillary forces may therefore reduce powder flow and lead to sticking or an increase in the tensile strength of the powder compacts. However, the capillary forces are strongly dependent on the moisture content in the powder bed [56]. Above a certain critical moisture content, the capillary forces may be exceeded by the force caused by the disjoining pressure, consequently reducing the bonding forces in a compact [53,57]. In dry or low moisture systems, capillary forces can be neglected [58].

The electric double layer force is another force closely related to the moisture content of the powder bed environment. It typically takes places between charged particle surfaces in polar liquids. The name "electric double layer" refers to the charged surface which is surrounded by oppositely charged ions resulting in two electrically charged layers. The electric double layer force arises if the electric double layers of two surfaces overlap when coming in close proximity [54]. It can also be found in a dry environment but only at particle sizes below 5 µm. The charging of particle surfaces in liquids, typically water or any liquid with a high dielectric constant, can occur via different mechanisms [59]. The selective adsorption of ions is the most important mechanism for previously uncharged surfaces. Particularly polyvalent anions often show a preferred adsorption tendency resulting in negatively charged particle surfaces [53]. The ions may be added to the water or may originate from the auto-ionization of the water. A further charging mechanism is the dissociation of

functional groups at particle surfaces such as carboxylic groups, which may dissociate in carboxylate anions and protons. In this case the surface is also charged negatively. The third charging mechanism occurs if two different surfaces are in very close proximity, allowing protons or electrons to move spontaneously from one surface to another. This mechanism is also known as contact electrification or triboelectric effect and results in the opposite charge of the two adjacent surfaces [59].

If non-conductive materials with excess charges are brought into contact, electrostatic forces or coulomb forces may arise. These long-range forces are relevant at particles sizes of above 5 µm and emerge if particles come into contact in an dry environment by the aforementioned triboelectric effect [53,60].

In general, the strongest forces between two adjacent particles are the Lifshitz-van der Waals forces, which are 10 times stronger than electrical and electrostatic forces. This relation between these forces remains unchanged, even if additional capillary forces are present.

Usually, if adhesion occurs, the forces mainly contributing to adhesion are the Lifshitz-van der Waals forces followed and enforced by the electrostatic forces or at moist conditions the capillary forces [53,61].

## *1.2.3.  Factors influencing sticking*

Because the adhesion is a multifactorial process, there are various factors, which may influence the degree of adhesion. A small selection of these factors is given in the next chapters.

### 1.2.3.1. *Composition of the tablet formulation*

The composition of the tablet formulation can influence both, the cohesive and the adhesive forces. The cohesive forces within the tablet may be increased by the addition of a high amount of binders [3]. Further influencing factors are the powder particle size, their crystal structure and crystal habit [62–66].

To reduce the adhesive forces, lubricants may be added to the tablet formulation to act as a so-called anti-adherent [67–71]. Magnesium stearate is the most frequently used lubricant because of its efficient friction and sticking reducing properties as well as its low cost [67,68,71–73]. However, it is also known for its negative effect regarding tablet strength as well as its prolonging effect on tablet disintegration and thus drug release [68]. These problems become even more pronounced with a prolonged powder blending time [74]. Moreover, magnesium stearate is known to form eutectic mixtures with different APIs such as ibuprofen, consequently lowering the melting point of these mixtures and increasing their sticking tendency [75,76]. Sodium stearyl fumarate is often suggested to be a good but expensive alternative to magnesium stearate because it exhibits similar lubrication properties with less chemical incompatibilities and a less pronounced prolonging effect on tablet disintegration [77]. Co-processed excipients such as Lubritose[TM] MCC, which consists of the dry binder microcrystalline cellulose (MCC) and the lubricant glycerol monostearate (GMS), are becoming increasingly popular for the direct compaction of tablets because their blending time sensitivity is reduced and less processing steps

for the preparation of the material to be tableted are needed [78]. However, these relatively novel excipients have not yet been examined as extensive as traditional excipients and their benefits still need to be further investigated.

1.2.3.2. *Process parameters during tableting*

Other attempts to reduce sticking of tablet formulations involve the adjustment of the tableting settings such as the compaction force and the compaction speed [79,80]. The increase of the compaction force may lead to an increase of the cohesion forces within the tablet and may exceed the adhesion forces between the tablet and the punch surface [34,81,82]. It is known that high compaction forces may also increase the temperature during compaction [70], which in turn may locally exceed the melting point of low-melting tablet components or eutectic mixtures and thus may affect their sticking tendency [81]. The compaction speed also has to be increased with caution because of its possible adverse effects on sticking and tablet properties such the tablet strength. The reduction of the compaction speed represents another option to reduce sticking. This reduction results in a prolongation in the dwell time and may increase the cohesive forces within the tablet, especially with plastically deforming formulation components [15].

1.2.3.3. *Roughness of punch surfaces*

As described before, the contact area between two surfaces plays an important role with regard to the strength of adhesion. Surface roughness as well as particle size and shape may affect the true contact area between two surfaces and are therefore essential factors influencing adhesion and consequently sticking during tableting [83,84].

With respect to tableting, the influence of the punch surface roughness on sticking is subject of controversial debate. In some studies it was found that a higher surface roughness promotes sticking [85,86]. However, in other studies it was described that a high surface roughness reduces sticking [46,87,88]. In general, a high punch surface roughness may either increase or decrease the true contact area between the adhesive particles, depending on their size and shape (Fig. 4). This true contact area may be decreased by the punch surface roughness assuming that the asperities of the surface, which result from the surface roughness, work as spacers between the adhesive particles and the respective surface. However, this relation is only valid, if the particle size is larger than the gap between two asperity tips (Fig. 4 a). If the particle size is smaller than this gap, adhesion is increased because the particles come in contact with the numerous valleys of the punch surface [53,89] (Fig. 4 b). The dependency of the extent of adhesion on the surface roughness and the particle size is strongly related to the extent of the van der Waals forces while it is only hardly related to the extent of the capillary forces, if they are also involved. The strength of the capillary forces is influenced by the contact angle, which increases with the punch surface roughness. However, it may also be influenced by other surface properties and is therefore strongly dependent on the current conditions [53,90].
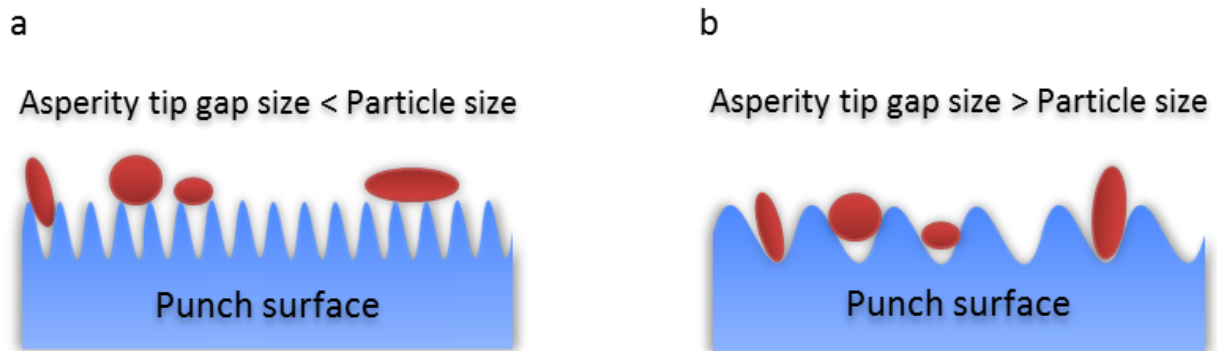
**Fig. 4:** Influence of the ratio asperity tip gap size and the particle size on the true area of contact. (a) If the gap size is smaller than the particle size the true area of contact is reduced. (b) If the gap size is larger than the particle size the true are of contact is increased. Modified from [53].

Therefore, there has been an increased interest in the identification of surface properties causing sticking problems to eventually develop optimized punch surfaces which are able to prevent this phenomenon. There has been substantial effort to visualize sticking residues on punch surfaces [49,91,92]. Abbott laboratories quantified the composition of sticking residues directly on the punch surfaces using scanning electron microscopy (SEM) combined with energy dispersive X-ray spectroscopy (EDS) [49,91]. However, the sticking pattern on the punch surfaces was not evaluated in the described studies. In the master thesis by James V. Thomas, sticking ibuprofen to the punch surface was visualized by SEM images of a removable punch tip after one compaction of plain ibuprofen and after 450 compactions of a 30 % ibuprofen formulation [92]. It was observed that sticking was more pronounced in the center of the punch. However, only one surface image per formulation and compaction was evaluated and the effect of subsequent compactions on the sticking pattern was not investigated.

In other studies, the effect of punch surface roughness on sticking was evaluated but in contrast to the aforementioned studies no investigations of punch surfaces with sticking residue on were performed [46,51,87,88,93].

For a thorough characterization of punch surfaces, 3D measurements are necessary as they provide more detailed information on the surface properties than 2D analysis [94]. However, taking only one surface parameter into account is not sufficient to describe the complex nature of punch surfaces because each surface parameter can give information on only one specific property of these surfaces [95]. Therefore, several 3D surface parameters were defined and standardized according to American Society of Mechanical Engineers (ASME), European project report EUR 15178 EN (EUR) and International Organization for Standardization (ISO) [96–99]. Some of these proposed surface parameters are unique parameters of the respective standard while the other parameters defined in the different standards are either identical or similar to each other, if they were calculated differently [100]. For characterization of the complex surface of tablet punches it is necessary to record a 3D image of the respective surface and to characterize it using various surface parameters. The parameters typically related to the adhesive behavior of a surface are the summit density (Sds), the mean summit curvature (Ssc), the developed interfacial area ratio (Sdr), the root mean square height (Sq), the skewness (Ssk) as well as the kurtosis (Sku) [101,102].

1.2.3.4. *Modification of punch surfaces*

Punches with applied coatings represents another option to reduce the adhesive forces between the tablet material and the punch surface with the additional benefit with regard to wear and corrosion resistance of the tooling [39,85,87,103,104]. However, the selection of the appropriate tooling for tableting a certain formulation can be difficult as coated tools are regarded as complex structured compound materials and their interaction with the material to be tableted is therefore difficult to predict [105,106].

There is a wide range of different punch coatings available on the market but only few have been systematically examined with regard to the reduction of sticking and wear. Costly trial-and-error tests are the result [45,85].

The most commonly used coating is hard chromium (HCr), a low-cost coating produced by electroplating [107–109]. The anti-sticking properties of HCr punches, however, have been reported to be similar to or even worse than uncoated punches [46,87]. Alternatively, coatings applied by physical vapor deposition (PVD) such as titanium nitride (TiN) or chromium nitride (CrN) can be used [104,107,110–112]. The most prevalent PVD coating is TiN [113–115]. However, investigations showed that CrN may be a better option as coating material for industrial tooling than both TiN and HCr [107,113,116]. Another coating which can be applied by either PVD or by chemical vapor deposition (CVD) is diamond-like carbon (DLC). DLC has become increasing popular in recent years because of its high hardness, abrasive and corrosive wear resistance, chemical inertness and its surface smoothness [105,117,118]. Images of differently coated punches are shown in Fig. 5.

Especially the resistance against different types of tooling wear such as abrasion and corrosion plays a significant role in the designated application of the respective coating and has been subject of many studies [105,106,110,113]. However, the suitability of the coating materials for the specific requirements of tablet punches with respect to wear phenomena and their resulting effect on sticking has not yet been sufficiently investigated.

**Fig. 5:** Exemplary images of differently coated punches.

1.2.3.5. *Surface free energy of solid materials*

The work of adhesion, which is defined as the energy required to separate two solids with a contact area of 1 cm² (Fig. 6 a), is closely related to the surface free energy of the respective solid materials, which is defined as the energy required to increase the surface area of the material by 1 cm² [53,59,119]. The work of cohesion is equivalent to the work of adhesion, if the two phases in contact are made of the same material (Fig. 6 b).
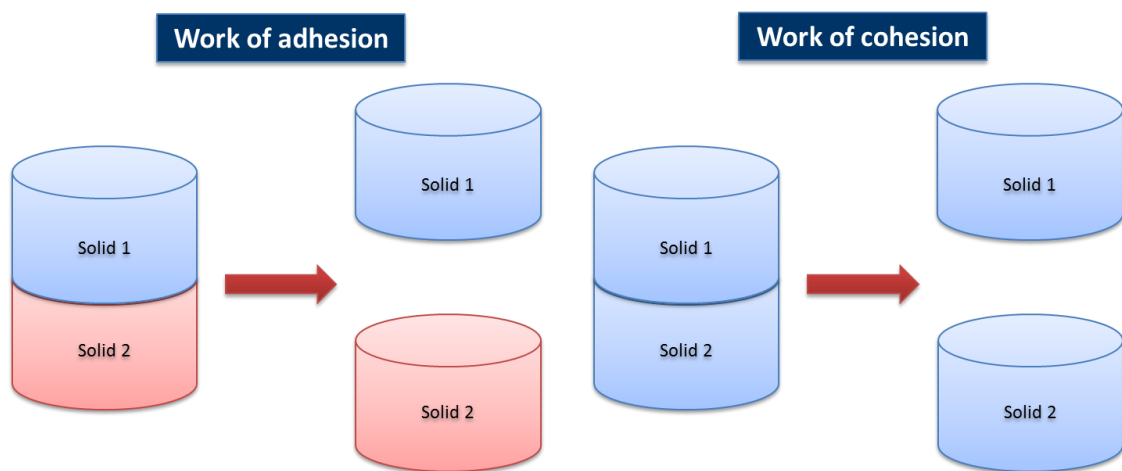


**Fig. 6:** Schematic representation of the work of adhesion (a) and the work of cohesion (b), modified from [53,54].

Because two new surfaces are formed after the separation, the work of adhesion has to exceed the surface free energies resulting from the newly formed surfaces of the two materials. The interfacial energy between the two materials is released after separation, consequently lowering the work of adhesion. Therefore, the work of adhesion may be calculated from the surface free energies of the respective materials and their interfacial energy using the Dupré equation (Eq.) [120]:

$$W_A = \gamma_1 + \gamma_2 - \gamma_{12} \qquad\qquad\qquad (Eq.\ 1)$$

where $W_A$ is the work of adhesion, $\gamma_1$ the surface free energy of solid 1, $\gamma_2$ the surface free energy of solid 2, and $\gamma_{12}$ the interfacial energy between the two solids.

The surface free energy of materials may therefore be used as a directly proportional indicator for the adhesiveness of the materials' surface [89,104,121,122]. Therefore, it may for instance be used for evaluating the surface modification of tableting punches with regard to their anti-sticking properties.

The surface free energy of materials is caused by various chemical bonding components, which may be reduced to the dispersion and the polar components of the material [123,124]:

$$\gamma = \gamma^d + \gamma^p \tag{Eq. 2}$$

where $\gamma$ is the surface free energy, $\gamma^d$ are the dispersion forces and $\gamma^p$ the polar forces.

To determine the surface free energy of solids, several approaches have been introduced One of these approaches is the so-called OWRK method, which was developed by Owens, Wendt, Rabel, and Kalble [125–127]. After the determination of the contact angles between a solid test surface  and at least three test liquids with known surface tensions as well as known polar and dispersive components, the dispersion and polar components of the solid test surface may be calculated with the linear Eq. of the OWRK method [128].

$$\frac{\gamma_l \cdot (1 + \cos\theta)}{2 \cdot \sqrt{\gamma_l^d}} = \sqrt{\gamma_s^p} \cdot \sqrt{\frac{\gamma_l^p}{\gamma_l^d}} + \sqrt{\gamma_s^d} \tag{Eq. 3}$$

where $\gamma_l$ is the surface free energy of the liquid, $\theta$ the contact angle of the liquid on the solid surface, $\gamma_l^d$ the dispersive component of the liquid, $\gamma_l^p$ the polar component of the liquid, $\gamma_s^p$ the polar component of the solid, and $\gamma_s^d$ the dispersive component of the solid. The surface free energy of the solid may then be calculated as the sum of its polar and dispersive components. However, the surface free energy may provide

inconsistent results in some cases because it can be influenced by the environmental

conditions and the solid surface roughness [121].

## 1.3.    Design of Experiments (DoE) in tableting investigations

Every process can be viewed as a system with the influencing factors as inputs and the respective responses as outputs (Fig. 7). The influencing factors can be further classified as either controllable, such as the settings of the process e.g., compaction force during tableting, or as uncontrollable, such as environmental changes, which are mainly responsible for the variability of the responses. These factors may either be numerical (e.g. setting of the compaction force to 5 kN or 19 kN) or categorical (e.g. tableting excipient A or B) [129].
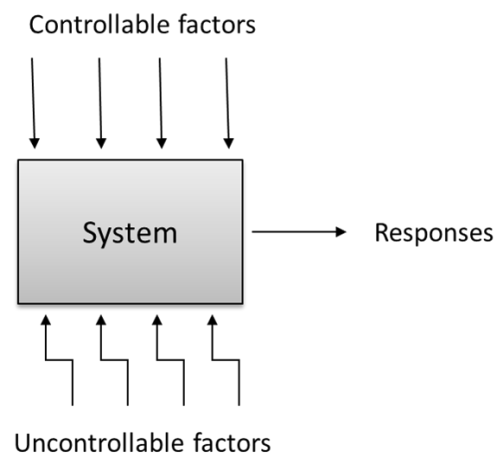
**Fig. 7:** A process depicted as a system with controllable and uncontrollable factors as inputs and responses as outputs.

To understand the effect of the many factors influencing multi-factorial processes such as sticking to tablet tooling, a statistical methodology is needed to avoid an unpractical amount of experiments on the one hand, while simultaneously analyzing the interaction of the factors on the other hand. Instead of varying the level of only one factor while keeping all other factor levels constant, as conducted in classical One-Factor-at-a-Time approaches, it is by far more efficient to vary all factor levels simultaneously [129,130]. This more efficient concept is implemented in the design of experiments (DoE) approach - a statistical methodology for planning and analyzing experiments with a minimal amount of experimental effort.

Two-factorial designs are the most frequently used DoE designs. They are also sometimes referred to as $2^k$ designs, where k stands for the amount of selected factors, because all selected factors are varied only at two levels and the resulting number of experimental runs may therefore be calculated by this formula. To describe the whole design space (Fig. 8), the two levels for the selected amount of factors are usually set to the minimum and maximum level. As these points are the extremes of the design space, they are also referred to as the vertices. Because the selected factors are only varied at two levels, this design model is limited to linear correlations. To check if the calculated model is truly linear, a third level of the respective factors is required which is set to the level in between the maximum and the minimum level and is therefore referred to as the "center point". If the deviation of the center point from the calculated response model is statistically significant, curvature is present and a linear response model is insufficient to describe the data.
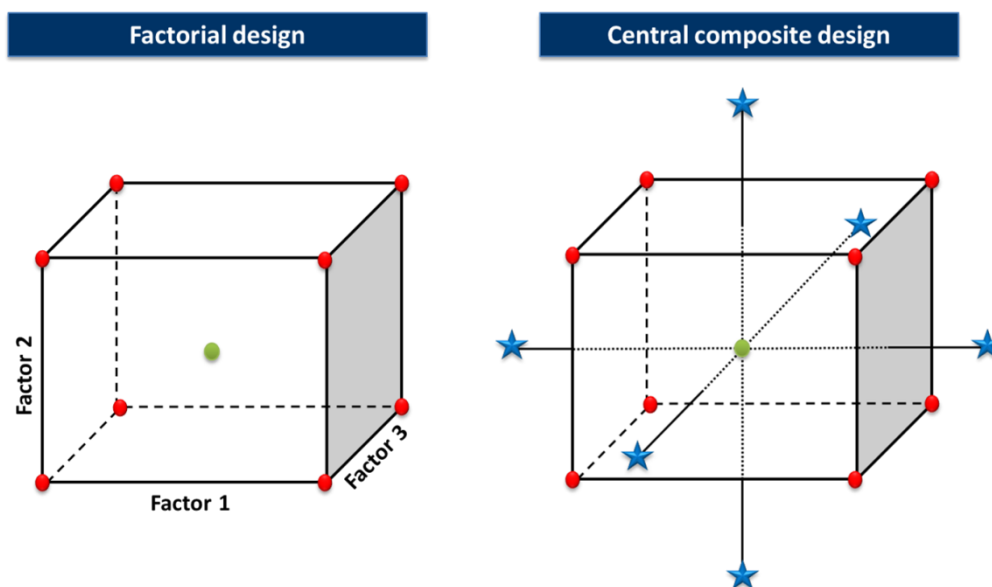


**Fig. 8:** Example of a factorial design and a central composite design with three factors. The red dots represent the vertices, the green dots the center point and the blue stars the star points of the design.

In the presence of a curvature, designs that represent higher order correlations are required such as the central composite design (Fig. 8), where so-called star points are added [131].

These well-established DoE methods have been used for many years but show several limitations [131]:

- Multifactorial operating constrains such as factor levels which are either impossible to execute or which may damage the equipment cannot be considered.

- The combination of numerical factors with categorical factors either requires an impractical amount of experiments with two-factorial designs or is impossible with central composite designs.

- The methods provide insufficient data for non-quadratic polynomial models such as cubic or higher-order models.

As computers can quickly calculate more complex optimal design points, computer-based algorithms can be used for the creation of designs without the above-mentioned constrictions and with an acceptable number of experiments. These designs are referred to as optimal designs. The most commonly used optimal design is the D-optimal design [132,133]. The D is an abbreviation for "determinant" because this computer-generated design is based on the D-optimality criterion to minimize the variance of the model coefficients and therefore to maximize the determinant of the Fisher Information Matrix [131,134]. Because D-optimal designs require more measurements at the boundary of the design region, they are recommended if this is the area of interest, e.g. in screening designs, where out of a large number of factors the most relevant have to be identified [135,136].

The I-optimal design, which is also referred to as Q-, V- or IV-optimal design, aims to minimize the variance of prediction over the whole design region [136,137]. In this case, the letter I stands for optimizing the "integrated variance". Because this design usually requires more measurements at the center of the design space in comparison to D-optimal designs, it is often used for investigations, where the prediction is the main focus [133,135].

To construct either of these computer-based designs, various algorithms have been applied for finding the optimal design points. Currently, most available DoE software offer two variations of the so-called exchange algorithms to find the optimal design: the point exchange and the coordinate exchange algorithm. Exchange algorithms begin with a random design built with a predetermined number of design points and subsequently calculate the respective optimality criterion (D- or I-optimal). The exchange algorithm then starts adding new design points while deleting existing design points to approximate the respective optimality criterion [138]. This procedure is repeated until no further changes are required to improve the design. The point exchange algorithm chooses the design points from a beforehand specified set of candidate points and may be used if only predetermined levels of factors are applicable [139]. In contrast, the coordinate exchange algorithm is not limited to certain design points and is therefore suitable for mainly continuous factors [138].

With a DoE approach it is possible to evaluate factor influences, to detect factor interactions and to predict process outcomes with a manageable number of experiments. Therefore, DoE has found various applications in the pharmaceutical field either as a tool for quality management or for research and development [132,140].

## 1.4.    Ibuprofen as model drug

Ibuprofen is a widely used nonsteroidal anti-inflammatory drug (NSAID), which is administered mainly orally in the form of tablets, usually with a high drug content (200-800 mg) [141].

However, the tableting of ibuprofen is challenging because of its poor flowability resulting from the high cohesivity of the powder particles as well as its poor compactibility because of the high viscoelastic deformation behavior of these particles [66,142]. Furthermore, ibuprofen shows a high sticking tendency to the tablet tooling [34,66,142]. One of the suggested causes for its sticking tendency is its low melting point of 75 - 78 °C [34]. It is suggested that the interparticulate friction during compaction results in localized high temperature spots on the newly formed tablet surface, where melting of powder components with a low melting point is induced. The subsequent rapid recrystallization resulting from the decrease of the compaction force and the temperature after the punches pass the compression rolls is assumed to cause adhesion to the tablet tooling [70,76]. In a study conducted by Thomas [92], sticking ibuprofen was visualized on the surface of a punch and it was presumed that particle fragments, which were partly deformed, were an indicator of two mechanisms of ibuprofen sticking: ibuprofen fragmentation during compaction with subsequent adherence to the punch or to the already adhered mass to the punch as well as squeezing and smearing on the punch surface. As a consequence of the poor tableting properties, granulation of ibuprofen powder formulations is often necessary [65,141,143]. However, to improve the economic efficiency of the tableting process, direct compaction is preferred over an additional time- and energy-consuming granulation step before compaction [9,62,141]. Nevertheless, a limitation of the direct compaction process is the drug content of the tablet formulation, which is often limited to approximately 30 % [8].

Because of the above-mentioned properties of ibuprofen, it is often used as a model substance in investigations involving sticking [66]. Therefore, the high sticking behavior of ibuprofen has been investigated intensively [34,46,48,76,141,144,145].

With regard to ibuprofen powder formulations, several attempts have been made to improve the tableting behavior of ibuprofen during direct compaction such as formulation optimization [46,146], crystal engineering [62,63,65,66,82,142], selection of the optimal ibuprofen grade [141] or the application of optimal storage conditions [147]. Another promising method for the improvement of ibuprofen tableting that has been subject to recent investigations is the nanocoating of ibuprofen powder particles with various excipients such as magnesium stearate [148] or fumed silica [149]. With both excipients, an improvement of powder flowability and tabletability was achieved. However, the sticking tendency was not investigated in these studies. Particularly to overcome sticking and tabletability problems with ibuprofen, BASF has developed a directly compressible ibuprofen grade in the form of nanocoated granules, which contain 85 % ibuprofen and 15 % excipients. These granules (Ibuprofen DC 85 W) are produced via roller compaction, followed by the nanocoating of the granules with fumed silica [150]. The tableting and anti-sticking properties of Ibuprofen DC 85 W have been reported to be excellent [151].

To improve tablet properties with regard to the tableting settings, a pre-compaction force is often applied in addition to the main compaction force, as it is known that pre-compaction may overcome tableting problems in some cases [12,20]. Usually, the pre-compaction force is lower than the main compaction force. However, in some studies various combinations of pre- and main compaction forces were investigated with conflicting results. In one study, it was reported that a pre-compaction force that is lower than the main compaction force may increase the tablet crushing strength,

while in another study contrasting results were found, revealing that a higher pre-compaction force may result in higher tablet tensile strengths [152,153]. In other studies, the compaction of various materials in more than two compaction events showed an improvement of some tablet properties, especially if brittle material was compacted [153,154]. However, the application of a multiple compaction has not been investigated yet with regard to sticking problems with ibuprofen. In rotary tablet presses, a pre-compaction station belongs to the standard equipment. With the FE tablet press series, Fette Compacting has developed tablet presses with even three compaction stations.

Moreover, another option to deal with sticking problems is  the application of differently coated punches, which may either increase or decrease the sticking tendency of ibuprofen during tableting [46,87,88,155]. However, the reasons for this coating-dependent adhesion behavior are still not fully understood.
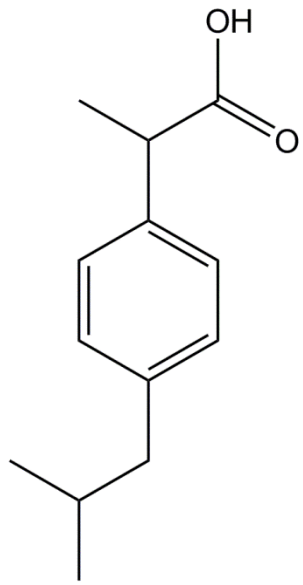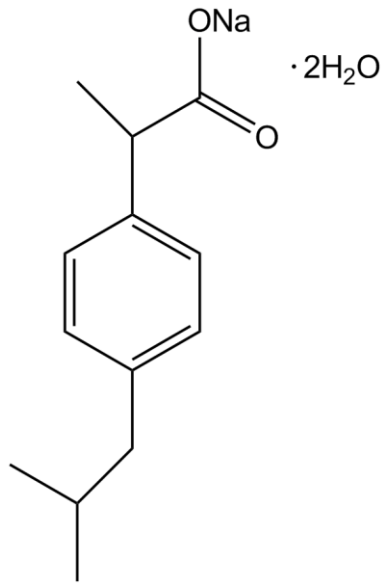
Recently, tablets containing the sodium salt of ibuprofen instead of its free acid are becoming increasingly popular because of their higher hydrophilicity and their resulting faster dissolution [71,156]. Although the melting point of ibuprofen sodium is significantly higher (198 °C) than its acidic counterpart, it has been reported that sticking of the salt can still be observed [157], which surprisingly decreases with increasing humidity [158]. Although its compaction behavior has been compared with that of ibuprofen acid [159], its sticking tendency has not yet been subject to a comparative investigation. Especially the sticking tendency to differently coated punches may improve the understanding of the processes leading or preventing sticking.

Ibuprofen exhibits a combined plastic and elastic compaction behavior and the predominating behavior is dependent on the selected tableting speed [160]. Moreover, ibuprofen shows brittle fragmentation to a small degree [63].

In comparison to ibuprofen, ibuprofen sodium dihydrate shows a higher plastic deformation tendency, which is most probably related to its crystal water acting as a plasticizer [159].

**Table 1:** Overview of the chemical structure and the properties of ibuprofen and ibuprofen sodium dihydrate.

| API | Ibuprofen | Ibuprofen sodium dihydrate |
|:---:|:---:|:---:|
| **Chemical structure** |  |  |
| **Molecular mass** | 206.28 [g/mol] | 264.26 [g/mol] |
| **Water solubility** | 0.01139 [g/l] (25 °C) [161] | 100 [g/l] (20 °C) [162] |
| **Melting point** | 75 - 78 °C | 198 °C |
| **Deformation behavior** | Plastic and elastic deformation with a small fraction of brittle fragmentation | Higher plastic deformation than ibuprofen |

# 2.        Objectives of this work

Sticking during tableting may lead to complications resulting in time-consuming and costly interventions. Even if small-scale tableting was successful, sticking problems may still become apparent on a production-scale. Although extensive research has been performed to identify the influencing factors and to reveal the underlying mechanisms of sticking, the phenomenon of sticking is still not fully understood.

For instance, the anti-adhesive effect of lubricants, especially of magnesium stearate, has been extensively described. However, the effect of other lubricants, such as co-processed compounds, has not yet been thoroughly investigated.

Another approach to deal with sticking problems that has been subject to intensive research in recent years is the application of differently surface-coated punches. The punch surface properties have been identified early on as a major factor influencing sticking. Two of these properties may affect the anti-sticking tendency of punch surfaces: its chemical composition and its surface texture. Although some of the coating materials could be identified as especially efficient in terms of their anti-sticking properties, there appears to be a lack of a systematic characterization of the punches' features regarding their chemical and surface texture. This may be caused by the difficult visualization of sticking material to the punch surfaces because of the usually bulky size of tablet punches.

The influences of tableting settings such as compaction force and compaction speed on the sticking tendency are better understood. However, the extent of their influence has mostly been investigated separately and not in combination with each other, which makes it difficult to identify the most influencing tableting parameter.

Therefore, the aim of this thesis was to systematically investigate these influencing factors and to reduce sticking during tableting.

In this context, it was of special interest to identify the most important influencing factors and to detect possible factor interactions. The aim was to specify whether the tableting settings, the lubricant types, the punch surface modifications or their interactions were the most critical parameters.

One of the main objectives of the thesis was to systematically characterize differently coated punch surfaces with respect to their anti-sticking performance, their hydrophilicity and their surface texture. Furthermore, the influence of the different hydrophilicity of the selected model drugs ibuprofen and ibuprofen sodium dihydrate on their sticking tendency to these different punch surface coatings was explored in-depth.

Because the influence of the punch surface texture is difficult to analyze, another major goal of the thesis was to develop a technique to visualize and characterize differently modified punch surfaces before and after tableting formulations containing the model drugs.

Overall, the aim of the present work was to reduce sticking complications during tablet production. Therefore, several approaches pursued in the previous investigations were transferred to production-scale tableting to significantly improve sticking problems.

# 3.     Materials and Methods

## 3.1.     Materials

### 3.1.1.     Materials used for the preparation of the powder blends

Ibuprofen 50 USP (IBU) and ibuprofen sodium dihydrate (IBU-Na) were kindly donated by BASF (Germany), fumed silica (Aerosil® 200) by Evonik (Germany) and MCC (Avicel® PH-102) by FMC BioPolymer (USA). Sodium stearyl fumarate (SSF, Lubripham® SSF) and Lubritose™ MCC (Lubritose™, a co-processed excipient produced by spray-drying, containing 98 % MCC and 2 % [w/w] glyceryl monostearate) were kindly provided by Lehmann & Voss (Germany). Glyceryl monostearate (GMS) was obtained from Alfa Aesar (USA) and magnesium stearate (MS) from Fagron (Germany).

Ibuprofen DC 85 W was kindly donated by BASF (Germany) and is a pre-formulated, roller compacted, directly compactable material, composed of 85 % ibuprofen and 15 % inactive ingredients such as MCC, croscarmellose sodium, and fumed silica. Ibuprofen DC 85 W is supplied in the form of granules coated with fumed silica nanoparticles to overcome tableting complications such as sticking.

An IBU powder formulation optimized for direct compaction was donated by BASF and was used for the production-scale tableting experiments of study 1 ("Factors influencing the sticking tendency of ibuprofen during direct compaction"). It was composed of 70 % [w/w] IBU together with 0.5 % MS as lubricant and MCC as dry binder. To meet the requirements for direct compaction, additional ingredients, which cannot be specified because of the confidentiality agreement with BASF, served as formulation optimizers.

Two other ibuprofen formulations (ibuprofen formulation A and ibuprofen formulation B) optimized for direct compaction were also donated by BASF to compare their

sticking properties with those of Ibuprofen DC 85 W in study 4 ("Production scale tableting of an optimized ibuprofen grade to decrease its sticking tendency"). Both formulations were provided as powders and composed of 70 % ibuprofen and 30 % inactive ingredients such as MCC and croscarmellose sodium. In contrast to ibuprofen formulation A, ibuprofen formulation B did not contain fumed silica.

### 3.1.2.   Materials used for tablet disintegration

Demineralized water was used for tablet disintegration testing. In addition, to exclude differences in wettability caused by the different lubricants of the produced tablets, a 0.3 % [w/V] surfactant solution containing polysorbate 80 from Caelo (Germany) was used for tablet disintegration testing.

### 3.1.3.   Materials used for high performance liquid chromatography (HPLC) analysis

For HPLC analysis, acetonitrile of high performance liquid chromatography (HPLC) grade from VWR (USA), phosphoric acid 85 % ROTIPURAN® from Carl Roth (Germany) and Milli-Q® water from Merck Millipore (Germany) were used. HPLC grade methanol from VWR (USA) was used for cleaning the punch surfaces and in study 1 to collect samples of IBU that was sticking to the punches.

### 3.1.4.   Materials used for impression molding

High-resolution silicone-A dental impression material (Provil® novo light; Heraeus Kulzer; Germany) was used for molding the punch surfaces. For fixing the molds, microtiter plates (96 wells) from Carl Roth (Germany) were used.

### 3.1.5.   Materials used for contact angle measurements

Diiodomethane and formamide from Alfa Aesar (USA) were used for the contact angle measurements.

## 3.2.    Factors influencing the sticking tendency of ibuprofen during direct compaction (study 1)

### 3.2.1.   Preparation of powder blends for direct compaction

All prepared powder blends contained 70 % [w/w] of sieved (1000 µm mesh) IBU as the API and 0.5 % [w/w] of sieved (315 µm mesh) Aerosil$^®$ 200.

For tablet manufacture, MS is usually used at concentrations between 0.25 % - 5.0 % [w/w] and SSF at concentrations between 0.5 % - 2.0 % [w/w] [163]. The concentration levels of the lubricants used in this study were chosen based on these commonly used concentration ranges. Additionally, to allow an accurate comparison between the lubricants, equal concentrations of the different lubricants in the formulations had to be applied. Because of the fixed composition of Lubritose$^{TM}$ (composed of 98 % MCC and 2 % GMS), formulations 1-3 (Table 2) consisted of 28.91 % MCC [w/w] and 0.59 % [w/w] of either GMS, MS or SSF. Formulation 4 contained 29.5 % [w/w] Lubritose$^{TM}$ as dry binder and lubricant, which corresponded to a composition of 28.91 % [w/w] MCC and 0.59 % [w/w] GMS. MCC and GMS were chosen as excipients in formulation 3 to provide a physical mixture of its co-processed equivalent Lubritose$^{TM}$ in formulation 4 for comparative purposes. The composition of the powder blends to be compacted is displayed in Table 2. All formulation components were mixed in a Turbula blender (T2F equipped with a 2 l container, Willy A. Bachofen, Switzerland) at 72 rpm for 10 min, sieved (1120 µm mesh) to remove  agglomerates and mixed again for additional 14 min. Batch sizes of 1.5 kg were prepared.

**Table 2:** Composition of the powder blends

| Formulation | Dry binder (% [w/w]) | Lubricant (% [w/w]) | Glidant (% [w/w]) | API (% [w/w]) |
|---|---|---|---|---|
| formulation 1 | 28.91 % Avicel® PH-102 | 0.59 % MS | 0.5 % Aerosil® 200 | 70 % ibuprofen 50 |
| formulation 2 | 28.91 % Avicel® PH-102 | 0.59 % SSF | 0.5 % Aerosil® 200 | 70 % ibuprofen 50 |
| formulation 3 | 28.91 % Avicel® PH-102 | 0.59 % GMS | 0.5 % Aerosil® 200 | 70 % ibuprofen 50 |
| formulation 4 | 29.5 % Lubritose™ (co-processed excipient with a corresponding compostion of 28.91 % MCC and 0.59 % GMS) | | 0.5 % Aerosil® 200 | 70 % ibuprofen 50 |

Prior to tableting, the powder blends were stored in an air-conditioned room at a temperature of 21 °C and a relative humidity (RH) of 45 % for at least 72 h.

50 kg of the IBU formulation optimized by BASF for direct compaction was delivered ready to use so that no further processing before tableting was needed.

### 3.2.2.   Determination of bulk density and flow properties

The Hausner ratio, angle of repose and the flow rate through an orifice of 10 mm diameter (BEP2 flowability tester, Copley Scientific, UK) were determined according to the European Pharmacopoeia (Ph. Eur.), chapter 2.9.36 "Powder Flow", to characterize the flow properties ofr the investigated powder blends. The Hausner ratio was calculated as the quotient of bulk and tapped volume. Bulk and tapped volumes were determined according to the Ph. Eur., chapter 2.9.34 "Bulk Density and Tapped Density of Powders", with a jolting volumeter (STAV 2003, J. Engelsmann, Germany). Prior to the experiments, the temperature and the RH of each formulation were measured with a thermohygrometer (HygroClip HC2-HP28 equipped with a HygroPalm HP23, Rotronic Instruments, UK). The determinations of the powder properties were repeated four times.

### 3.2.3.   Influence of lubricants on ibuprofen melting

The melting point of IBU and the influence of the lubricants on its melting point were determined by differential scanning calorimetry (DSC) with a DSC 1 (Mettler-Toledo, USA). Plain IBU and IBU together with 0.83 % [w/w] of each lubricant were tested. Samples containing Lubritose$^{TM}$ consisted of IBU and 41.67 % [w/w] Lubritose$^{TM}$ to ensure the same lubricant concentration. The samples (7 mg, n = 5) were heated at scan rates of 3 K/min in aluminum pans under nitrogen atmosphere. The onset of melting was determined using the STAR$^{e}$ evaluation software (Mettler-Toledo, USA).

*3.2.4. Direct compaction on a laboratory scale*

Tableting of formulation 1 was performed in single punch mode on an instrumented rotary tablet press (FETTE 102i, FETTE Compacting, Germany) in an air-conditioned room (21°C and 45 % RH) using round concave punches (FETTE Compacting, Germany) of 10 mm diameter (maximum recommended compaction force of 24.5 kN). The investigated punch tip coatings were chromium nitride (FCG-CRN), titanium nitride (FCG-TIN) and hard chromium (FCG-HCP). Uncoated punches (FCG-U) served as reference. All selected punches were new and unused. The Fill-O-Matic fill shoe was set to 50 rpm and the compaction speed to 30 rpm (dwell time = 21.83 ms). Compaction runs of 27 tablets each were performed. The first and the last tablet of each run were discarded. Tablet weight was set to 310 mg. Compaction force was adjusted to 5 kN, 12 kN and 19 kN, respectively. Each compaction run was performed in triplicate. After each compaction run, the upper and lower punches were removed from the tablet press to collect samples of sticking IBU from the respective punch surfaces. After sampling, each punch was thoroughly cleaned from any remaining formulation residues for following compaction runs.

Additional tableting runs of formulations 1 – 4 were conducted under the same conditions three years after the initial experiments described above. The same punches as from the first experiments were selected except for the fact that over three years the punches were used for various other tableting trials. All punches were equally used for the same amount of compaction runs and mainly for the compaction of IBU formulations. The selection of the punch tip coating and the formulation as well as the adjustment of the compaction force to 5 kN, 12 kN (center point) and 19 kN, respectively, was conducted according to the DoE design described below.

### 3.2.5. Direct compaction on a production scale

The IBU formulation optimized by BASF for direct compaction was tableted on an instrumented production-scale rotary tablet press (FE55, FETTE Compacting, Germany) with 60 punch stations using oblong 18 x 7 mm concave punches (maximum recommended compaction force of 69.1 kN). The investigated punch tip coatings were the same as described above. Compaction speed was set to 60,000 tablets/h (dwell time = 19.96 ms), pre-compaction force to 2 kN and tablet weight to 571 mg. Two compaction runs of 30,000 tablets each were performed. The main compaction force was adjusted to 8 kN or 12 kN, respectively. Because initial tableting runs already caused high sticking, the die table was kept constant at 21 °C by external cooling (ProfiCool Novus PCNO 10, National Lab, Germany), which was confirmed by infrared temperature measurements of the die table.

### 3.2.6. Quantification of ibuprofen sticking

To quantify the amount of sticking API to the punch surface, the stem of the punches was carefully cleaned and sticking IBU was collected by rinsing the surface with 10 ml methanol for HPLC analysis.

For the experiments on a laboratory scale, this procedure was repeated after each compaction run and both the upper and lower punch surfaces were rinsed to quantify the sticking IBU. For the experiments on a production scale, four upper punches per coating were randomly selected after each compaction run. Prior to rinsing the surfaces, photographic images of the four selected punches were taken with a camera (8 megapixel Olympus E-300, Olympus K. K., Japan). However, rather bad images were captured with this camera. Therefore, the camera of the smartphone Samsung Galaxy S6 (16 megapixel Samsung Galaxy S6 camera, Samsung, South Korea), which provided higher quality images, was used to take the tablet tooling images.

The HPLC system (Chromaster, USA) was equipped with a LiChrospher® RP-18e (125 mm length x 4 mm width, 5 µm particle size) column (Merck, Germany). The mobile phase consisted of 60 % acetonitrile and 40 % Milli-Q® water adjusted to pH 2.0 with phosphoric acid. The flow rate was set to 2 ml/min and the injected sample volume was 20 µl. Ultraviolet (UV) detection of IBU was performed at 214 nm. Validation of the HPLC method was conducted in-house. The limit of quantification was 0.01 µg/ml with a signal-to-noise ratio of 12:1 (n = 6). Absorbance was linear in the working concentration range between 0.3 µg/ml and 43 µg/ml ($R^2$ = 0.9998) tested with 5 freshly prepared IBU solutions of different concentrations (n = 3). The specificity was tested with a plain IBU solution (n = 3), IBU solution (n = 3) with the used excipients (matrix) at the same ratio as illustrated in Table 2 with 5 dilutions within the linear concentration range of 0.3 µg/ml and 43 µg/ml and a plain matrix solution. No significant peaks were detected with the plain matrix solution. The recovery of IBU calculated for the investigated concentration range was 99.21 % ± 2.7 % for the plain IBU solution and 100.30 % ± 3.40 % for the IBU solution with excipients (matrix). The variability of the HPLC method was examined with three sets of freshly prepared IBU solutions with added matrix at 5 different dilutions within the concentration range of 0.3 µg/ml and 43 µg/ml. The accuracy was within 95 and 105 %, the precision for all concentrations was less than 3.5 %.

### 3.2.7.  *Characterization of the tablets*

At least 24 h after compaction, tablet disintegration of 6 tablets per compaction run was examined with a disintegration tester (ZT 72, Erweka, Germany) according to the conditions of the Ph. Eur. for uncoated tablets in chapter 07 "Dosage Forms" and subchapter "Tablets". Additional disintegration tests were run using a 0.3 % polysorbate 80 aqueous solution under the same conditions. The crushing strength, diameter and thickness of 5 tablets per compaction run were determined using a hardness tester (TBH 525 WTD, Erweka, Germany). The tablets were weighed (Mettler AT400, Mettler Toledo, USA) before determination of the crushing strength.

Tablet tensile strength was calculated using the Eq. for biconvex tablets published by Pitt et al. [164]:

$$\sigma_f = \frac{10P}{\pi D^2}\left(2.84\frac{t}{D} - 0.126\frac{t}{W} + 3.15\frac{W}{D} + 0.01\right)^{-1} \qquad\qquad \text{(Eq. 4)}$$

where $\sigma_f$ is the tablet tensile strength (N/m²), P the crushing strength (N), D the tablet diameter (m), t the tablet thickness (m) and W the tablet central cylinder thickness (m).

The true density of 3 tablets compacted at 5 kN and 19 kN, respectively, and lubricated with either MS or SSF was determined with a helium pycnometer (AccuPyc 1330, Micromeritics Instrument Corp., USA). The tablet porosity was calculated using the following Eq.:

$$\text{Porosity} = 1 - \text{solid fraction} = 1 - \frac{\text{apparent tablet density}}{\text{true tablet density}} \qquad\qquad \text{(Eq. 5)}$$

## 3.2.8.  Design of Experiments

The statistical and factorial analysis was performed with the Design Expert® software (version 8.0.7.1; Stat-Ease, USA). For laboratory scale tableting of formulations 1 - 4, a D-optimal design was used to analyze the effects of the numerical factor compaction force and the two categorical factors punch tip coating and lubricant. The chosen factor levels for the design can be found in Table 3. A D-optimal design is a response surface method used as a tool for DoE where the computer-generated design is based on the D-optimality criterion to maximize the determinant of the Fisher Information Matrix (X'X) [131,134]. D-optimal designs are commonly used when both categorical and numerical factors have to be combined in the DoE [131,134]. A combination of the point exchange and coordinate exchange algorithm were used to find the optimum design points. As a result, the design included 112 tests consisting of 80 vertex and 32 center points. Up to three different punches with the same coating were used for each compaction run to eliminate systematic errors.

**Table 3:** Categorical and numerical factor levels (12 kN = center point).

| factor | level 1 | level 2 | level 3 | level 4 |
|---|---|---|---|---|
| compaction force (A) | 5 kN | 19 kN | - | - |
| punch tip coating (B) | hard chromium (FCG-HCP) | uncoated (FCG-U) | titanium nitride (FCG-TIN) | chromium nitride (FCG-CRN) |
| lubricant (C) | glyceryl monostearate (GMS) | sodium stearyl fumarate (SSF) | magnesium stearate (MS) | Lubritose™ MCC (Lubritose™) |

Sticking to the upper and the lower punch surfaces, disintegration time and tensile strength were selected as responses. The IBU amount sticking to the punches was quantified after 27 tablets were produced by each punch. Because the first and the last tablet of each run were discarded, 25 tablets per compaction run were gathered

for tablet characterization. From these 25 tablets per compaction run, 6 tablets were randomly chosen for tablet disintegration and 5 for the determination of the tensile strength. The mean of each response was calculated and used as the respective response for each of the 112 design points. The least significant differences (LSD) and the confidence intervals were calculated for the mean predictions.

## 3.3.    Impression molding as a novel technique for the visualization of ibuprofen sticking to tablet punch surfaces (study 2)

### 3.3.1.    *Suitability testing of the molding technique to provide detailed surface impressions*

#### 3.3.1.1. *Molding and surface data acquisition*

Each punch surface was cleaned with methanol and molded using the high-resolution silicone-A dental impression material. After 5 min of curing, the molds were placed and fixed on microtiter plates. Surface measurements of all investigated surfaces were conducted with a high-resolution disk scanning confocal microscope (µsurf custom, NanoFocus, Germany). An objective with a 100 x fold magnification was used to obtain surface data of a 160 µm x 160 µm sample area, an x, y resolution of 0.16 µm and a z resolution of 0.06 µm. All obtained surface images had a maximum vertical displacement range of 25 µm and a minimum of 98 % of recorded surface pixel.

#### 3.3.1.2. *Surface data processing*

All obtained surface data were automatically processed using a template in the µsoft Analysis Premium software (vers. 5.1, NanoFocus; a derivative of MountainsMap® Analysis software by Digital Surf, France) developed for tooth enamel texture analysis. All surface data (Fig. 9 a) obtained from the molds were inverted imprints of the original punches and therefore had to be mirrored in z direction (Fig. 9 b). For the surface data acquired from the original punch surfaces, this step was not necessary. All surfaces were leveled by subtracting the least square plane from the whole surface area (Fig. 9 c) and subsequently denoised using a median filter 5 x 5 pixels (Fig. 9 d). Outliers were removed with a median filter 3 x 3 pixels (Fig. 9 e) and non-recorded points (≤ 2 %) were replaced by the mean of the neighboring points (Fig. 9 f). Form alterations were removed by fitting a second-order polynomial

to the surface area (Fig. 9 g) resulting in the final surface image (Fig. 9 h) which was characterized with 58 3D surface parameters (ISO, ASME, EUR and miscellaneous) (Table 4). The surface parameters of all data sets were normalized to their maximum value and principal component analysis (PCA) was performed using the Unscrambler X software (vers. 10.1, Camo, Norway).
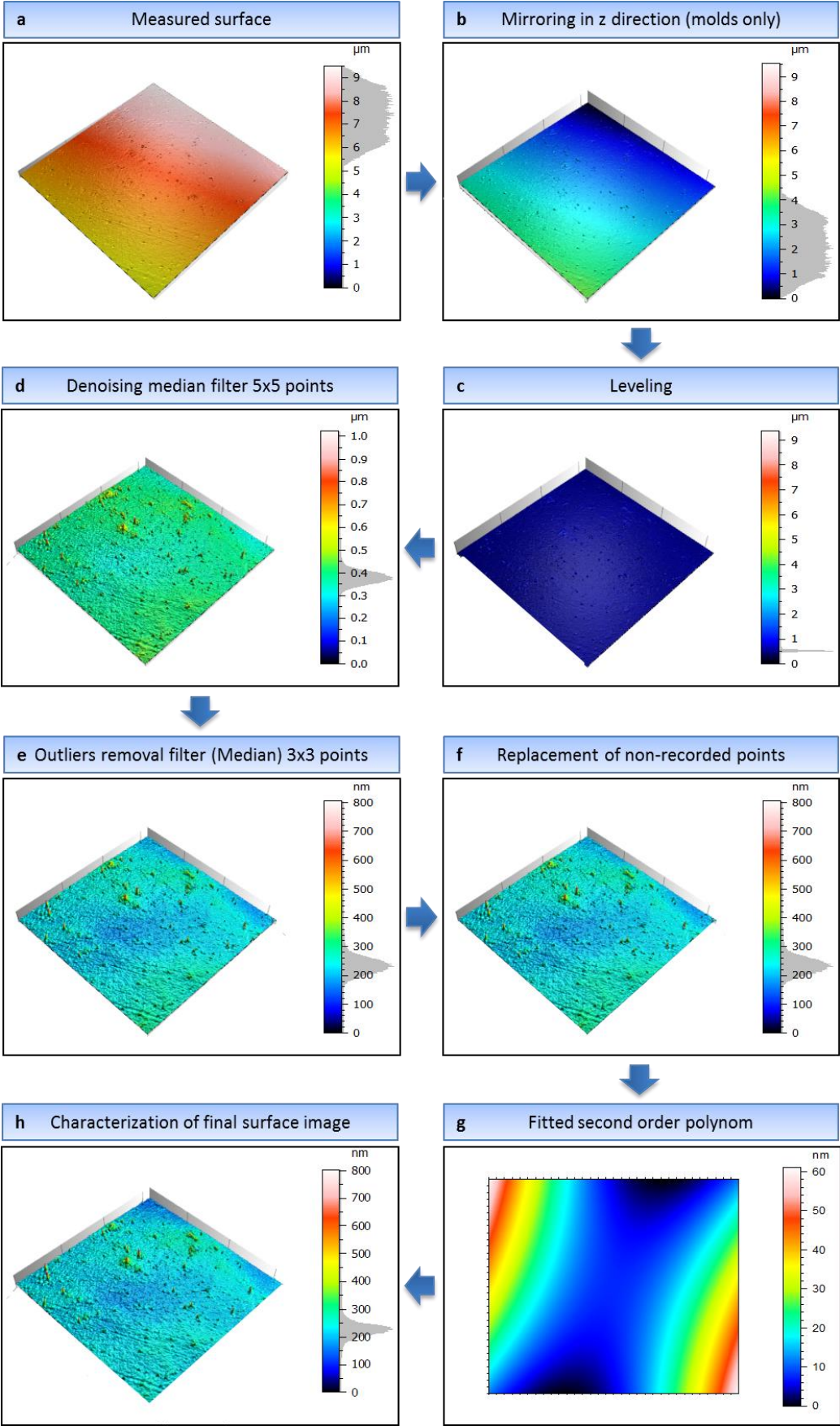
**Fig. 9:** Surface data processing. The image sizes were 160 µm x 160 µm and the height frequency distribution is depicted in grey.

**Table 4:** The 58 standardized surface parameters analyzed in the study.

| Group | Statistical parameter | Abbreviation |
|---|---|---|
| **Amplitude parameters ISO 25178** | Root mean square height | Sq |
| | Skewness | Ssk |
| | Kurtosis | Sku |
| | Maximum peak height | Sp |
| | Maximum pit height | Sv |
| | Maximum height | Sz |
| | Arithmetic mean height | Sa |
| **Functional parameters ISO 25178** | Areal material ratio | Smr (c = 0.1 µm under the mean plane) |
| | Areal material ratio | Smr (c = 0.01 µm under the highest peak) |
| | Inverse areal material ratio | Smc (p = 10 %) |
| | Extreme peak height | Sxp (p = 50 %, q = 97.5 %) |
| **Spatial parameters  ISO 25178** | Auto-correlation length | Sal (s = 0.2) |
| **Hybrid parmaters ISO 25178** | Root mean square gradient | Sdq |
| | Developed interfacial area ratio | Sdr |
| **Functional parameters (volume) ISO 25178** | Material volume | Vm (p = 10 %) |
| | Void volume | Vv (p = 10 %) |
| | Peak material volume | Vmp (p = 10 %) |
| | Core material volume | Vmc (p = 10 %, q = 80 %) |
| | Core void volume | Vvc (p = 10 %, q = 80 %) |
| | Pit void volume | Vvv (p = 80 %) |
| **Feature parameters ISO 25178** | Density of peaks | Spd (pruning = 1 %) |
| | Arithmetic mean peak curvature | Spc (pruning = 1 %) |
| | Ten-point height | S10z (pruning = 1 %) |
| | Five-point peak height | S5p (pruning = 1 %) |
| | Five-point pit height | S5v  (pruning = 1 %) |
| | Mean dale area | Sda  (pruning = 1 %) |
| | Mean hill area | Sha  (pruning = 1 %) |
| | Mean dale volume | Sdv (pruning = 1 %) |
| | Mean hill volume | Shv  (pruning = 1 %) |
| | Peak material portion | Smr1 (unfiltered) |
| | Valley material portion | Smr2 (unfiltered) |
| **Fractal analysis** | Fractal dimension (3D) | Fractal dimension (3D) |
| | Slope | Slope |
| **Isotropy analysis** | Isotropy | Isotropy |
| | 1st direction | 1st direction |
| | 2nd direction | 2nd direction |
| | 3rd direction | 3rd direction |
| **Motif analysis** | Number of motifs | Number of motifs |
| | Mean height | Mean height |
| | Mean area | Mean area |
| | Mean volume | Mean volume |
| **Furrow analysis** | Maximum depth of furrows | Max depth of furrows |
| | Mean depth of furrows | Mean depth of furrows |
| | Mean density of furrows | Mean density of furrows |
| **Hybrid parmaters EUR 15178N** | Summit density | Sds |
| | Mean summit curvature | Ssc |
| | Fractal dimension | Sfd |
| **Functional parameters EUR 15178N** | Inverse areal material ratio | Sdc (p = 10 %, q = 80 %) |
| | Core roughness depth | Sk (Gauß filter, 0.025 mm) |
| | Reduced peak height | Spk (Gauß filter, 0.025 mm) |
| | Reduced valley depth | Svk (Gauß filter, 0.025 mm) |
| | Upper bearing area | Sr1 (Gauß filter, 0.025 mm) |
| | Lower bearing area | Sr2 (Gauß filter, 0.025 mm) |
| **Functional indices EUR 15178N** | Surface bearing index | Sbi |
| | Surface core fluid retention index | Sci |
| | Surface valley fluid retention index | Svi |
| **Other 3D parameters** | Developed area | Sdar |
| **Amplitude parameters ASME B46.1** | Area waviness height | SWt (Gauß filter, 0.025 mm) |

3.3.1.3. *Analysis of punch surfaces*

The method's suitability to provide surface images, which were precise enough to detect even fine differences between different punch surface modifications, had to be verified in a first step. Because tableting punches are too large to fit below the disk scanning confocal microscope, the punches were physically cut close to the barrel-to-tip chamfer to make them shorter. For this purpose, cut punches with six different surface modifications were measured. Uncoated cut punches (FCG-U), roughened uncoated cut punches (FCG-R) as well as cut punches coated with FCG-HCP, FCG-CRN, FCG-TIN, and diamond-like carbon (FCG-DLC) were analyzed. The disk scanning confocal microscope was used for all surface measurements. To examine the impression precision of the molds, surface measurements of both, the cut punches and their respective molds were conducted (Fig. 10). Three non-overlapping areas were measured per punch and respective mold. The surface data processing was conducted as described in section 3.3.1.2. Additionally, a second data processing cycle was analogously performed without applying the filters used in step d and e. As a result, four data sets were obtained: filtered and non-filtered surface data of the original punches and of the molded punches.
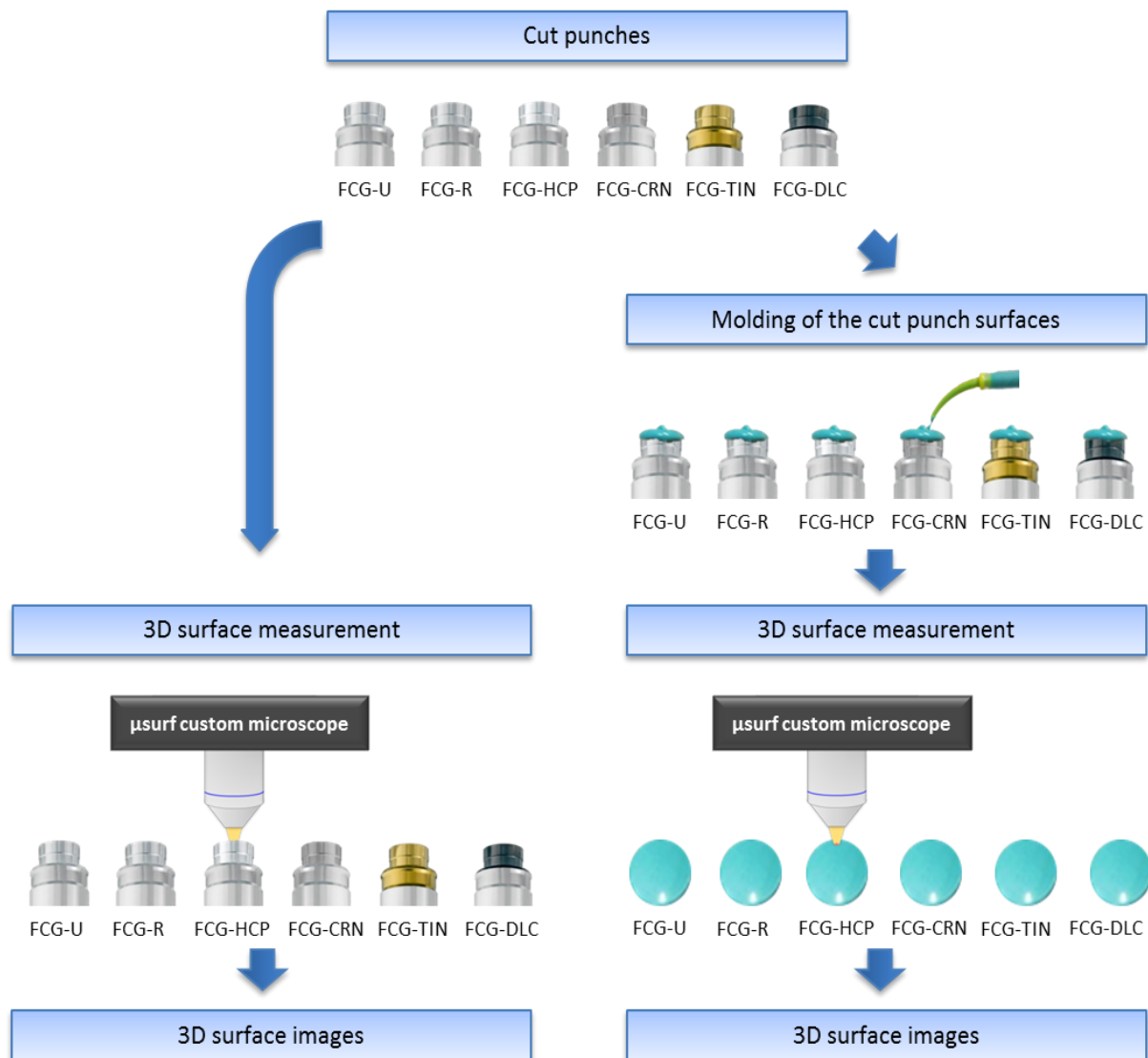
**Fig. 10:** Molding and surface measurement of six differently surface treated cut punches.

### 3.3.2. Suitability testing of the molding technique for the investigation of punch wear

The suitability of the method to detect punch wear was tested in a next step. Therefore, two FCG-TIN punches were selected, which had been used during tablet production of a highly abrasive formulation and had already been discarded because of their worn condition. The two fully-sized, heavily worn FCG-TIN punches were molded, analyzed and compared to the mold of the cut, unused FCG-TIN punch.

*3.3.3.   Evaluation of the sticking behavior to punch surfaces*

3.3.3.1. *Preparation and direct compaction of the powder blend*

All prepared powder blends contained 28.91 % or 48.91 % MCC [w/w], 0.59 % [w/w] MS, 0.50 % [w/w] sieved (315 µm mesh) Aerosil® 200 and 70 % or 50 % [w/w] either sieved (1000 µm mesh) IBU or IBU-Na, respectively, as the API.

The composition of the powder blends to be compacted is displayed in Table 5. All formulation components were mixed in a Turbula blender (T2F equipped with a 2 l container, Willy A. Bachofen, Switzerland) at 72 rpm for 5 min.

**Table 5:** Composition of the investigated powder blends

| Formulation | Dry binder | Lubricant | Glidant | API |
|---|---|---|---|---|
| formulation IBU | Avicel® PH-102 (28.9 % [w/w]) | MS (0.6 % [w/w]) | Aerosil® 200 (0.5 % [w/w]) | IBU (70 % [w/w]) |
| formulation IBU-Na (70 %) | Avicel® PH-102 (28.9 % [w/w]) | MS (0.6 % [w/w]) | Aerosil® 200 (0.5 % [w/w]) | IBU-Na (70 % [w/w]) |
| formulation IBU-Na (50 %) | Avicel® PH-102 (48.9 % [w/w]) | MS (0.6 % [w/w]) | Aerosil® 200 (0.5 % [w/w]) | IBU-Na (50 % [w/w]) |

Prior to tableting, the powder blends were stored in an air-conditioned room at a temperature of 21 °C and a RH of 45 % for at least 72 h. Furthermore, the uniformity of the formulation IBU-Na (50 %) blend was tested by sampling the blend in 4 different locations. The IBU-Na content was determined by solving the samples in Milli-Q® water, filtering and analyzing them with an ultraviolet-visible (UV/VIS) spectrometer (Agilent 8453, USA) at 264 nm wavelength. The resulting mean drug content of 54.54 % with a standard deviation (SD) of 0.71 % was considered acceptable.

Tableting of the powder blends was performed in single punch mode on an instrumented rotary tablet press (FETTE 102i, FETTE Compacting, Germany) in the

same air-conditioned room using round concave punches (FETTE Compacting, Germany) of 10 mm diameter. The Fill-O-Matic fill shoe was set to 50 rpm and the compaction speed to 5 rpm. The compaction force was adjusted to 19 kN. These settings were chosen to reduce the sticking extent of the APIs to a level which allows a distinctive investigation of the punches' surfaces structures leading to sticking. The tablet weight was decided to be 260 mg.

### 3.3.3.2. *Procedure for suitability testing of the molding technique for the visualization of sticking*

The molding method had to be tested for its suitability to visualize sticking residue on the punches in a third step. For this purpose, fully-sized production punches coated with FCG-U, FCG-TIN and FCG-CRN were molded before, after one and after three compaction runs using formulation IBU and IBU-Na (70 %) (Table 5). Before molding, loosely adhering powder was removed from each punch surface with compressed air (6 bar). The respective molds were analyzed using the disk scanning confocal microscope applying the same surface data processing as described in section 3.3.1.2.

### 3.3.3.3. *Analysis of the sticking behavior to punch surfaces*

The sticking behavior of different punch surfaces without the additional influences resulting from the coating material was determined in a next step. Therefore, punches with different surface textures but the same coating material (FCG-CRN) (Table 6) were molded before and after 1, 2, 5, 10 and 25 compaction runs of formulation IBU-Na (50 %) (Table 5). Loosely adhering powder was removed from each punch surface with compressed air (6 bar) before molding. Each compaction run was performed in triplicate. The 50 % formulation was used to prevent excessive sticking and therefore to allow a higher number of compaction runs. Using the disk

scanning confocal microscope, each mold was measured at three different locations: in the center ("center"), 1.6 µm afar from the center ("intermediate") and 3.2 µm afar from the center ("edge") (Fig. 11). All surface data was processed as described in section 3.3.1.2.

**Table 6:** Differently texturized FCG-CRN punches used for evaluation of the sticking behavior.

| Punch | Surface description |
|---|---|
| standard (old) | FCG-CRN standard produced punches. Used over 4 years for laboratory scale IBU and IBU-Na tableting. Smooth surface finish. |
| standard (new) | FCG-CRN standard produced punches. Not used prior to the present study. Smooth surface finish. |
| special | FCG-CRN non-standard punches produced by an alternative manufacturing process. Not used prior to the present study. Smooth surface finish. |
| ceramic blasted | FCG-CRN standard produced punches. Surface roughened prior coating with abrasive blasting using ceramic grit. "Medium" surface roughness. |
| corundum blasted | FCG-CRN standard produced punches. Surface roughened prior coating with abrasive blasting using corundum grit. "Heavy" surface roughness. |
| circular | FCG-CRN standard produced punches. Surface not polished prior coating. Rough, circular texture. |
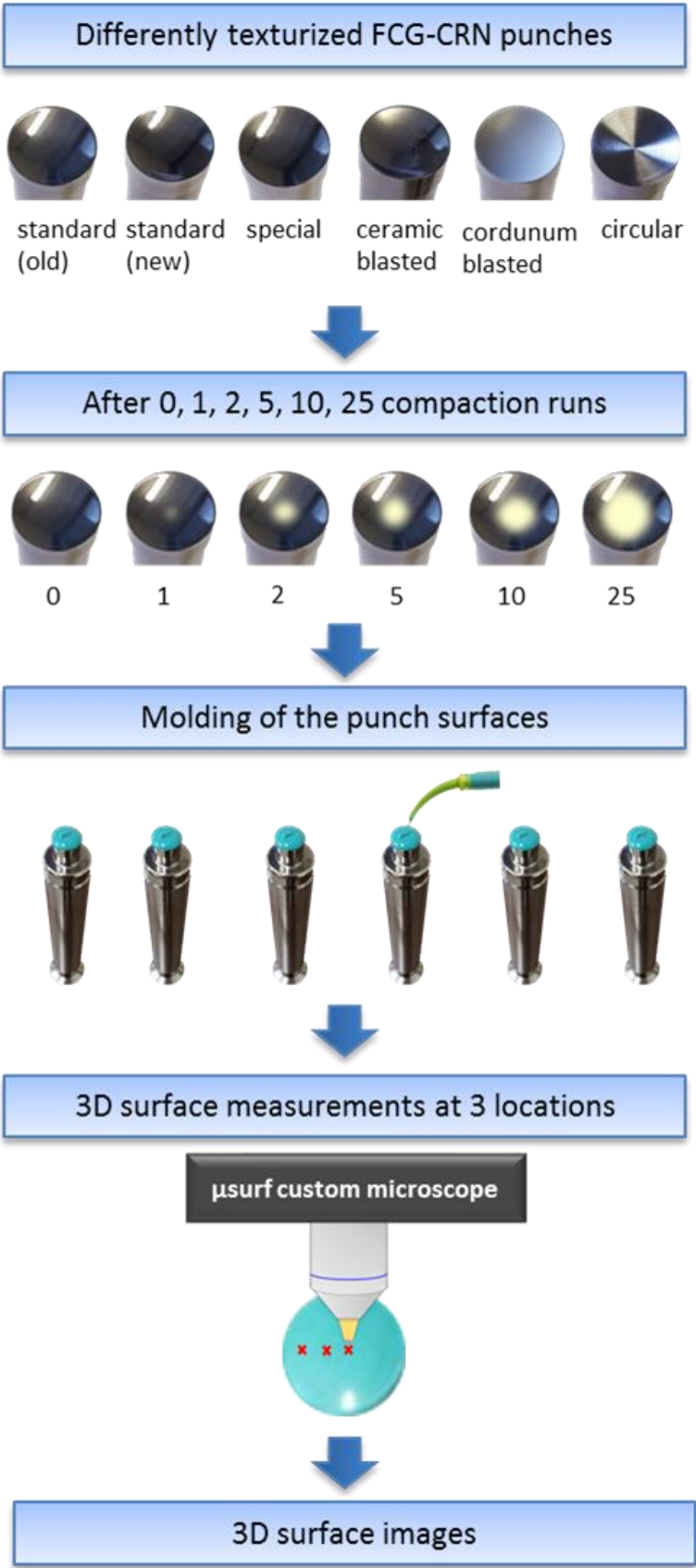
**Fig. 11:** Molding and surface measurement of six differently texturized FCG-CRN punches.

3.3.3.4. *Quantification of API sticking*

After 25 compaction runs, the upper and lower of each differently texturized FCG-CRN punches were removed from the tablet press to collect samples of sticking IBU-Na from the respective punch surfaces. The sticking amount of IBU to the investigated punches was not quantified because the acidic IBU reacted with the impression material. To quantify the amount of sticking IBU-Na to the punch surface, the stem of the punches was carefully cleaned and sticking IBU-Na was collected for HPLC analysis by rinsing the punch surface with 4 ml of Milli-Q$^®$ water adjusted to pH 2.0 with phosphoric acid. This 4 ml IBU-Na solution was transferred into a 10 ml volumetric flask. The flask was filled up to 10 ml with 6 ml of acetonitrile. The HPLC system (Chromaster, USA) was equipped with a LiChrospher$^®$ RP-18e column (125 mm length x 4 mm width, 5 µm particle size; Merck, Germany). The mobile phase consisted of 60 % acetonitrile and 40 % Milli-Q$^®$ water adjusted to pH 2.0 with phosphoric acid. The flow rate was set to 2 ml/min and the injected sample volume was 20 µl. Absorbance was linear in the concentration range between 0.3 µg/ml and 40 µg/ml ($R^2$ = 0.9998). UV detection of IBU was performed at 214 nm.

## 3.4.    Sticking tendency of hydrophobic ibuprofen and hydrophilic ibuprofen sodium dihydrate to differently coated tablet punches (study 3)

### 3.4.1.    Methods for the investigation of the sticking behavior of ibuprofen and ibuprofen sodium dihydrate

#### 3.4.1.1. *Design of Experiments*

The statistical and factorial analysis was performed with the Design Expert® software (vs. 8.0.7.1; Stat-Ease, USA). A D-optimal design was used to analyze the effects of the compaction speed, the compaction force and the punch tip coating on the tableting of both, the IBU and the IBU-Na formulations. D-optimal designs are commonly used if both categorical and numerical factors have to be combined in the DoE [131,134]. As a result, each design included 40 design points. To further improve the resulting prediction models, both designs were augmented with 20 additional design points chosen based on the I-optimality criterion. I-optimal designs are commonly used if the response surface has to be modelled with good precision [133,135]. Each resulting augmented design included 60 design points. The point exchange algorithm was used to find the optimum design points. The selected factor levels for the design are based on preliminary tests and can be found in Table 7. A compaction speed of 5 rpm was the minimum adjustable compaction speed of the tablet press. A maximum compaction speed of 55 rpm was chosen because higher speeds caused pronounced capping of the IBU-Na tablets. A minimum compaction force of 5 kN was chosen as the lowest level for the main compaction to ensure that at each design point a mechanically stable tablet was produced. A maximum compaction force of 19 kN was selected as the highest level to cover a design space, which is as large as possible.

The sticking amount of IBU and IBU-Na to the differently coated upper and lower punch tips were chosen as responses. Models for each response of the DoE were

statistically evaluated and chosen based on an analysis of variance (ANOVA). With the ANOVA, the significance of model, the lack of fit, $R^2$, adjusted $R^2$ and predicted $R^2$ were tested. Non-significant model terms were excluded, if they were not required to support factor hierarchy.

**Table 7:** Chosen factor levels for the DoE designs.

| factor | level 1 | level 2 | level 3 | level 4 | level 5 |
|---|---|---|---|---|---|
| compaction speed (A) | 5 rpm | 55 rpm | - | - | - |
| compaction force (B) | 5 kN | 19 kN | - | - | - |
| punch tip coating (C) | chromium nitride (FCG-CRN) | titanium nitride (FCG-TIN) | uncoated (FCG-U) | hard chromium (FCG-HCP) | diamond-like carbon (FCG-DLC) |

3.4.1.2. *Direct compaction of powder blends containing ibuprofen and ibuprofen*

      *sodium dihydrate*

All prepared powder blends contained 28.9 % Avicel® PH-102 [w/w], 0.6 % [w/w] MS, 0.5 % [w/w] sieved Aerosil® 200 (315 µm mesh) and 70 % [w/w] of either sieved IBU or IBU-Na (1000 µm mesh), respectively, as the APIs. All powder blend components were mixed in a Turbula blender (T2F equipped with a 2 l container, Willy A. Bachofen, Switzerland) at 72 rpm for 10 min, sieved (1120 µm mesh) to remove agglomerates and mixed again for additional 15 min. Prior to tableting, the powder blends were stored in an air-conditioned room at a temperature of 21 °C and a RH of 45 % for at least 72 h. In the same air-conditioned room, tableting of the powder blends was performed in single punch mode on an instrumented rotary tablet press (FETTE 102i, FETTE Compacting, Germany) equipped with round concave punches (FETTE Compacting, Germany) of 10 mm diameter. The Fill-O-Matic fill shoe was set to 50 rpm. Tablet weight was decided to be 250 mg. The adjustment of the compaction force as well as the compaction speed and the selection of the punch tip coating was conducted according to the DoE design. Compaction runs of 27 tablets each were performed for each DoE design point. The first and the last tablet of each run were discarded.

### 3.4.1.3. *Quantification of the sticking amount of ibuprofen and ibuprofen sodium dihydrate to the punches*

It is known that the sticking residue to punches is often enriched with the API and may be composed of up to 95 % API [47,49]. The amount of sticking IBU and IBU-Na to the punches was therefore considered as a measure for the amount of sticking residue. After each compaction run both the upper and lower punch surfaces were rinsed to quantify the sticking IBU and IBU-Na amount, respectively.

To quantify the amount of sticking IBU to the punch surfaces, the stem of the punches was carefully cleaned and adhering IBU was collected for HPLC analysis by rinsing the punch surface with 4 ml of acetonitrile. These 4 ml of resulting IBU solution were transferred into a 10 ml volumetric flask. The flask was filled up to 10 ml with additional 2 ml of acetonitrile and 4 ml of Milli-Q® water adjusted to a pH 2.0 with phosphoric acid. In the same manner, sticking IBU-Na was collected by rinsing the punch surface with 4 ml Milli-Q® water adjusted to a pH 2.0 with phosphoric acid. These 4 ml IBU-Na solution were also transferred into a 10 ml volumetric flask, which was filled up to 10 ml with 6 ml of acetonitrile. In both cases, no more adhering residues were visible on the rinsed punch surfaces.

The obtained samples were analyzed with a HPLC system (Chromaster, USA) which was equipped with a LiChrospher® RP-18e column (125 mm length x 4 mm width, 5 µm particle size, Merck, Germany). The mobile phase consisted of 60 % acetonitrile and 40 % Milli-Q® water adjusted to a pH 2.0 with phosphoric acid. The flow rate was set to 2 ml/min and the injected sample volume was 20 µl. UV detection of ibuprofen was performed at 214 nm. Absorbance was linear in the working concentration range between 0.03 µg/ml and 21 µg/ml ($R^2 = 0.9998$).

*3.4.2. Methods for the investigation of the anti-sticking properties of the punch tip coatings*

3.4.2.1. *Adhesive force analysis*

The colloidal probe technique [165–167] was applied to analyze the adhesion force of IBU and IBU-Na particles to the different punch tip coatings. Because tableting punches are too large to fit into the atomic force microscope (AFM), flat round punches, coated with the materials described above, were cut close to the barrel-to-tip chamfer to make them shorter. The spring constants of each used tip-less AFM cantilever (µMash, CSC37 series, Innovative Solutions, Bulgaria) were determined using the thermal method [168]. A single particle of either IBU or IBU-Na, respectively, was glued to these tip-less cantilevers using the method described by Jonat et al. [169]. Force-distance curves of both APIs were recorded in air at 25 °C and 25 % RH in a 8 x 8 grid of measurement points covering a 10 x 10 µm area of each investigated punch. The force-distance measurements were conducted with a JPK NanoWizard® II (JPK Instruments, Germany).

3.4.2.2. *Contact angle analysis*

Contact angles of water, formamide, diiodomethane and molten IBU were measured on the surfaces of the differently coated cut punches described in 3.4.2.1. All measurements were performed fourfold using the sessile drop method (OCA 20, DataPhysics, Germany). A volume of 2 µL of all liquids with the exception of molten IBU were dispensed using the dispense units of the OCA 20. The dispersion component and the polar component as well as the surface free energies of each punch tip coating were calculated using the OWRK method [125,126,128]. To obtain the contact angles of IBU, the API was molten at 80 °C, cooled down to room temperature at which it remained liquid and was dispensed onto the investigated punch surfaces with a micropipette (Eppendorf, Germany). This procedure was not

performed with IBU-Na because of its high melting point and thus the difficult handling.

### 3.4.2.3. *Surface texture analysis*

The surface textures of the fully-sized punches, which had been used for the tableting experiments, were acquired by molding the surfaces with a high-resolution silicone-A dental impression material (Provil® novo light, Heraeus Kulzer, Germany) and subsequent 3D surface measurements (μsurf custom, NanoFocus, Germany). The obtained surface data was processed, characterized with 57 standardized surface parameters and subsequently analyzed by principal component analysis (PCA) using the Unscrambler X software (vs. 10.1, Camo, Norway). The details of this method are described in [170].

## 3.5.    Production-scale tableting of an optimized ibuprofen grade to decrease its sticking tendency (study 4)

### 3.5.1.    Evaluation of the tableting behavior of Ibuprofen DC 85 W

The tableting behavior of Ibuprofen DC 85 W on a production scale rotary tablet press (FE55, FETTE Compacting, Germany) with three compaction stations (first station: pre-compaction, second station: intermediate compaction and third station: main compaction) was analyzed with a DoE approach. The influence of a pre compaction, intermediate compaction and main compaction force on the two tablet properties crushing strength and tablet disintegration time was evaluated.

#### 3.5.1.1. *Design of Experiments*

Statistical and factorial analysis was performed with Design Expert® software (vs. 8.0.7.1; Stat-Ease, USA). An I-optimal design was used to analyze the effects of the three compaction forces (pre-compaction, intermediate compaction, and main compaction). An I-optimal design is a response surface method used as a tool for DoE where the computer-generated design is based on the I-optimality criterion to minimize the integral of the prediction variance across the design space [135,137]. From the two available exchange algorithms (coordinate and point exchange), the point exchange algorithm was selected because this algorithm allows one to find the optimum design points from a predetermined set of candidate points. Selected possible candidate points were vertices, centers of edges, constraint plane centroids, axial check points and the overall center points. As a result, the design included 35 design points, which were arranged in two blocks. The chosen factor levels for the design were based on preliminary tests and can be found in Table 8. The compaction force of 5 kN was chosen as the lowest factor level for the main compaction force to ensure that at each design point a mechanically stable and sufficiently strong tablet would be produced. The compaction force of 11 kN was selected as the highest

factor level because even higher compaction forces did not result in a pronounced increase of the crushing strength. The same maximum value for all three compaction forces were chosen to allow a full analysis of all possible compaction force combinations and their effect on the chosen responses, as conflicting results have been found in the literature with higher pre- or main compaction forces, respectively.

The tablet disintegration time and the crushing strength were selected as responses. For each design point, 6 tablets were randomly chosen for tablet disintegration and 20 for the determination of the crushing strength. The mean value of each response was calculated and used as the respective response for each of the 35 design points.

Models for each response of the DoE were chosen and statistically evaluated based on an ANOVA. The ANOVA was tested for significance of model, lack of fit, $R^2$, adjusted $R^2$ and predicted $R^2$. Non-significant model terms ($p < 0.05$) were excluded, if they were not required to support hierarchy. For model validation, 12 additional tableting runs were conducted at different factor levels than those used to calculate the models.

**Table 8:** Chosen factor levels for the DoE design.

| factor | low level | high level |
|---|---|---|
| standard pre-compaction force (A) | 0 kN | 11 kN |
| addional intermediate compaction force (B) | 0 kN | 11 kN |
| standard main compaction force (C) | 5 kN | 11 kN |

### 3.5.1.2. *Direct compaction of Ibuprofen DC 85 W*

Ibuprofen DC 85 W was tableted with the instrumented production-scale rotary tablet press equipped with 60 punch stations using oblong (18 mm x 7 mm) concave uncoated punches. The compaction speed was set to 100,000 tablets/h and the tablet mass to 471 mg. The compaction forces were chosen according to the DoE design. After the compaction forces achieved low relative standard deviations (≤ 7 %), tableting was conducted for approximately 10 min for each design point. As the compaction forces were remained constant, this time period for data collection was considered sufficiently long, especially regarding the comparability and the feasibility of an experimental design including the 35 design points.

The tablet disintegration time of 6 tablets per design point was determined with a disintegration tester (ZT 72, Erweka, Germany) according to the conditions of the Ph. Eur. for uncoated tablets. The tablet mass and the crushing strength of 20 tablets each were determined at different time points with a tablet tester (Checkmaster 4.1, FETTE Compacting, Germany) throughout the whole tableting run. Subsequently, the mean and the standard deviation of all samples per tableting run were calculated.

## 3.5.2.  *Evaluation of the sticking behavior of Ibuprofen DC 85 W*

The sticking tendency of Ibuprofen DC 85 W was evaluated by long term tableting runs (2 h) and subsequent quantification of the sticking ibuprofen residue on the punch tip surfaces of differently coated punches. Furthermore, the sticking amount of Ibuprofen DC 85 W was compared to the sticking amount of the two other ibuprofen formulations (A and B) optimized for direct compaction.

### 3.5.2.1. *Direct compaction of the ibuprofen formulations*

Tableting of all three ibuprofen formulations was conducted on an instrumented production-scale rotary tablet press (FE55, FETTE Compacting, Germany) with 60 punch stations using differently coated oblong (18 mm x 7 mm) concave punches. The selected punch coatings are shown in Table 9.

**Table 9:** Selected punch tip coatings.

| Coating | Abbreviation | Number of punches assambled |
|---|---|---|
| Chromium nitride multilayer with an oxide toplayer | FCG-CR+ | 8 |
| Chromium nitride | FCG-CRN | 9 |
| Hard chromium | FCG-HCP | 8 |
| Titanium nitride | FCG-TIN | 9 |
| Titanium aluminium nitride | FCG-TAN | 9 |
| Physical Vapor Deposition Chromium | FCG-PCR | 9 |
| Uncoated | FCG-U | 8 |

Ibuprofen DC 85 W  was  compacted  at  the  following  conditions  (Table  10):  a pre-compaction force of 3 kN, main compaction force of 8 kN, a compaction speed of 120,000 tablets/h and a run time of 2 h, resulting in 4000 compaction events per punch. The tablet strength was approximately 80 N and the tablet mass was set to 471 mg, which corresponds to a 400 mg ibuprofen dose. The die table temperature

was measured by an infrared sensor. It was 22 °C before starting the tableting runs, increased to 28 °C after 1 h and to 31 °C after 2 h of tableting.

The ibuprofen formulation A was compacted with a target tablet mass of 571 mg, again corresponding to a 400 mg ibuprofen dose as well (Table 10). Except for tablet mass, the same tableting settings as described for Ibuprofen DC 85 W were chosen. However, tableting had to be stopped after approximately 500 produced tablets because of a high amount of sticking ibuprofen to some punches. As a consequence, the compaction speed had to be reduced to 60,000 tablets/h to reduce sticking. A main compaction force of 8 kN was still applied, however, to reduce the contact time between the punches and the formulation, no pre-compaction performed. The die table was cooled to 22 °C with the internal vortex cooling system of the tablet press. Tableting was conducted for 2 h, resulting in 2000 compaction events per punch.

To assess the influence of the additional (intermediate) compaction force on ibuprofen sticking, the ibuprofen formulation B was compacted in two compaction runs with a target tablet mass of 571 mg, again corresponding to 400 mg ibuprofen (Table 10). During both runs, the compaction speed was set to 60,000 tablets/h, a main compaction force of 8 kN was applied and the die table was cooled to 21 °C by the internal vortex cooling as well as by an external cooling system (ProfiCool Novus PCNO 10, National Lab, Germany). The first compaction run was conducted for 30 min and a pre-compaction force of 2 kN was applied. In the second compaction run, tableting was conducted for 50 min with a pre-compaction force of 1 kN and an intermediate compaction force of 3 kN.

**Table 10:** Selected tableting settings for the investigation of ibuprofen sticking.

| Formulation | Tablet mass | Compaction speed | Run time | Pre-compaction force | Intermediate compaction force | Main compaction force | Cooling |
|---|---|---|---|---|---|---|---|
| Ibuprofen DC 85 W | 471 mg | 120,000 tablets/h | 2 h | 3 kN | 0 kN | 8 kN | no |
| Ibuprofen formulation A | 571 mg | 60,000 tablets/h | 2 h | 0 kN | 0 kN | 8 kN | internal |
| Ibuprofen formulation B | 571 mg | 60,000 tablets/h | 30 min | 2 kN | 0 kN | 8 kN | internal and external |
| Ibuprofen formulation B | 571 mg | 60,000 tablets/h | 50 min | 1 kN | 3 kN | 8 kN | internal and external |

### 3.5.2.2. *Quantification of ibuprofen sticking*

It is known that the sticking residue on punches is often enriched with the API if the excipients are less adherent and may be composed of up to 95 % API [47,49]. The amount of sticking ibuprofen to the punches was therefore considered a measure for sticking residue. To quantify the amount of sticking ibuprofen to the punch surfaces, the body of the punches were carefully cleaned and any residual ibuprofen was collected by rinsing the surface with 10 ml of methanol for HPLC analysis.

After the compaction of Ibuprofen DC 85 W, four upper and four lower punches from each punch tip coating were randomly selected and both the upper and lower punch surfaces were rinsed to quantify the sticking ibuprofen. After the compaction of the ibuprofen formulations A and B, four upper punches per coating were randomly selected after the respective compaction runs. Prior to rinsing the surfaces, photographic images of the four selected upper punches were taken with a digital camera (16 megapixel Samsung Galaxy S6 camera, Samsung, South Korea).

The HPLC system (Chromaster, USA) was equipped with a LiChrospher® RP-18e column (125 mm length x 4 mm width, 5 µm particle size, Merck, Germany). The

mobile phase consisted of 60 % acetonitrile and 40 % Milli-Q® water adjusted to pH 2.0 with phosphoric acid. The flow rate was set to 2 ml/min and the injected sample volume was 20 µl. UV detection of ibuprofen was performed at 214 nm. Absorbance was linear in the working concentration range between 0.3 µg/ml and 43 µg/ml ($R^2$ = 0.9998).

# 4. Results and Discussion

## 4.1. Factors influencing the sticking tendency of ibuprofen during direct compaction (study 1)

### 4.1.1. Bulk density and flow properties of the differently lubricated powder blends

The measured properties of the powder formulations were similar to each other (Fig. 12). The maximum difference between the bulk density means of each formulation was 0.046 g/ml (difference between formulation 1 and 4). The Hausner ratios varied between the Ph. Eur. classifications of "good" (1.12 - 1.18) and "fair" (1.19 - 1.25) and therefore fulfilled the requirements for direct compaction. The flow rate was similar with all formulations and, according to the Ph. Eur. classification, the angles of repose indicated "good" to "excellent" flow properties. The different formulations were therefore considered to be suitable for direct compaction and to be comparable to each other with regard to the compaction-relevant properties.
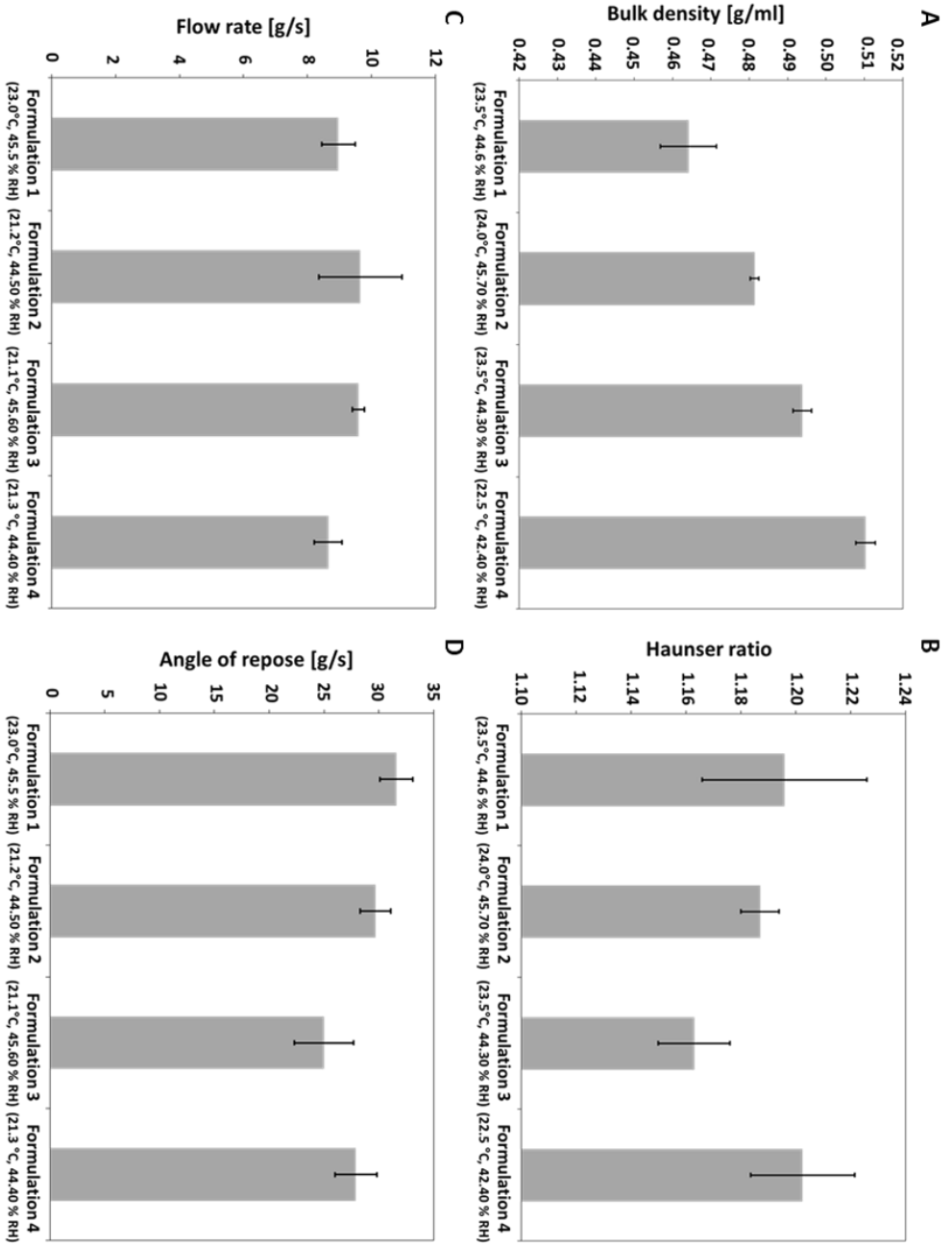
**Fig. 12:** (A) Bulk density, (B) Hausner ratio, (C) flow rate and (D) angle of repose for each laboratory-scale formulation at the respective bulk temperature and RH (means ± SD, n = 4).

## 4.1.2.  *Influence of lubricants on ibuprofen melting*

The results of the DSC measurements are depicted in Fig. 13. The mean melting point of plain IBU was 76.18 °C as expected for racemic IBU [171]. The melting point of IBU was reduced when mixed the lubricants and the extent of melting point reduction was similar for all lubricants. IBU is known to form low-melting eutectic mixtures with stearate lubricants such as MS, calcium stearate, stearic acid and stearyl alcohol [75] which may lead to an increased sticking tendency [76]. Therefore, it is assumed that MS, GMS and SSF also reduced the melting point of IBU due to the formation of an eutectic mixture. The co-processing procedure of GMS with MCC in Lubritose$^{TM}$ did not significantly affect the melting point reduction of IBU caused by GMS.
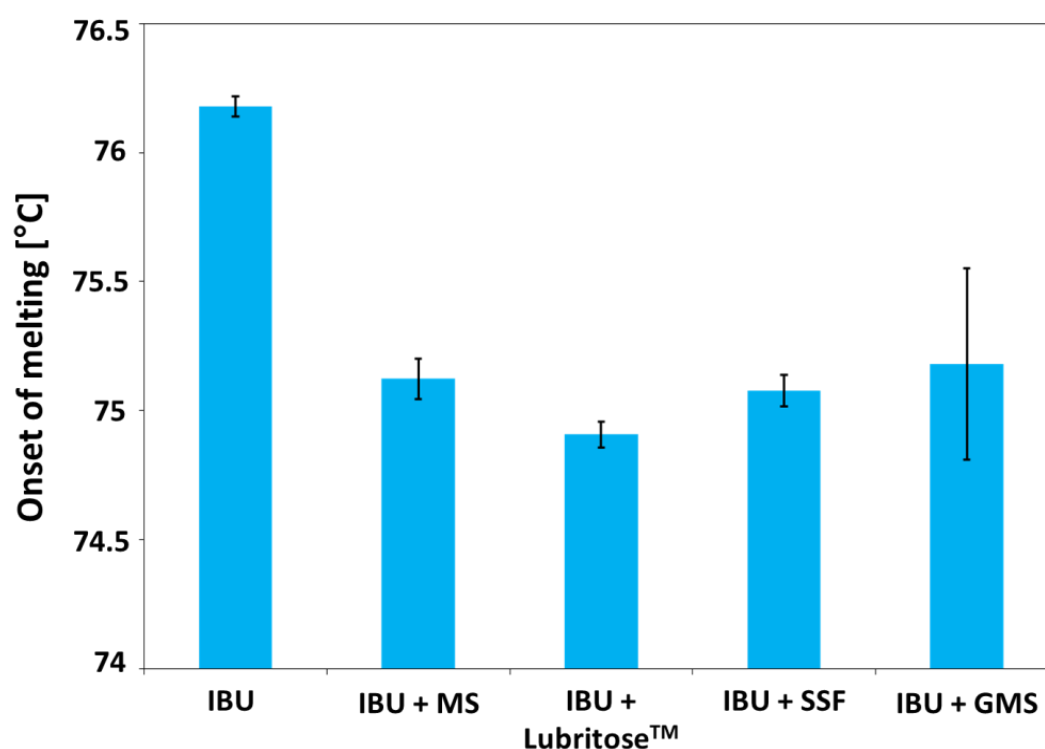


**Fig. 13:** Onset of melting of plain IBU and IBU together with 0.83 % [w/w] of each lubricant (means ± SD, n = 5)

## 4.1.3. Design of Experiments Model Evaluation

Models for each response of the DoE were statistically evaluated and chosen based on an ANOVA. The ANOVA was tested for significance of model, lack of fit, R², adjusted R² and predicted R². Non-significant model terms were excluded. Additionally, power transformations of the data were conducted according to the Box-Cox plot recommendation. If data transformation had to be carried out according to this recommendation, the ANOVA of the resulting model was tested again as described above. The ANOVA of the final response models are presented in Table 11.

**Table 11:** ANOVA of the DoE models based on the Box-Cox plot recommendation

| Model | Sticking to the upper punch | Sticking to the lower punch | Disintegration time | Tensile strength |
|---|---|---|---|---|
| | p-value | p-value | p-value | p-value |
| **Transformation** | Square root | Natural logarithm | Natural logarithm | None |
| **Model** | Significant | Significant | Significant | Significant |
| **Compaction force (A)** | 0.0001 | 0.0001 | 0.0001 | 0.0019 |
| **Punch tip coating (B)** | 0.0001 | 0.0001 | Non-significant | 0.0009 |
| **Lubricant (C)** | 0.0038 | 0.0001 | 0.0001 | 0.0008 |
| **Interaction AB** | 0.0001 | 0.0001 | Non-significant | Non-significant |
| **Interaction AC** | Non-significant | Non-significant | 0.0001 | Non-significant |
| **Interaction BC** | 0.032 | 0.0136 | Non-significant | Non-significant |
| **A²** | Non-significant | Non-significant | 0.0001 | 0.0001 |
| | | | | |
| **Lack of fit** | Non-significant | Significant | Non-significant | Non-significant |
| **R²** | 0.9230 | 0.9265 | 0.9482 | 0.4359 |
| **Adjusted R²** | 0.9071 | 0.9113 | 0.9442 | 0.3921 |
| **Predicted R²** | 0.8866 | 0.8916 | 0.9382 | 0.3336 |
| **Adequate precision** | 26.238 | 31.508 | 48.806 | 13.025 |

## 4.1.4.  Influence of the selected factors on ibuprofen sticking to the punch tips

The ANOVA of the responses sticking to the upper and lower punch tip revealed a significant model (Table 11). Furthermore, the models had high R², adjusted R² and predicted R² values as well as a high adequate precision value indicating good models for correlation analysis.

The lack of fit was not significant for the response sticking to the upper punch. Therefore, this model could be used for precise predictions as well. However, the lack of fit was significant for sticking to the lower punch indicating that the model did not fit the data sufficiently. This may be due to third-order effects of the factors, which could be detectable with additional experiments. This model is not suitable for precise predictions. However, the other statistical values establish its suitability for detection and explanation of the influences affecting sticking to the lower punch.

Sticking to the upper and lower punch tip depended on all selected factors. A significant two factor interaction was found between the compaction force and punch tip coating (AB) (Fig. 14 A and C). At the lowest compaction force the amount of sticking IBU to the differently coated punches increased in the following order: FCG-CRN < FCG-TIN < FCG-U < FCG-HCP. The FCG-CRN punches had the lowest overall amount of sticking API and no adhering formulation was visibly observed. With increased compaction force, sticking was overall reduced and the differences in the sticking tendency of the coatings were strikingly decreased. It is known that high compaction forces may induce an increase of the temperature during compaction [70], which may locally exceed the melting point of low-melting materials and thus affect the sticking tendency [81]. However, it has also been reported that a temperature increase during compaction may cause an elevated tablet tensile strength [70,172,173]. The reduction in IBU sticking with increased compaction force

has been observed in other studies as well [34,79,82] and has been explained by the increase of cohesion forces within the tablet exceeding the adhesion forces between the tablet and the punch surface [34,81,82]. The results of the present study were therefore explained by the increased cohesion forces within the tablet. These high cohesion forces even exceeded the presumably also increased adhesion forces between tablet and punch surface caused by the elevation of the temperature resulting in localized IBU melting. The amount of sticking IBU to the FCG-CRN punches was not affected by compaction force, which was attributed to extremely low adhesion forces between the FCG-CRN coating and the tablet. Even at the lowest compaction force, the cohesion within the tablet still exceeded the adhesion force of the tablet surface to the FCG-CRN.

Another two factor interaction was detected between the punch tip coating and lubricant (BC) (Fig. 14 B and D). The amount of sticking API was mostly influenced by the selected coating of the punches and the compaction force as described above. However, especially the lower FCG-HCP punches were also affected by the choice of lubricant. The highest amount of sticking was detected for the blend lubricated with Lubritose$^{TM}$, followed by GMS and MS. The blend with SSF as lubricant caused the least amount of sticking. Overall, SSF had the best anti-sticking properties of all examined lubricants. The effect of the lubricants on sticking was less important for the upper punches. This observation is presumably related to the different detachment directions of the tablet from the upper and lower punch. This observation was explained by the following hypothesis: The tablet is detached from the upper punch by the pull up movement of the punch. In this case, the contact time between the tablet and punch surface is relatively short and the lubricant can only reduce adhesion forces on limited spots. In the case of the lower punch, the tablet is slid over the punch surface over an extended time period allowing the lubricant to

reduce friction and adhesion forces over a longer distance. Thus, the anti-adherent effect of the lubricant becomes more apparent with the lower punch. It would be interesting to investigate how an increased tableting speed would influence this effect. Further research to clarify this influence and to explore effects of increased tableting speed should be conducted.
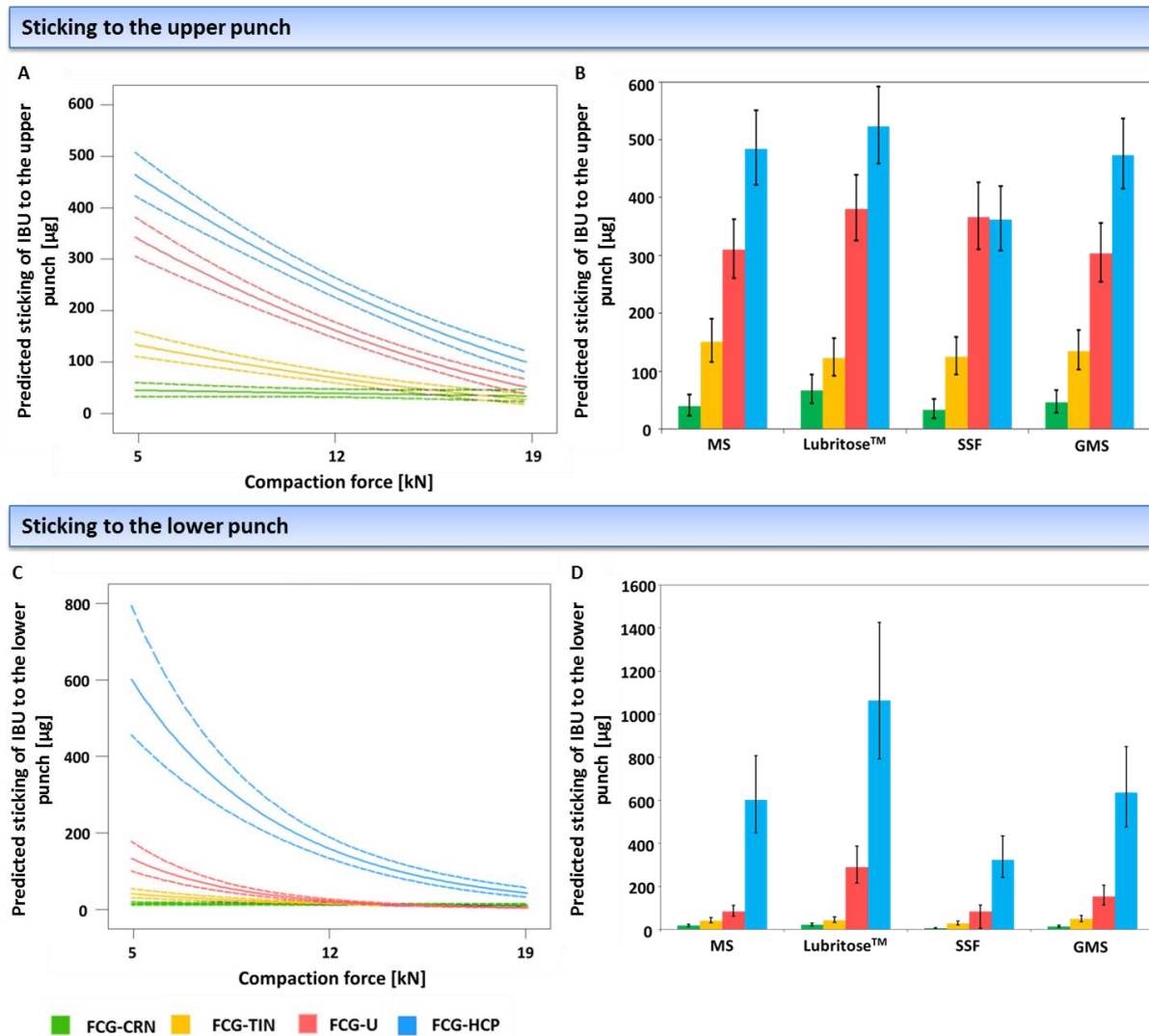


**Fig. 14:** (A, C) Two-factor interaction plots of the factors "compaction force" and "coating material" for the response "sticking IBU to the upper punch" and "sticking IBU to the lower punch", displayed with confidence bands. (B, D) Two-factor interaction plots of the factors "coating material" and "lubricant" at 5 kN compaction force for the response "sticking IBU to the upper punch" and "sticking IBU to the lower punch", displayed with LSD bars.

*4.1.5. Influence of the selected factors on tablet disintegration*

A significant model was detected by the ANOVA for the response "disintegration time" (Table 11). The model fitted the original data well, as the lack of fit was non-significant. Additionally, high R², adjusted R² and predicted R² values as well as a high adequate precision value indicated a good model for correlation and prediction.

The disintegration time depended on the compaction force, selected lubricant and their respective interaction (AC) (Fig. 15 A): The disintegration time increased with increasing compaction force from 5 kN to 12 kN (center point) but decreased again at 19 kN. In general, with increasing compaction force tablet cohesion forces become stronger resulting in prolonged disintegration times [174]. At higher compaction forces, however, elastic deformation of the powder during compaction increases while plastic deformation remains almost constant. As a result, tablets compacted at high compaction forces exhibit a higher elastic recovery. It is assumed that the bonding forces within the tablets compacted at 19 kN and consequently their disintegration times were reduced by this effect [175].

The disintegration time was also highly influenced by the added lubricant. The addition of lubricants to a tablet formulation is known to potentially prolong the tablet disintegration time due to an increase in tablet hydrophobicity [174]. In the present study, the disintegration time was increased by the selected lubricants in the following order: MS < Lubritose$^{TM}$ < SSF < GMS. Only at the lowest compaction force, the disintegration time of the formulations containing GMS and SSF were similar.
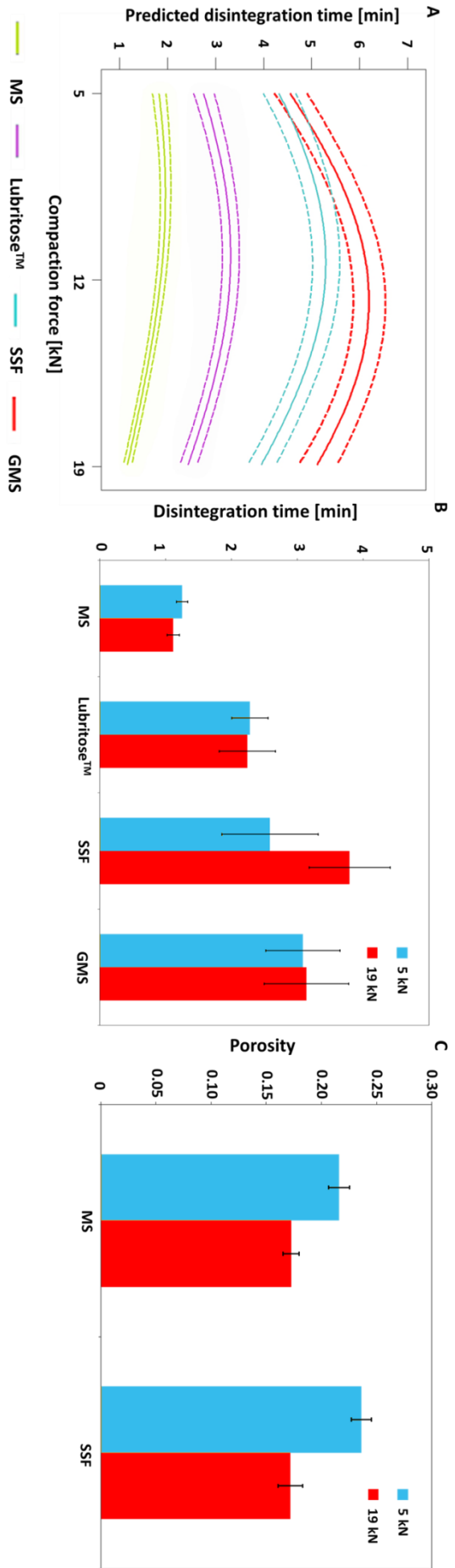
**Fig. 15:** (A) Two-factor interaction plot of the factors "compaction force" and "lubricant" on the response "disintegration time" displayed with confidence bands. (B) The disintegration time of tablets compacted at 5 kN and 19 kN, respectively, in 0.3 % polysorbate 80 solution (means ± SD, n = 6). (C) The porosity of tablets lubricated with either MS or SSF compacted at 5 kN and 19 kN, respectively (means ± SD, n = 3).

Interestingly, tablets lubricated with the co-processed Lubritose[TM] disintegrated faster than tablets lubricated with the physical mixture of MCC and GMS. In the study by Mužíková and Muchová, the disintegration times of plain Lubritose[TM] tablets were compared to tablets produced from the physical mixture of MCC and GMS without any other ingredients [78]. In contrast to the findings in the present study, Mužíková and Muchová reported only minor differences in the disintegration times between the two formulations. However, the mixing time for the powder blends was only 2.5 min and tablets were produced with a texture analyzer without a filling device. The differences in the disintegration times between the IBU containing MCC/GMS formulations in the present study can be explained by the longer blending time and the additional mixing by the paddle movements of the Fill-O-Matic. Previous studies have already shown that lubricants can extend the disintegration time with prolonged blending [68,74,174,176]. Unlike its physical mixture, the co-processed Lubritose[TM] is insensitive to the mixing time and therefore, disintegration is not prolonged with these tablets.

The results of the tablets lubricated with MS and SSF were surprising because SSF is known as an excellent lubricant leading to lower disintegration times in comparison to MS because of its lower hydrophobicity and lesser mixing sensitivity [78,177–179]. It was therefore assumed that the lubricants interacted with the IBU in the formulation. Yet, no distinguishing interaction between IBU and the selected lubricants could be detected by the DSC analysis. However, IBU is known to be very hydrophobic [65,66,142]. It is therefore assumed that the high IBU content of the tablets masked the water-repelling effect of the added lubricant and led to disintegration times independent of the hydrophobicity of the lubricants. Thus, other factors than wettability may have influenced the differences in the disintegration times of these tablets such as porosity, swelling or moisture absorption [174]. To verify this

hypothesis, additional disintegration tests were run with a 0.3 % surfactant solution as disintegration medium (Fig. 15 B). The tablets chosen for these additional experiments were compacted at the lowest (5 kN) and the highest (19 kN) level of the factor "compaction force" to cover the whole range of the design space. The role of the added surfactant was to prevent differences in the wettability resulting from the differently lubricated tablets. Thus, possible differences in the disintegration times must be caused by other factors. The reduction of the surface tension of water by the surfactant caused an overall decrease in the disintegration times of all tablets, especially if GMS and SSF were used as lubricants. Still, the order of the disintegration times in the surfactant-containing medium was the same as in plain water. This supports the hypothesis that other factors than wettability are likely to influence the disintegration of tablets containing a high IBU amount. Furthermore, the influence of the tablet porosity was determined using the tablets lubricated with MS and SSF, respectively, because the results of the disintegration time experiments were unexpected (Fig. 15 C). However, no correlation between the disintegration times and the porosity was observed. Further studies should be conducted to understand the underlying mechanisms leading to these unexpected results.

The disintegration time of tablets may give further insight into the cohesion forces and excipient interaction in a tablet, which may be helpful to understand the mechanisms of tablet sticking. However, no direct correlation between the disintegration time and tablet sticking could be derived from the present data.

## 4.1.6. Influence of the selected design factors on tablet tensile strength

For the response "tablet tensile strength" a significant model was identified by the ANOVA (Table 11). The lack of fit was non-significant, indicating a sufficient fit of the model with the original data. The $R^2$, adjusted $R^2$ and predicted $R^2$ values as well as the adequate precision are sufficient, but higher values would have been desirable. These values indicate that additional factors, which were not included in the model, might have had an influence on the tensile strength.

All selected factors (compaction force, punch tip coating and lubricant) had a significant influence on the tensile strength. No two-factor interactions were detected for the response "tablet tensile strength". The tensile strength of all tablets was above 1.8 N/m², indicating a sufficient mechanical strength of the tablets (Fig. 16). Similar to the disintegration time, the tensile strength increased with the compaction force from 5 kN to 12 kN and decreased at compaction forces up to 19 kN (Fig. 16 A). This behavior has already been described for IBU tablets and is associated with a higher elastic recovery of the tablets at high compaction forces [142,180]. The coating of the punches also had an influence on the tensile strength (Fig. 16 B). This might be caused by minor differences in the lengths of the punches resulting in slightly higher tablet weights and thus compaction forces. To examine this presumption, the weights of the tablets resulting from each compaction run (n = 5 per compaction run) were evaluated by the DoE but no correlation to the punch tip coating could be found. The mean tablet weight resulting from all compaction runs was 300.63 mg ± 1.53 mg, n = 560. As a result, no distinct reason for the correlation between tensile strength and punch tip coating could be provided. Considering the only slight differences in the tensile strengths and the $R^2$ values of the model, further investigations are needed.
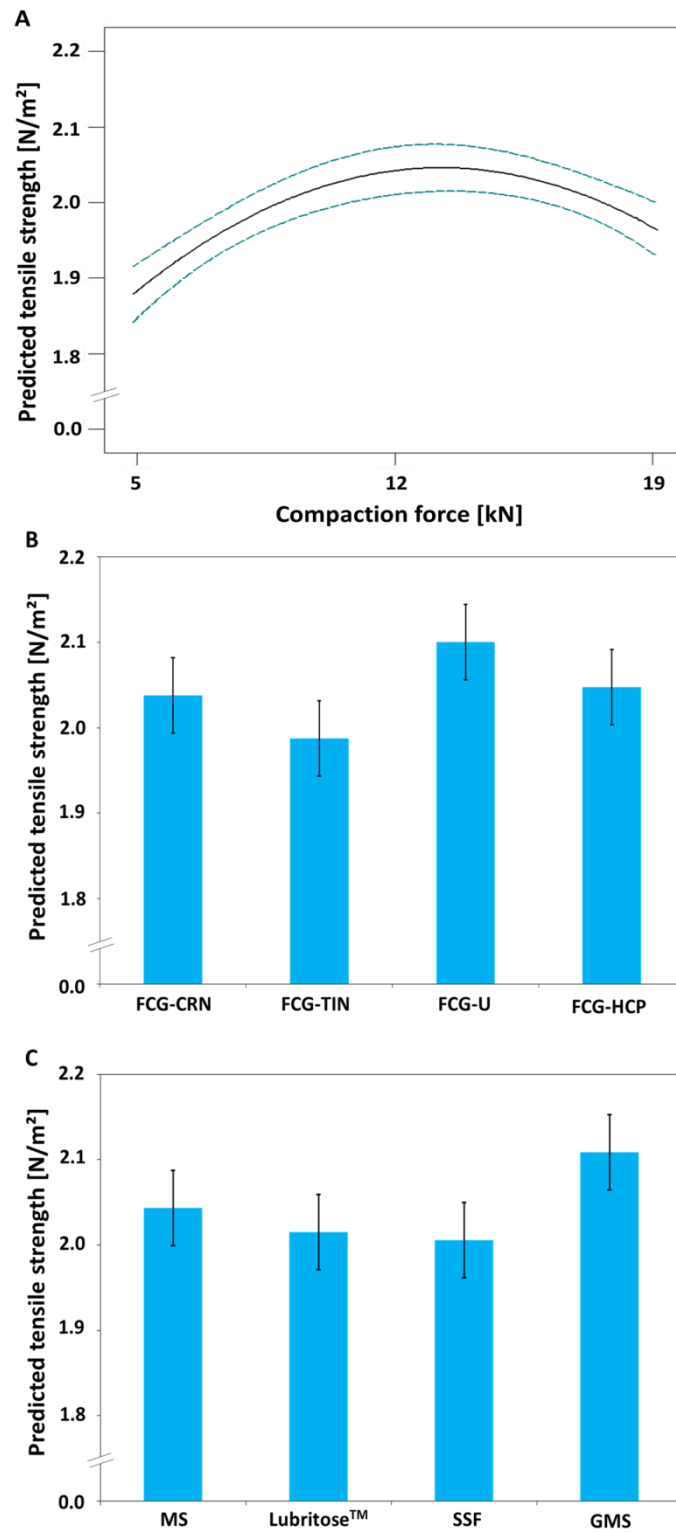
**Fig. 16:** Main effect plots of (A) "compaction force" (predicted tensile strength displayed with confidence bands), (B) "punch tip coating" at 5 kN compaction force and (C) "lubricant" at 5 kN for the response "tablet tensile strength" (predicted tensile strength ± LSD bars).

The choice of the added lubricants also affected the tablet tensile strength (Fig. 16 C). Lubricants are known to reduce the mechanical strength of tablets [68]. In the present study, the tablet tensile strength was reduced by SSF, MS and Lubritose$^{TM}$ to a similar extent, while tablets lubricated with GMS led to slightly higher tensile strengths.

The tensile strength is a measure for the mechanical strength of the tablets and may therefore provide reasons for tablet sticking. However, similar to the disintegration time the tensile strength in the present study did not give sufficient information on the sticking of the tablet formulations.

*4.1.7.   Comparison of ibuprofen sticking to unused and used upper and lower*

*punches*

In Fig. 17 the amount of sticking IBU to differently coated unused punches at varying compaction forces is shown in comparison to the amount of sticking IBU to the same punches after three years of usage. For the upper and lower punches, no significant differences in sticking behavior were observed with FCG-HCP and FCG-CRN coatings before and after three years of usage. Over the investigated three years, adhesion of IBU to FCG-HCP remained high and was dependent on the compaction force whereas with FCG-CRN adhesion remained low and independent on the compaction force. The adhesion tendency of IBU to both unused FCG-TIN coated and uncoated (FCG-U) punches was very low and independent of the compaction force. However, over the course of three years the sticking tendency increased with both FCG-TIN and FCG-U punches especially at low compaction forces. The FCG-U punches were particularly sensitive to wear over time as they exhibited remarkably higher API sticking in comparison to their unused state. In contrast to the results in the present study, Roberts et al. found that less sticking occurs to "old" FCG-U punches than to "new" ones [46]. However, the classification "old" or "new" punch was conducted based only on the surface quality of the punches. It remains unclear, if the punches were already of different surface quality when purchased, if they were purchased from different suppliers or if the supplier changed the surface finish method over time.

Different reasons for wear of tablet tooling have been described in the literature [40]. According to this study, the predominant reasons for tablet tooling wear are abrasion and corrosion. Abrasive wear is highly correlated to material hardness. Of the selected coatings, FCG-TIN commonly shows the highest hardness, followed by FCG-CRN and then FCG-HCP [103]. Because FCG-TIN turned out to be more

sensitive to sticking than FCG-CRN over the three years, abrasion is unlikely to be the main cause of the wear phenomenon in this case. Corrosive wear on the other hand is another cause that needs to be considered as the punches were mainly used for tableting of IBU, which is a weak acid that can cause corrosion of steel surfaces. Several studies have shown that FCG-CRN demonstrate a higher corrosive resistance than FCG-TIN most likely due to its denser microstructure [113,116,181]. Therefore, corrosive wear is assumed to be the major cause of increasing sticking to the punches. Consequently, corrosive wear resistance should be a main criterion in the selection of a suitable punch coating for the prevention of sticking. However, further investigations are needed to confirm the causes for these phenomena.

All investigated coatings applied to the upper punches (Fig. 17 A) as well as to the lower punches (Fig. 17 B) showed similar sticking tendencies, while in general sticking was less pronounced with the lower punches. This observation may be result from the strong tangential detachment forces between tablet and lower punch resulting from the momentum of the take-off bar. In contrast, vertical detachment forces between tablet and upper punch resulted only from the vertical withdrawal of the upper punch. In all cases, sticking to the FCG-HCP punches was most pronounced among all coatings.

So far, the present study is the first to compare the performance of the same punches with different coatings after three years of identical usage. The results of the present study revealed that wear of the punches affected sticking negatively. Punch tip coating may reduce these wear phenomena. FCG-CRN coatings displayed the best anti-sticking properties over time.
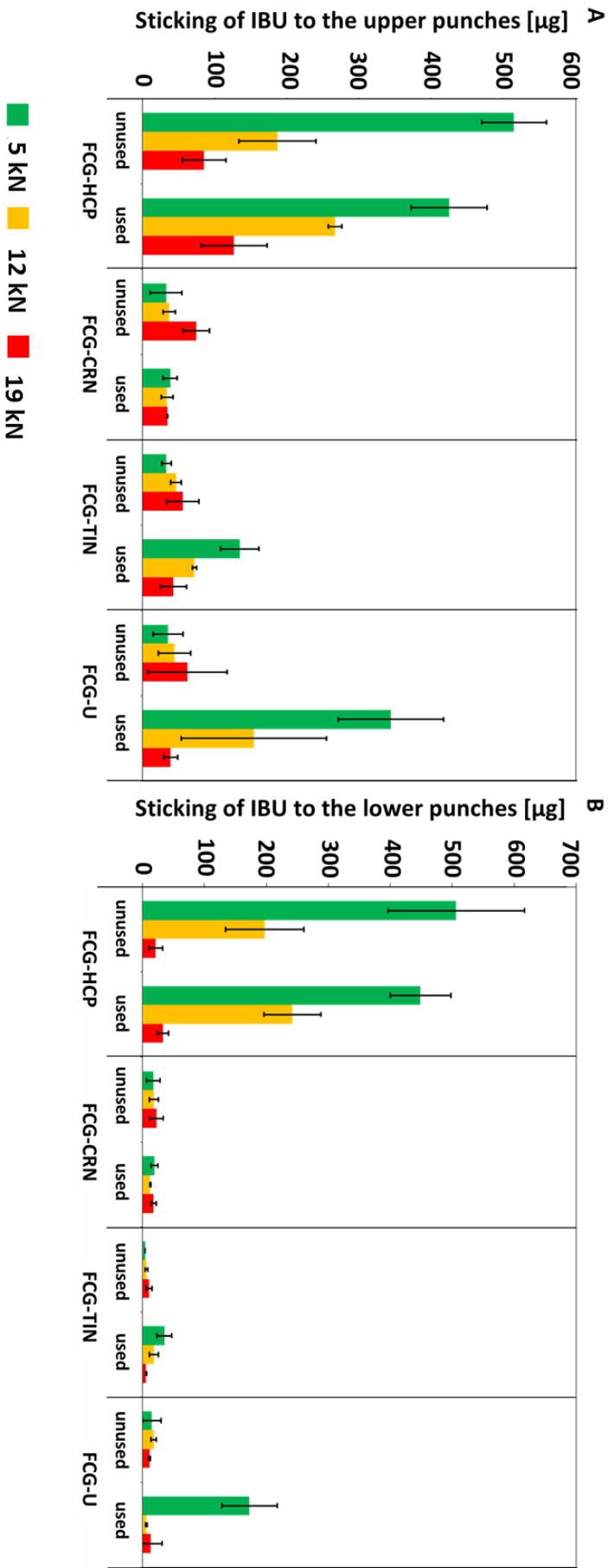
**Fig. 17:** Comparison of the amount of sticking IBU to unused and used, differently coated (A) upper punches and (B) lower punches at 5, 12 and 19 kN compaction force, respectively (means ± SD, n = 3).

*4.1.8.  Comparison of ibuprofen sticking to coated punches on a laboratory vs.*

*production scale*

The results of the sticking experiments on the production rotary press under production conditions (Fig. 18) were similar to the findings under laboratory conditions. The highest amount of sticking IBU was found on FCG-HCP punches at the low main compaction force of 8 kN (Fig. 18 A). The high SD reflects the inhomogeneity of the adhering residues on the FCG-HCP punch surfaces which are depicted in Fig. 18 B. No visible sticking was observed on the other investigated punches, which was confirmed by HPLC analysis where only negligible IBU amounts were detected. An example of punch surfaces with no visible sticking API is shown in Fig. 18 B (FCG-TIN). It should be noted that 500 compression events per punch were recorded and the sticking amount might most likely increase at all punches with a higher number of compaction runs closer to commercial production. In previous studies, it was found that the amount of IBU sticking may reach a plateau after even less than 500 compaction runs [47]. However, the predictability of this plateau may change depending on the API concentration level [145]. The anti-sticking tendencies of the examined punches matched the afore-mentioned laboratory scale examinations performed with unused punches: FCG-U, FCG-TIN coated and FCG-CRN coated punches all exhibited a similar low sticking tendency while FCG-HCP punches showed a high amount of sticking API. At the highest compaction force of 12 kN no sticking was observed with any of the examined punches, which is also consistent with the results of the laboratory scale experiments.
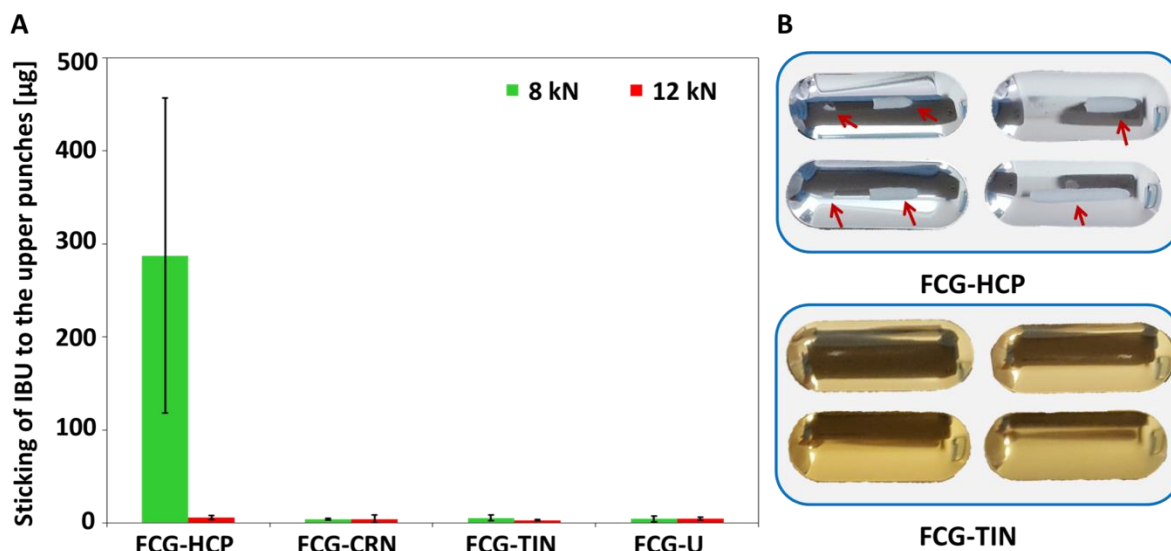
**Fig. 18:** Sticking amount of IBU to differently coated upper punches after tableting on a production rotary press. (A) Amount of sticking IBU to each punch tip coating at 2 kN precompaction force and either 8 kN or 12 kN main compaction force (means ± SD, n = 4). (B) Photos of the 4 selected upper punch tip surfaces of the FCG-HCP and FCG-TIN coated punches after compaction at 8 kN main compaction force; visible adhering IBU stains are marked with an arrow.

It has to be emphasized that the production scale experiments were conducted to investigate if the correlations found on the laboratory scale also apply to the larger production scale. They were not conducted as scale-up experiments and should not be interpreted as such. The production scale experiments were conducted under the following differences in the production conditions, mostly to approximate the real manufacturing conditions as close as possible. The first notable difference was the variable composition of the IBU formulations. The formulation used for the laboratory scale experiments was not optimized with regard to the transferability to larger tableting presses. It was formulated with as little additional excipients as possible to enable an unbiased evaluation of the investigated factors leading to IBU sticking. The only optimization that was performed was the addition of Aerosil® 200 to meet the minimum requirements needed to carry out the laboratory scale experiments. In

contrast, the formulation used for the production scale experiments was optimized by BASF for production scale tableting with additional and non-disclosed excipients. However, as the formulations were both composed mostly of IBU, MCC and MS, they were still chosen for general comparison. Another difference between production scale and laboratory scale tableting was the shape of the selected punches. It is well known that the shape of the punch affects the particle movement in the compact during compaction and consequently the density distribution of the tablet [182–184], which also affects the sticking tendency of IBU tablets [144]. As the density distribution also differs between oblong and round tablets [185], sticking tendency is not comparable between the two different punch shapes either. However, a comparison between the performances of the coatings was possible, because the same coatings were used for each examination. The last difference was the choice of the tableting parameters. The chosen dwell times differed only slightly (laboratory scale: 19.96 ms; production scale: 21.83 ms) but the chosen "low" and "high" compaction forces were significantly different. The selected compaction forces resulted from the different punch shape and the composition of the formulation. A compaction force not less than 8 kN lead to strong enough tablets (hardness: 31 N ± 4 N, n = 10) while higher compaction forces than 12 kN did not result in an increase of the tablet hardness (hardness: 67 N ± 5 N, n = 10).

Despite all the described differences, the data of the production scale experiments still confirmed the outcome of the laboratory scale single-punch examinations. These results suggest that screening investigations of the most suitable punch tip coatings for a specific API formulation may be conducted on a cost-efficient and material-sparing laboratory scale. However, corrosive wear phenomena need to be taken into consideration which can change the performance of the chosen coating dramatically over time as shown in the laboratory scale trials.

## 4.1.9. Conclusion

This study demonstrates that various factors affecting adhesion of ibuprofen to punches can be detected in an economical way with a laboratory scale set-up. However, the results of this work are specific to ibuprofen. Additional studies of APIs with different sticking properties and higher melting points should be conducted in the future for a more profound insight to the reasons leading to sticking. Especially in combination with a design of experiments, several factors and their interactions could be investigated in-depth. It was shown that the main factors affecting ibuprofen sticking are the compaction force and the punch tip coating. Furthermore, an interaction between punch tip coating and selected lubricant was detected which turned out to be more relevant for sticking of ibuprofen to the lower punch tip. Moreover, the selection of the lubricant had a major impact on the disintegration time of the resulting tablets. Surprisingly, the mechanism behind the variation of the disintegration times was not the difference between the wettability of the resulting tablets and needs further investigation. These results may also be obtained under production-scale tableting conditions. Furthermore, it was demonstrated that the application of the appropriate punch tip coating can improve sticking and wear problems simultaneously. Overall, chromium nitride-coated punches provided the best results with regard to these complications and are therefore recommended to be used for overcoming sticking and wear problems during ibuprofen tableting.

## 4.2.    Impression molding as a novel technique for the visualization of ibuprofen sticking to tablet punch surfaces (study 2)

### 4.2.1.    *Suitability of the molding technique for providing detailed surface impressions*

In this study, the suitability of a molding technique to provide a precise and distinguishable imprint of different punch surfaces was evaluated. The resulting surface parameters (Table 4) acquired from the direct measurement of six different cut punches were compared with the respective parameters acquired from the measurement of the respective molds.
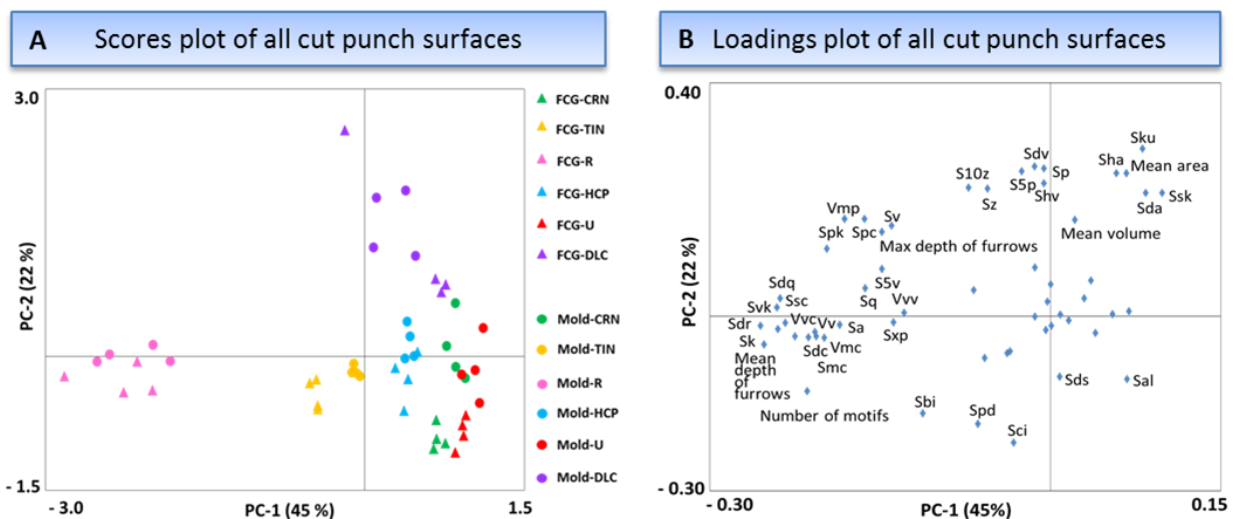


**Fig. 19:** (A) PCA scores plot and (B) loadings plot of the surface data acquired from the direct measurement of the differently coated cut punches and from their respective molds.

Both data sets were processed including all filters described in section 3.3.1.2 and the resulting surface data was evaluated with a PCA. In the PCA scores plot (Fig. 19 A) both, the directly measured punches and their molds, clustered along principal component (PC)-1 and PC-2 according to their respective surface treatment, independent of whether the surface data were acquired by direct measurement or measurement of the mold. The molded surfaces exhibited the tendency to cluster slightly higher -in the direction of PC-2- than the directly measured surfaces. The respective loadings plot was used to interpret the common surface properties of the

clustered punches (Fig. 19 B). The surface parameters of the isotropy group, fractal analysis, sdar, furrow density, both smr parameters, sr1, sr2, smr1, smr2 and svi (Table 4) had a factor loading of lower than 0.1 with both PC-1 and PC-2 and were therefore not considered to be essential for the distinction of the differently treated punch surfaces. The loadings plot revealed that the PC-1 distinguished between surfaces with high (Spk, Smc, Sxp) and comparably rounder (Ssc, Spc) peaks, with steep valleys (Svk, S5v, Sv, max depth of furrows, Sdq), and with an intricate (Sdr, Sk, number of motifs, Sa, Sq, Sdc) and voluminous (Vv, Vvc, Vvv, Vmc, Vmp, Vm) texture. It was concluded that the PC-1 corresponded with the general surface property "roughness". In contrast, PC-2 described surfaces which were relatively flat (Sbi, Sci), with a low peak density (Sds, Spd) but an excess of peaks in comparison to valleys (high Ssk). However, existing peaks and valleys were relatively large (S10z, Sz, mean volume and area of motifs, Sha, Shv, Sda, Sdv, Sp) and the peaks and valley structures are unevenly distributed and irregularly high or deep (low Sal, high Sku) in comparison to the overall surface. It was therefore concluded that PC-2 stands for the "homogeneity" of the surfaces. PC-1 clusters the surfaces in the order of FCG-R > FCG-TIN > FCG-HCP ≈ FCG-DLC > FCG-CRN > FCG-U from "rough" to "smooth" and PC-2 separates "inhomogeneous" from "homogenous" surfaces, mainly separating the FCG-DLC surface from the remaining surfaces. The slight shift of the mold surface data towards PC-2 might be the result of tiny bubbles embedded in the mold, which are unavoidable during molding to a certain extent. The different surfaces could successfully be distinguished and both methods (direct measurement and measurement of the molds) achieved similar results, showing that the molds produce high quality replica of the real surfaces.

Up to this point, all surface data were processed by applying denoising and outlier removing filters as recommended for reflective surface data acquired from non-

contact measurements [186]. In a second data set, no denoising and outlier removal filter was used. With the directly measured data (Fig. 20 A), no distinction between the different punch surfaces was possible without any additional filtering whereas the mold surface data could successfully be distinguished from each other (Fig. 20 B). This observation may be explained by higher interferences resulting from a larger intensity of reflected light on the metallic surfaces of the cut punches. The molds were composed of silicone-A which showed less reflection. As a result, the molded surfaces were less sensitive to filtering.
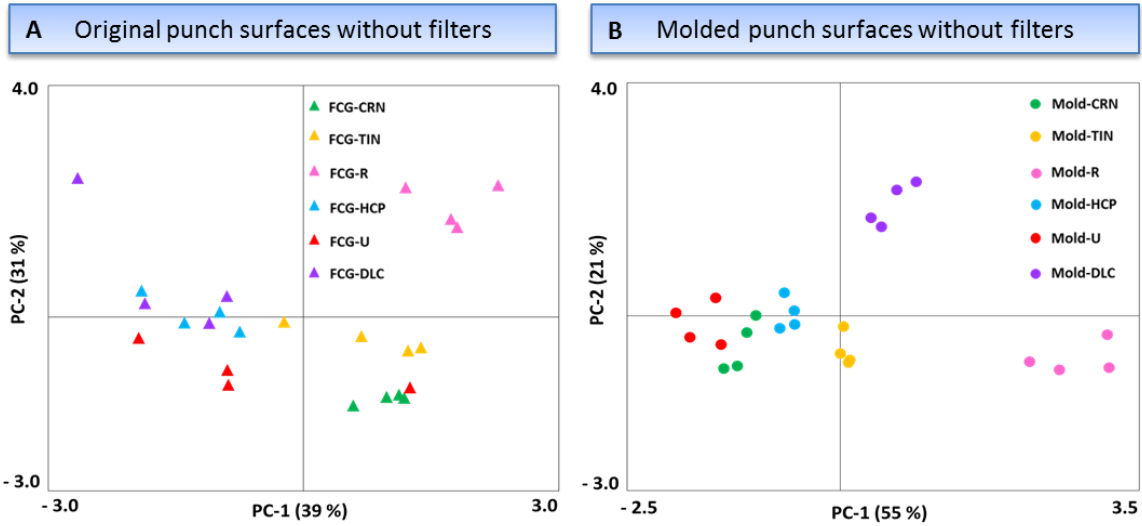


**Fig. 20:** (A) PCA scores plot of the not denoised surface data acquired from the direct and the mold measurement of the differently coated cut punches. (B) PCA scores plot of the unfiltered surface data acquired from the direct and the mold measurement of the differently coated cut punches.

*4.2.2.   Suitability of the molding technique for the investigation of punch wear*

The applicability of the molding technique to identify used and worn surfaces was investigated by molding two different FCG-TIN punches which were used during production-scale tableting of a highly abrasive formulation and had been discarded because of the decreased quality of the resulting tablets. The molded worn punch surfaces were measured at five randomly chosen non-overlapping areas (160 µm x 160 µm). The surface data was pre-processed as described in Fig. 9 without the additional filtering steps 4 and 5. When evaluated in relation to the other punch surfaces with a PCA (Fig. 21 A) it became evident that the worn punches had no common surface parameter which allowed them to be categorized as "worn". Some sampled areas clustered together with the unused molded FCG-TIN coating indicating similar surface quality for these areas. However, other sampled areas of the worn FCG-TIN punches were distributed along the PC-1 in either direction. According to the loadings plot, PC-1 and PC-2 again stood for the surface "roughness" and surface "homogeneity", respectively. As the PC-1 stood for the general "roughness" of the surfaces it was concluded that wear of the FCG-TIN punches may lead to smoothened or roughened areas on the punch surface. The worn punches were not affected by PC-2. Apparently, wear of punches did not affect the "homogeneity" of the measured areas in terms of unevenly distributed irregular high peaks or valleys. It was concluded that the abrasive wear of FCG-TIN punches resulted in inhomogeneous surface areas which had less common surface parameter values and therefore showed a decreased tendency to cluster in a PCA, where a strict surface classification is needed.
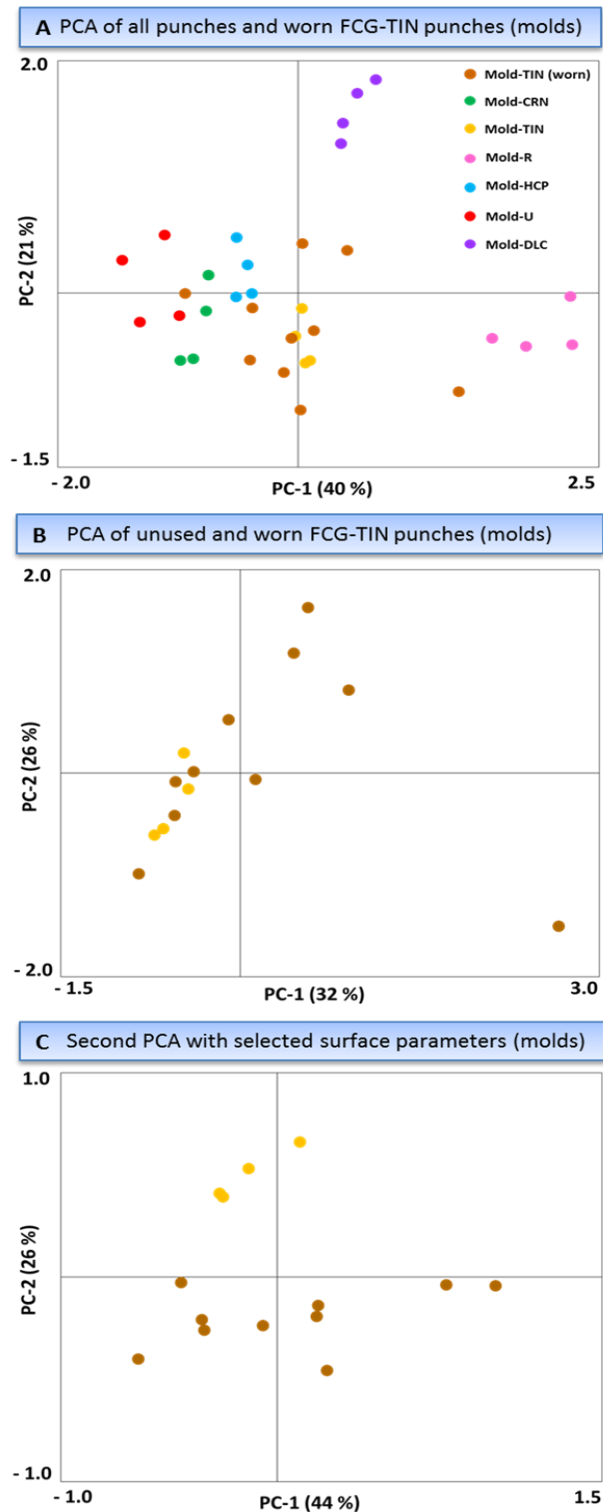
**Fig. 21:** (A) PCA scores plot of surface data acquired from the measurement of the molded differently coated cut punches together with the molded worn FCG-TIN punches. (B) Initial PCA scores plot of surface data acquired from the measurement of the molded FCG-TIN coated cut punches together with the molded worn FCG-TIN punches. (C) Second, optimized PCA scores plot of surface data acquired from the measurement of the molded FCG-TIN coated cut punches together with the molded worn FCG-TIN punches.

To allow a better comparison between punches with the same surface coating but different wear, another PCA was conducted with only the surface data of the unused and both used FCG-TIN punches, excluding the other surface coated punches and the uncoated punch (Fig. 21 B). Similar to the first PCA, the unused FCG-TIN samples clustered closely together with some of the worn FCG-TIN punch samples. This first cluster was therefore labelled as "intact" FCG-TIN surface area and was found in the negative part of PC-1. Only area samples of the worn punches shifted to the positive part of PC-1, indicating that these punches show signs of punch wear and should be discarded. Using the respective loadings plot (not shown) for interpretation, the shift to the positive part of PC-1 may indicate that several of the areas of the worn punches had comparably round peaks (high Spc) with similar heights (Sal) and were more voluminous overall as well as "rough" (Smc, Sxp, SWt, Sa, Sq, Sdc, Vv, Vvc, Vvv, Vmc, Vmp, Vm).

Interestingly, in PC-5 a clear distinction between the unused and used punches was possible. Therefore, another PCA was conducted using only these parameters, derived from the respective loadings plot, which have a high influence on PC-5 (Fig. 21 C). All unused FCG-TIN punches clustered at positive PC-2 scores while all used punches clustered at negative PC-2 scores. According to the respective loadings plot (not shown) all unused punches had higher Sdr, Sk, Spk, Ssc, Sr1 and mean depth of furrows values than the worn punches. The worn punches showed higher values of Shv, mean height of motifs, maximum depth of furrows and the second direction. The unused surfaces apparently had a generally rougher surface texture with pronounced and pointed peaks and furrows than the worn punches. In contrast, the worn punch surfaces were characterized by less pronounced peaks and furrows with a few being exceptionally high or steep, respectively. However, it has to be noted that PC-2 explained only 26 % of the data variance of the preselected data

and was originally created from PC-5. To prevent a coincidental observation, further investigations are needed.

### 4.2.3. *Evaluation of the sticking behavior to different punch surfaces*

4.2.3.1. *Suitability of the molding technique for the visualization of sticking*

The molding technique used in the present study was tested in preliminary experiments for its potential to visualize sticking residues on the punches. For this purpose, fully-sized production punches with three different surface coatings were molded before and after one and three compaction runs, respectively. Initially, a formulation containing IBU was selected but was quickly replaced by the IBU-Na formulation because the acidic IBU reacted with the silicone-A polymer of the impression material. The molding of the punches with the IBU-Na formulation after 1 and 3 compactions runs, respectively, was successful and no interaction between the formulation residues on the punches and the impression material was observed. The resulting surface images showed the successful visualization of the sticking formulation to the punches. The IBU-Na formulation 70 % showed such a high sticking tendency that it covered almost of all of the punch surface after only 3 compaction runs. To acquire more nuanced punch surface images with accumulating sticking residue after even 25 compaction runs, formulations with only 50 % API amount were used in a following investigation.

4.2.3.2. *Evaluation of the sticking behavior to differently texturized punch surfaces*

*using the selected surface parameters*

To determine the sticking behavior to different punch surfaces without the additional influences resulting from the coating material, punches with different surface textures but with the same coating material (FCG-CRN) were investigated (Fig. 22 A). The punches were molded before and after 1, 2, 5, 10, and 25 compaction runs. Each mold was measured at three different locations: in the "center", at the "intermediate" and at the "edge" location.
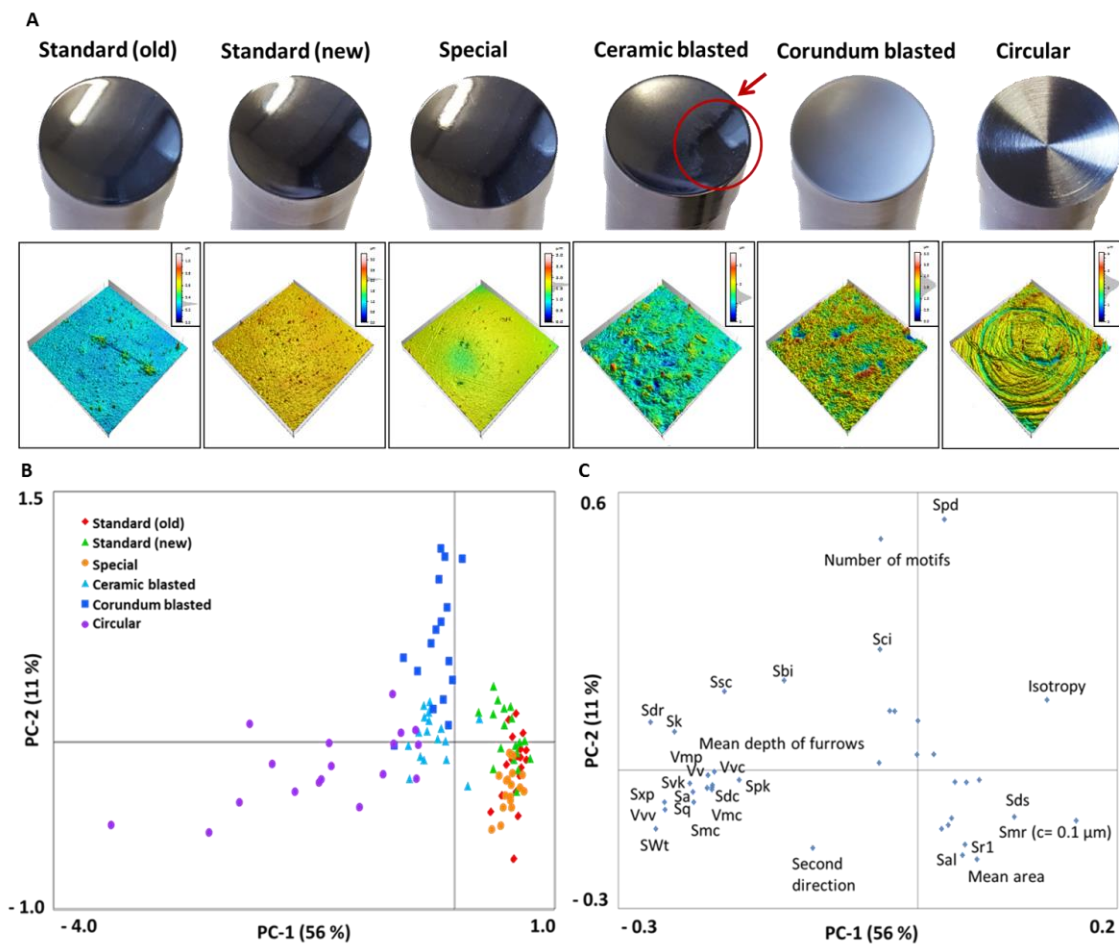


**Fig. 22:** (A) Photographic and surface images of the differently texturized FCG-CRN punches. The incomplete blasted area of the ceramic blasted punches is marked in red. (B) The respective PCA scores plot and (C) the loadings plot of the surface data acquired from the measurement of the differently texturized FCG-CRN punches prior tableting.

To characterize the differently texturized punch surfaces the resulting surface parameters of all measurements before tableting were analyzed in a first PCA. This PCA allowed a distinction between the different surface textures of the punches. However, a different distinction was observed when also considering the measurement location. In contrast to the differently coated cut punches, the production punches used in this investigation were biconcave. Therefore, the measured areas at the "edge" were steeper than the areas closer to the "center" of the molds. Apparently, some surface parameters were sensitive to this resulting steepness at some measurement locations of the molds. This sensitivity manifested itself in a cluster of mainly the "edge" data points at negative PC-1 and PC-2 scores (data not shown). The steepness-dependent parameters were identified (S5p, S5v, S10z, Sz, Sv, Sp, Shv, Sdv, Sha, Svi, Sda, Spc, Sdq mean height, max depth of furrows and mean volume of motifs) and excluded from all following analyses. After this exclusion, an optimized PCA scores plot (Fig. 22 B) of the punches before tableting was obtained. The more texturized surfaces like the "circular" and the two blasted punches clustered at negative PC-1 scores, while the smoother surfaces of the "standard (old)", "standard (new)", and "special" punches clustered at positive PC-1 scores. Two data points from the sample areas of the ceramic blasted punches were found at positive PC-1 scores. Inadvertently, the blasting procedure for producing the ceramic blasted punches did not enclose the whole surface area of the punch, which still had areas in the smooth surface finish (Fig. 22 A). Therefore, these areas clustered close to the smooth punches in the PCA scores plot (Fig. 22 B). Surfaces with "denser" surface textures (number of motifs, Sdr) had higher PC-2 scores. The "denser" corundum blasted surfaces was distinguished by the PC-2 from the ceramic blasted punches. Furthermore, the "special" punches all cluster at

negative PC-2 scores, presumably caused by their lack of distinctive surface textures.

After characterization of the differently texturized punches and exclusion of curvature-dependent surface parameters, a full analysis of the surface data including all compaction runs (from 0 to 25 runs) was conducted by another PCA. The resulting PCA scores plot was complex and had to be interpreted with respect to different influencing variables: the different number of compaction runs, the different surface textures of the punches, and the different measurement locations on the punch surfaces. In Fig. 23 the resulting PCA scores plot is displayed depending on these three variables with different sample grouping colors (Fig. 23 A-C). The most important variable influencing the order of the PCA scores data was the number of compaction runs (Fig. 23 A). The data points before tableting (run 0) clustered at negative PC-1 and positive PC-2 scores and started shifting towards positive PC-1 but negative PC-2 scores after 1 and 2 tableting runs. With increasing tableting runs the surface data continued clustering towards positive PC-1 scores but started shifting to positive PC-2 scores again until most of the 25 tableting run surface data reached positive PC-1 and PC-2 scores. Examining the surface images, it was clearly visible that the amount of formulation residue stuck to the punch surfaces increased with the number of tableting runs. According to the loadings plot (Fig. 23 D), clean punch surfaces had higher Smr values than punch surfaces with sticking residue. Sticking residue on punch surfaces increased all texture parameters related to "roughness" of the surface: higher and comparably round peaks (Ssc, Spk, Sxp , Smc, Sbi), steeper valleys (Svk, mean depth of furrows) and a coarser (Sdr, Sk, Sa, Sq, Sdc, SWt) and more voluminous texture (Vv, Vvc, Vvv, Vmc, Vmp) of the surfaces.
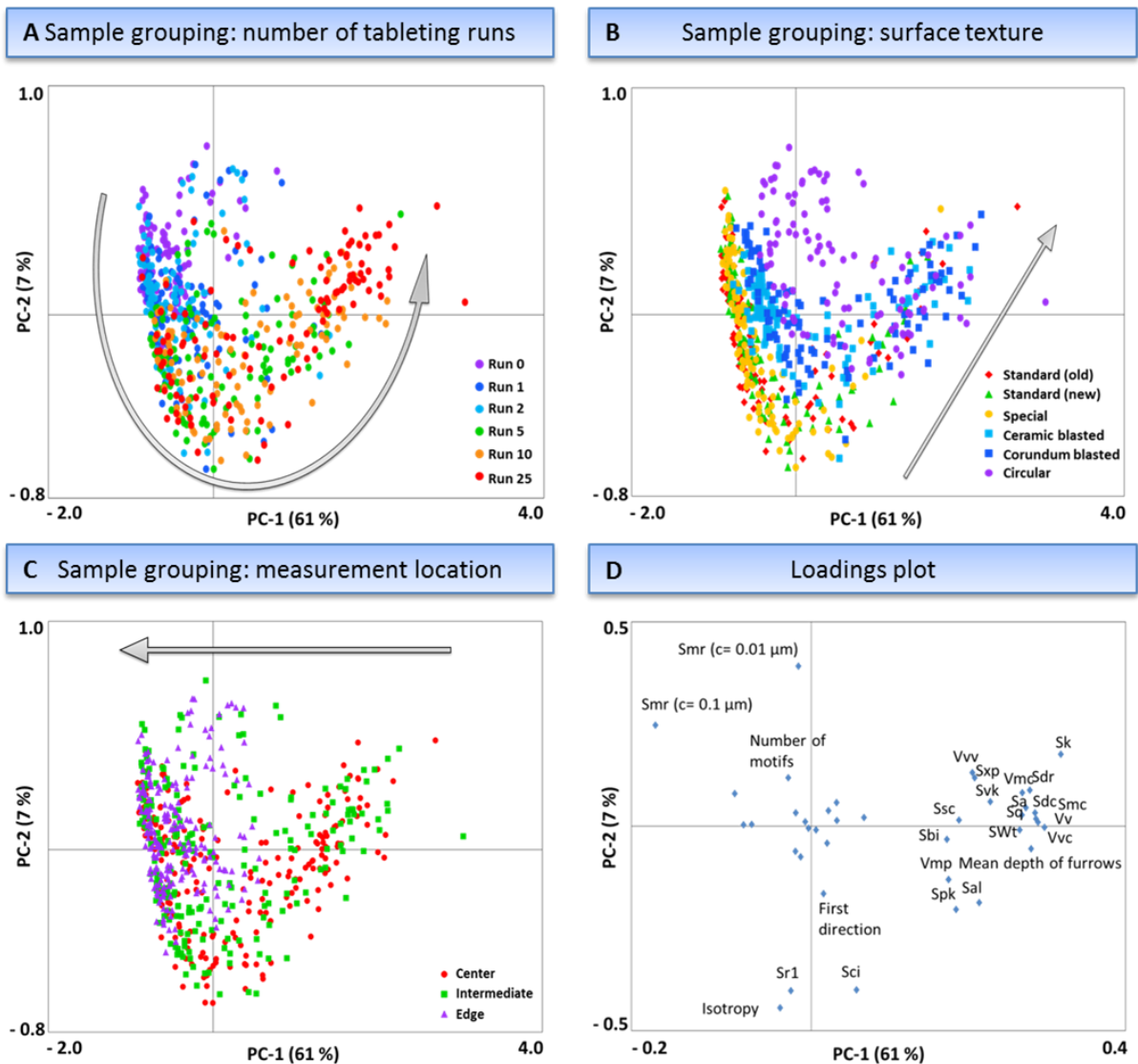
**Fig. 23:** (A, B, C) PCA scores plots and (D) Loadings plot of the surface data acquired from the measurement of the differently texturized FCG-CRN punches. Sample grouping colors of the same PCA scores plot were changed according to the respective variable: (A) number of tableting runs, (B) surface texture, and (C) measurement location.

The second effect that determined the location of the PCA scores was the punch surface texture (Fig. 23 B), which influenced PC-1 and PC-2. A good differentiation between the smoother ("standard (old)","standard (new)" and "special" FCG-CRN coated punches) and the rougher (ceramic, corundum blasted, "circular" FCG-CRN punches) surfaces was possible with both, PC-1 and PC-2. The "circular" punches could be distinguished from the other punches by PC-1, most probably because of

their anisotropic surface structure. The surface data were sorted by the PCA in the direction of positive PC-2 scores with increasing roughness, which became most obvious in the negative PC-1 scores plot section. It is important to note that the rougher punches dominated in the positive PC-2 section, which means that these punches also showed a higher amount of sticking residue on the punch surfaces if considering the data shown in Fig. 23 A.

The third influence that took effect on the cluster position of the data points in the PCA was the measurement location of the surface data (Fig. 23 C). The surface data acquired at the "edge" of the punch were found at negative PC-1 scores, while the surface data acquired at the "center" and "intermediate" location of the punch showed no clustering tendency. When correlating this finding with the cluster pattern of progressing tableting runs, it was shown that the larger the distance from the punch center the less sticking residue on the surface segment. When considering the same PCA with only the surface data of the respective measurement location, this observation became even more obvious (Fig. 24). The differentiation between the increasing number tableting runs was most distinct with the data acquired at the punch "center". These differences started to lessen with the "intermediate" data until at the punch "edge" only minimal differences –interestingly in the negative PC-2 direction- in the data were observed. These results are also in accordance with the visible inspections of the punches after tableting.
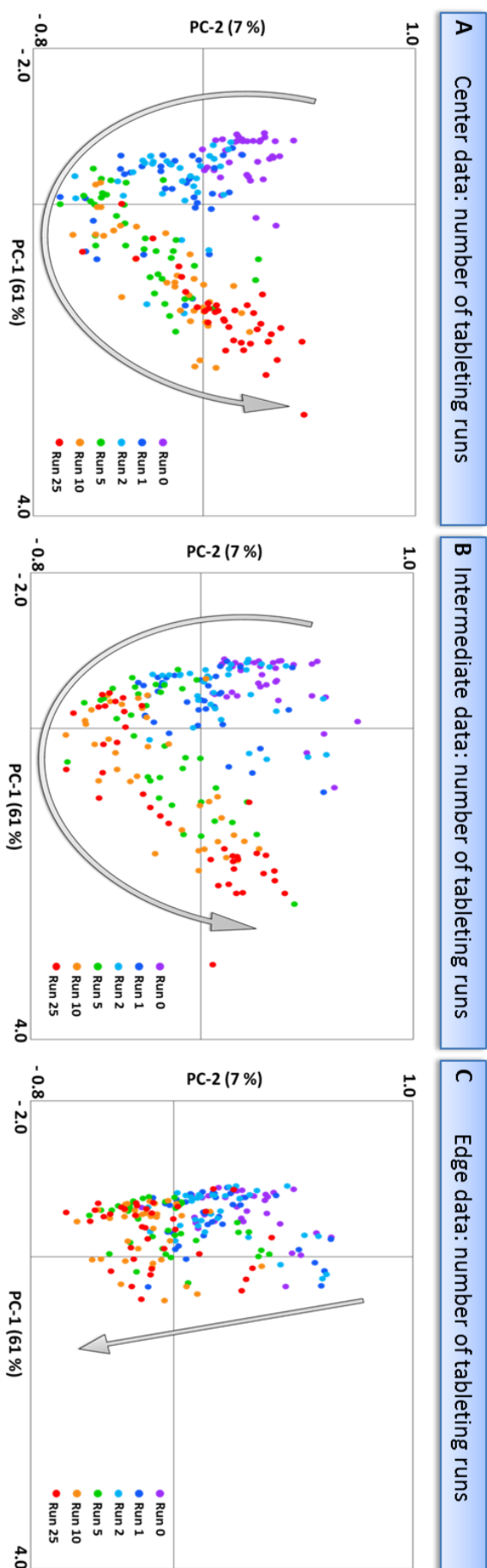
**Fig. 24:** PCA scores of the surface data acquired from the measurement of the differently texturized FCG-CRN punches in (A) "center", (B) "intermediate" and (C) "edge" position; coloring according to the number of tableting runs.

4.2.3.3. *Evaluation of the sticking behavior to differently texturized punch surfaces*

 *with surface images*

Examples of the differently texturized punches after 0 – 25 tableting runs are depicted in Fig. 25 for examination of the sticking behavior on the surfaces. After 1 tableting run small as well as large adhering particle agglomerates were distributed more or less over the whole punch surfaces. After the next tableting run, no pronounced differences were observable. The ceramic blasted, corundum blasted and "circular" punches had large and clearly visible pits and valleys, which were not filled with adhering residue after 1 or 2 tableting runs. It seemed as if sticking occurred preferably at the border of these pits.
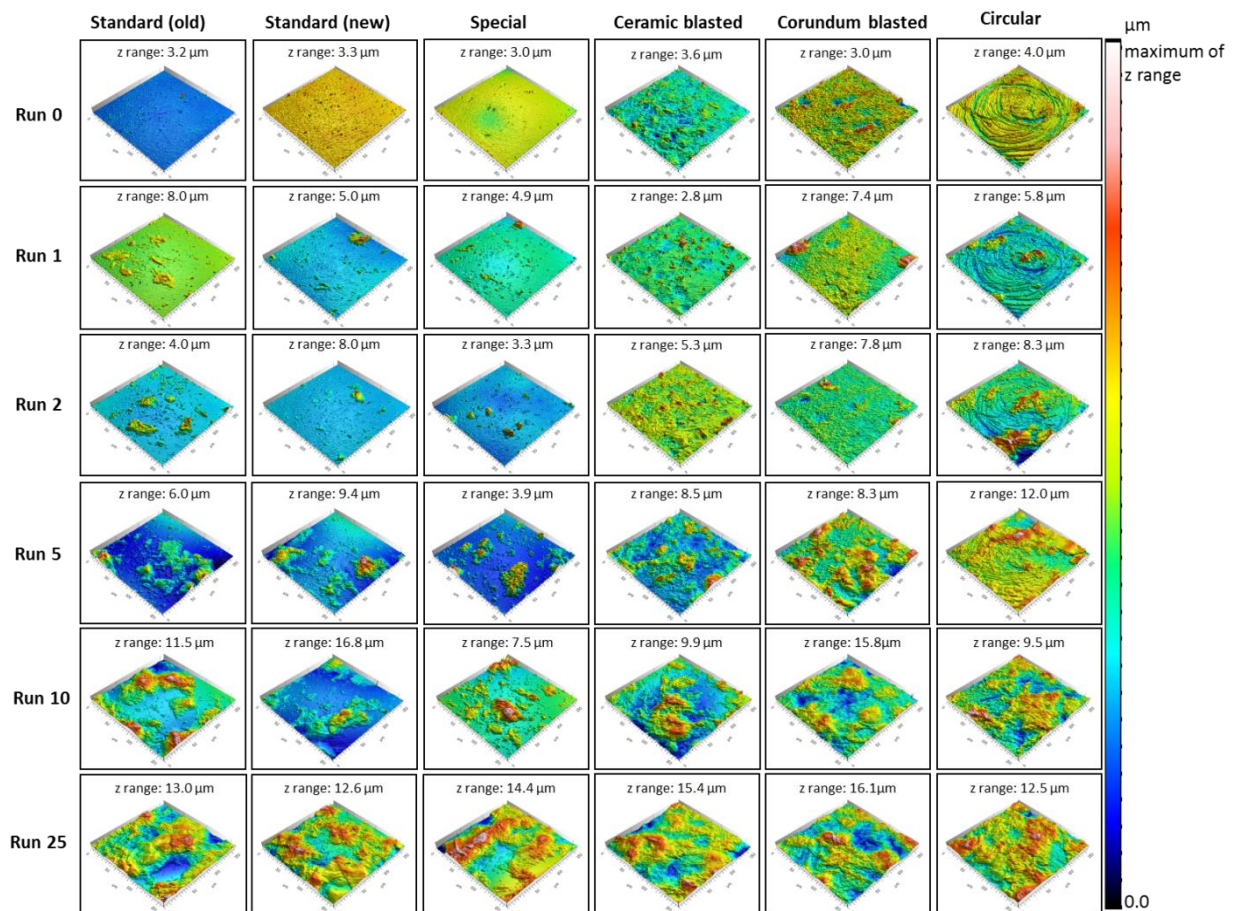


**Fig. 25:** Selection of the surface images of the differently texturized FCG-CRN punches taken at the "center" position after 0, 1, 2, 5, 10, and 25 tableting runs.

It has to be noted that it was impossible to analyze exactly the same areas after each compaction run. Only the "circular" punches had such unique textures in the central position that made images at the approximately same location possible as long as the surface was not covered with too much sticking residue. The tableting runs 0 – 5 of the "circular" punches were therefore magnified and depicted in Fig. 26.
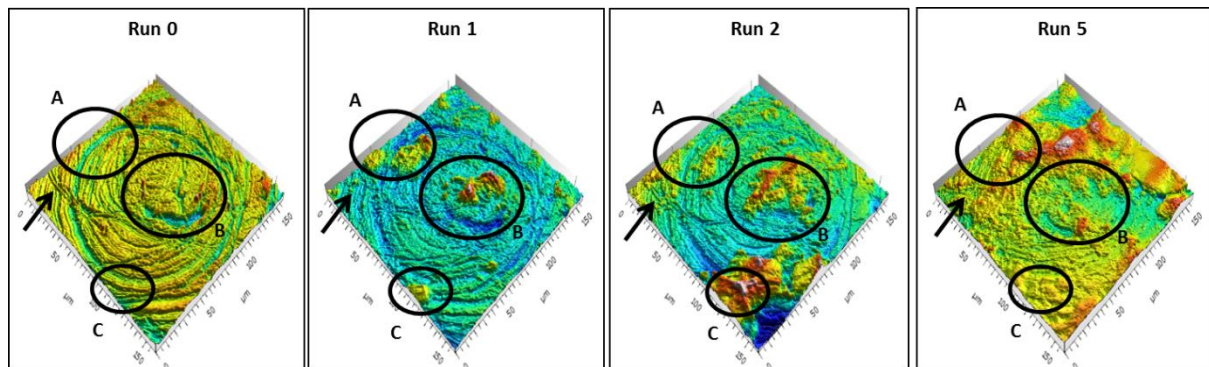


**Fig. 26:** Surface images of one of the "circular" FCG-CRN punches taken at the "center" position after 0, 1, 2, and 5 tableting runs. The circles and the arrow in the image of run 0 depict structures which undergo a pronounced change with increasing tableting runs.

After 1 tableting run of the "circular" punch, the unique structures of the punch before tableting (run 0) were still clearly visible, but the edges were not as sharp, most probably resulting from very fine adhering particles. Some very fine valleys (run 0, marked with an arrow) were filled after 1 run and partly reappeared after the next run. After tableting run 1, large particle agglomerates could be found in some regions of the surface close to the borders of the valleys. These adhering formulation fragments filled out the narrower and less steep valleys while the larger and steeper valleys were not affected. Therefore, the following sticking mechanism which has been suggested before [89] was assumed: the adhering particles become trapped in the narrow valleys between the asperities while they may escape the border valleys. After the second tableting run the two effects described before became apparent: the amount of the sticking residue in region A decreased while the residues in regions B

and C increased. Especially in region C the increase of the residue was particularly pronounced and the resulted pattern suggested that the residue increase started at the small fragment from run 1 as a seed crystal. After 5 tableting runs, an even larger punch area was covered with residue. The same trend to larger areas covered with coherent formulation residue was observed with all punches depicted in Fig. 25. The extent of the areas covered with residue on the surfaces appeared to correlate with the amount of sticking ibuprofen quantified by HPLC.

In Fig. 27 example surface images of the differently texturized punches are displayed according to the measurement location after 25 tableting runs. As expected, the farther away from the "center" the less sticking residue could be observed on the punches, which confirmed the results of the PCA. Interestingly, the farther away the images were taken from the punch "center" the more they resembled the "center" images taken after less tableting runs. It can therefore be concluded that next to the sticking pattern at the "center" also the radius of the sticking residue distinguishes between punches with a low and a high sticking tendency. During compaction, the powder in the edge region close to the die wall undergoes less powder movement because of restricting higher frictional forces resulting from the die wall [184]. Different shear forces and a heterogeneous density distribution of the tablets are the result [187]. Therefore, high density areas can be found at the edges of tablets, while the low density areas can be found in the central region, where sticking is more likely to occur. Similar assumptions have been suggested by other authors as well [144,188,189].
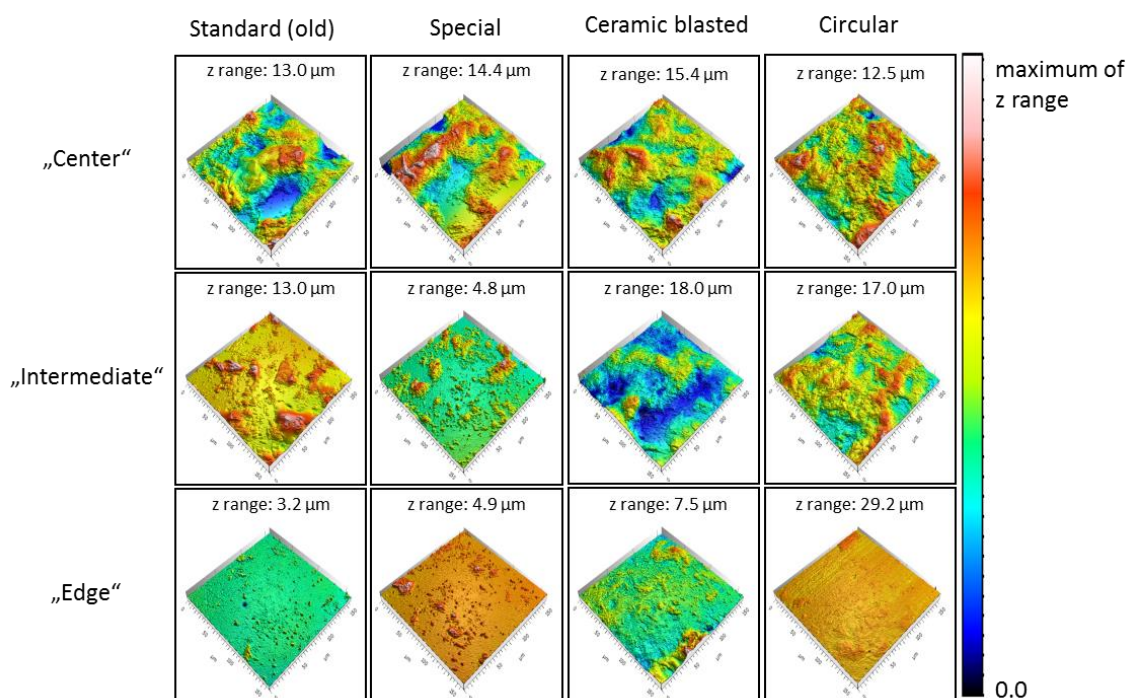
**Fig. 27:** Selection of the surface images of the "standard (old)", "special", "ceramic blasted" and "circular" FCG-CRN punches taken after 25 tableting runs at the "center", "intermediate" and "edge" position.

4.2.3.4. *Comparison of surface parameter data with HPLC data*

To verify the assumption that sticking was higher with the "rougher" punches, the sticking residues on the different punch surfaces were collected by rinsing the surfaces and quantified by subsequent HPLC analysis. The results of the HPLC analysis are shown in Fig. 28. The amount of sticking IBU-Na on the surfaces increased in the following order: Special < standard (new) < standard (old) < ceramic blasted < circular ≈ corundum blasted. The ceramic blasted punches had a very high SD, most probably because of their aforementioned incomplete surface modification.
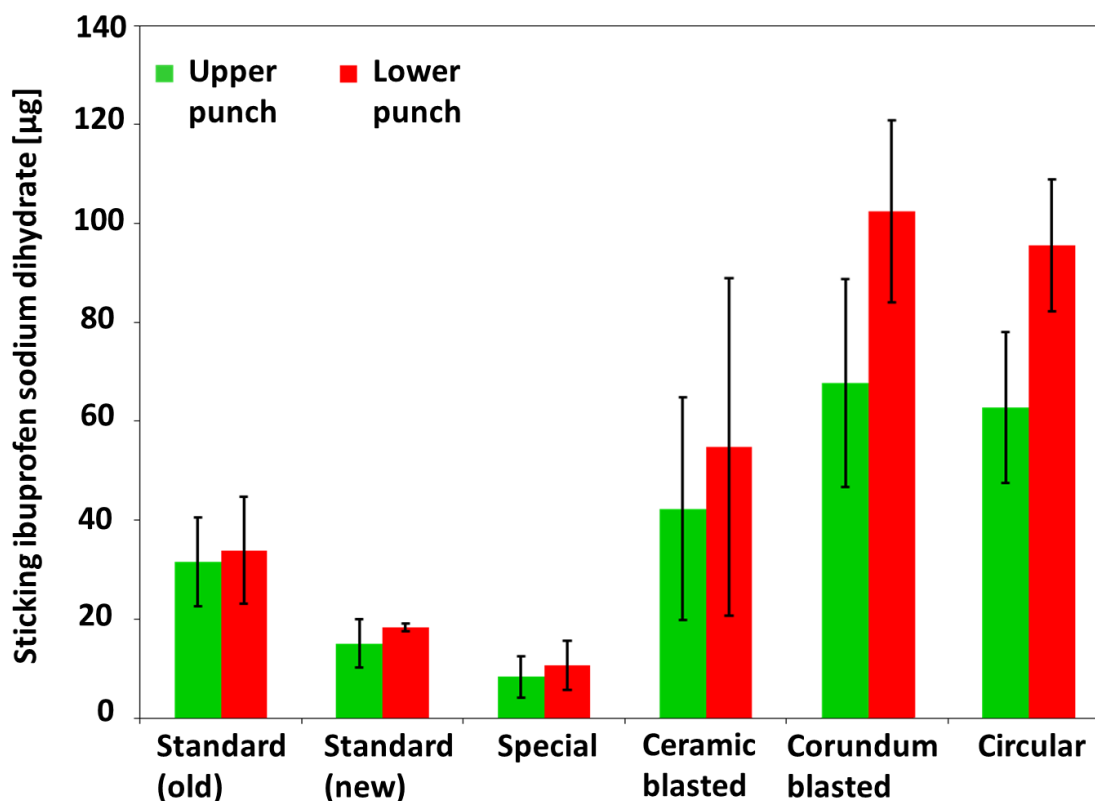
**Fig. 28:** Comparison of the amount of sticking IBU-NA to differently texturized FCG-CRN punches determined by HPLC (means ± SD, n = 3).

The HPLC data confirmed the results from the PCA evaluation: the "rougher" surfaces showed a higher sticking tendency (Fig. 23 B). However, the selected surface parameters apparently were not adequate to detect the differences in the sticking amount between the "smoother" punches "standard (old)", "standard (new)" and "special". While the PCA of the surface parameters identified all "smoother" punches as equal with regard to their relatively low sticking tendency, a more pronounced differentiation was obtained by HPLC. The lowest amount of sticking API was found on the "smoothest" punch surface, i.e. the "special" FCG-CRN coated punch surface. Higher amounts of sticking API were found on the two "standard" punches, most probably because of their slightly higher texturized surface.  Only with the PCA performed with the surface data of the clean punches before tableting it was possible to detect differences between the "special" and the two "standard" coated

punches (Fig. 22 B). The PCA including all tableting runs did not allow this distinction. Moreover, the HPLC data indicated that the new "standard" FCG-CRN coated punch showed a slightly lower sticking tendency than the older "standard" FCG-CRN coated punch. Apparently, the wear of the punches also had an effect on the sticking tendency. However, wear did not manifest itself in the differences between the surface data of the newer and older punches. There are two possible explanations to the insufficient identification of differences between these two surfaces. One possibility might be that the precision of the method -either the molding itself or the quality of the available surface parameters- was insufficient to detect these small differences. Another possibility might be that the differences between the older and newer punches were not caused by changes in the surface texture but rather by changes in the chemical composition of the surfaces. The "standard (old)" FCG-CRN punches had only been used with IBU or IBU-Na tableting formulations, which are likely to cause corrosive wear due to the acidic nature of IBU. In a previous study conducted in our lab, it was found that the wear phenomenon leading to increased IBU sticking to differently coated punches was more pronounced with FCG-TIN than with FCG-CRN coated punches [155]. Because FCG-TIN is known for its higher abrasive wear resistance but lower corrosive wear resistance than FCG-CRN, and both punches were equally used for mainly IBU formulation tableting, it had already been assumed that the wear phenomena was of corrosive nature. The results of the surface evaluation in the present study may further reinforce this hypothesis. The corrosion of the surface had apparently started to affect the chemical composition of the punch but had not yet started to alter the surface texture. However, further investigations are necessary to confirm the origin of these observations.

*4.2.4. Conclusion*

The present study demonstrated that the high-resolution molding of punches is a valuable method for punch surface analysis. In combination with 3D surface measurements, it was proven that this method is suitable for punch surface characterization, punch wear identification and sticking behavior analysis. The quantification and characterization of the surfaces with standardized surface parameters was successful and may be used for future investigations to avoid a complex and non-uniform image analysis. In cases where the reflection of the metallic punches interferes with the measurement, molding the surface may improve the measurement. The limits of the method were the impossible identification changes in the chemical composition of the punches as well as the impossible observation of sticking with acidic powder components because of the sensitivity of the impression material to acids. The analysis of the sticking behavior on differently texturized punches showed that sticking occurred mainly at the center of the punch and gradually increased with the number of tableting runs. It was also demonstrated that the smoother the punch surface the less formulation residue containing ibuprofen sodium dihydrate tended to stick. With the presented method, it is possible to identify the most suitable punch surface modification for sticking prevention with minimal tableting runs and therefore minimal material consumption. Furthermore, the presented novel technique allows the observation of the sticking behavior on the surfaces with the potential to optimize the punch surfaces. Future applications of the presented method should include the investigation of formulations with variable particle sizes and shapes as well as with other APIs and other excipients such as lactose or mannitol.

### 4.3. Sticking tendency of hydrophobic ibuprofen and hydrophilic ibuprofen sodium dihydrate to differently coated tablet punches (study 3)

#### 4.3.1. *Investigation of the sticking behavior of ibuprofen and ibuprofen sodium dihydrate*

The sticking behavior of IBU and IBU-Na was investigated by one DoE each. The results of these DoE models are shown in Table 12. Significant models were detected by the ANOVA for the responses sticking of IBU and IBU-Na to the upper and lower punches.

**Table 12:** ANOVA results of the DoE models.

| Model | IBU sticking to the upper punch<br>p-value | IBU sticking to the lower punch<br>p-value | IBU-Na sticking to the upper punch<br>p-value | IBU-Na sticking to the lower punch<br>p-value |
|---|---|---|---|---|
| Transformation | None | None | None | None |
| Model | Significant | Significant | Significant | Significant |
| Compaction speed (A) | 0.0112 | 0.0001 | Non-significant | 0.0001 |
| Compaction force (B) | 0.0001 | 0.0001 | 0.0001 | 0.0001 |
| Punch tip coating (C) | 0.0001 | 0.0001 | 0.0001 | 0.0001 |
| Interaction AB | 0.0432 | 0.0001 | 0.0064 | 0.0063 |
| Interaction AC | 0.0040 | 0.0001 | Non-significant | Non-significant |
| Interaction BC | 0.0001 | 0.0001 | 0.0178 | Non-significant |
| $A^2$ | 0.0005 | Non-significant | Non-significant | Non-significant |
| $B^2$ | 0.0001 | Non-significant | 0.0001 | Non-significant |
| $C^2$ | Non-significant | Non-significant | Non-significant | Non-significant |
| Interaction ABC | 0.0001 | 0.0001 | 0.0393 | 0.0001 |
| Interaction $AB^2$ | Non-significant | Non-significant | Non-significant | 0.0003 |
| Interaction $A^2C$ | Non-significant | Non-significant | Non-significant | Non-significant |
| Interaction $AC^2$ | Non-significant | Non-significant | Non-significant | Non-significant |
| Interaction $B^2C$ | 0.0001 | Non-significant | Non-significant | Non-significant |
| Interaction $BC^2$ | Non-significant | Non-significant | Non-significant | Non-significant |
| Lack of fit | Non-significant | Non-significant | Non-significant | Non-significant |
| $R^2$ | 0.9752 | 0.9601 | 0.9343 | 0.9323 |
| Adjusted $R^2$ | 0.9558 | 0.9401 | 0.8978 | 0.8927 |
| Predicted $R^2$ | 0.9035 | 0.8995 | 0.7608 | 0.8087 |
| Adequate precision | 32.759 | 26.872 | 16.495 | 14.386 |

All models fitted the original data well, as the lack of fit was non-significant. Additionally, high R², adjusted R² and predicted R² values as well as high adequate precision values indicated good models for correlation and prediction. Whenever possible, higher order model terms were excluded to simplify the models.

The selected factors and/or many of their interactions showed a significant influence on the sticking tendency of both APIs. To interpret the effect of the factors "compaction speed" and "compaction force", the response surfaces of the sticking tendency of both APIs to the differently coated upper and lower punch tips were used. Exemplary response surfaces for the FCG-DLC upper and lower punches are displayed in Fig. 29.
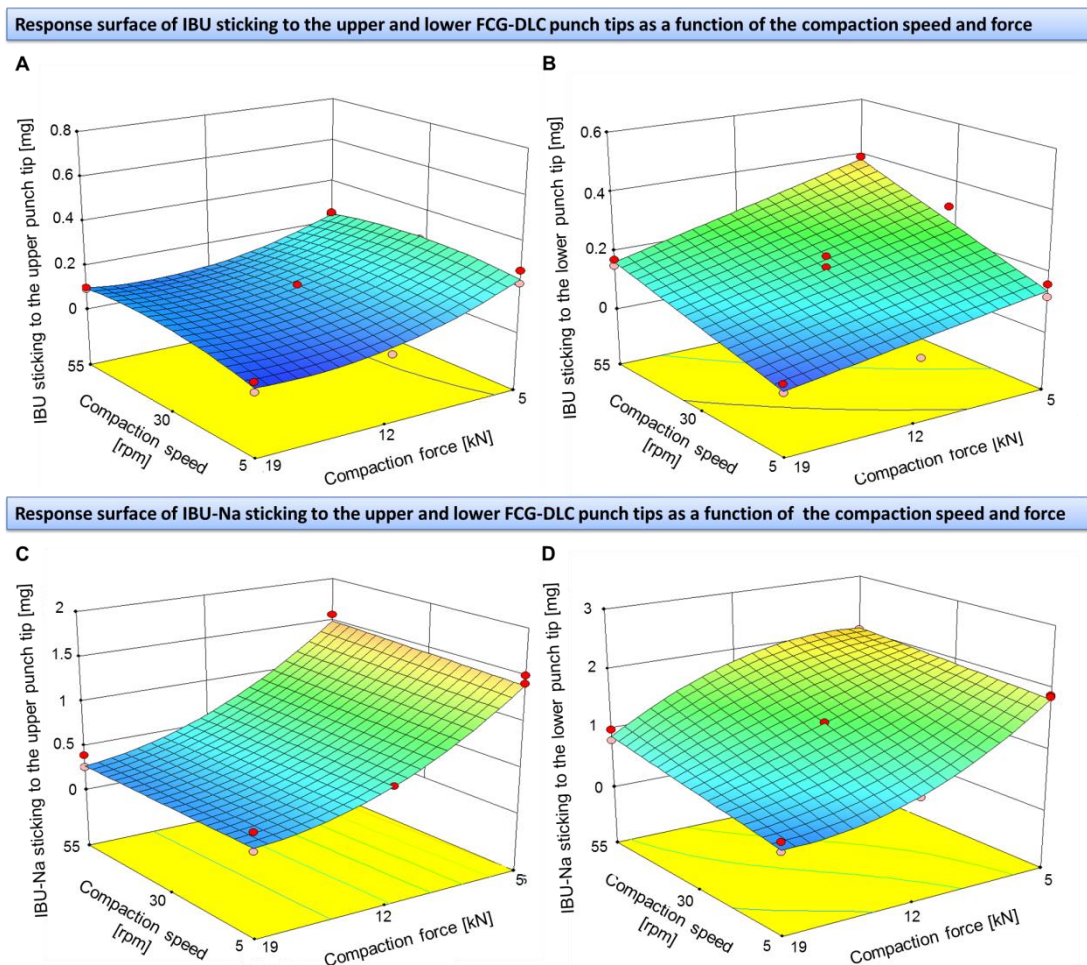


**Fig. 29**: Exemplary response surfaces of IBU sticking to the (A) upper and to the (B) lower FCG-DLC punch tips and response surfaces of IBU-Na sticking

The influence of the compaction speed and compaction force on IBU sticking has already been described in the literature [79,80]. As expected, the sticking amount of IBU in the present study increased with increasing compaction speed and decreased with increasing compaction force with both the upper and lower punches (Fig. 29 A and B). However, the effect of the compaction speed on the sticking tendency was less pronounced with the upper than with the lower punches. This observation is also reflected by the ANOVA of the sticking models of IBU because of the higher p-values of the factor A (compaction speed) as well as the interaction AB (compaction speed and force) in the upper punch sticking model in comparison to the lower punch sticking model (Table 12). A similar observation was made with the response surfaces of the sticking tendency of IBU-Na to the upper and lower punch tips (Fig. **29** C and D). The influence of the single factor "compaction speed" was even considered non-significant on IBU-Na sticking to the upper punch (Table 12). The reduction of API sticking with increasing compaction forces may be explained by an increase of the cohesion forces within the produced tablets, which exceed the adhesion forces between the tablets and the punch tip surfaces and therefore result in a less pronounced sticking tendency [34,82]. The influence of the compaction speed may be explained in the same manner. It has been described before that with increasing tableting speed the percentage elastic deformation exceeds the percentage plastic deformation of IBU tablets, which may result in less dense and thus softer tablets [160]. Therefore, it may be concluded that an increase in tableting speed also weakens the cohesive forces inside the tablets resulting in an increase in tablet sticking to the punches, although to a lesser extent than the compaction forces. The more pronounced influence of the compaction speed on sticking to the lower punch than to the upper punch may be explained by the different detachment mechanisms of the tablet from the respective punch surfaces. While the tablet is

detached from the upper punch by the pull-up movement of the punch, the tablet is detached from the lower punch by a take-off bar. While both detachment events are faster at high compaction speeds, the momentum of the take-off bar is also increased, which results in an additional effect of the compaction speed on the cohesion failure of the tablet. In general, sticking of both APIs to the lower punches was more pronounced, which further confirms this hypothesis.

Furthermore, it was observed that IBU-Na showed a higher sticking tendency than IBU. The sticking mechanism of IBU that has been explained by its low melting point cannot be applied to IBU-Na because its melting point is by far higher (198 °C). Although there are indicators that partial melting of IBU occurs [190], it was never directly proven. Sticking of IBU can be reduced by cooling the tablet press, which is often considered an indicator for the melting theory [191]. However, it is also known that many interactive forces may be influenced by the temperature. The observation that IBU-Na shows an even higher sticking tendency than IBU suggests that other mechanisms than sintering on the punch surfaces leads to sticking of these APIs. This assumption may be supported by studies, which show that similar drugs such as flurbiprofen and ketoprofen also stick to the punch surfaces – in the case of the latter to an even higher extent than IBU itself although both have a higher melting point (110 °C and 94 °C, respectively) [45,192]. Furthermore, independent of whether melting occurs or not, the nature of the bonds between the IBU particles and the punch surface has never been explained. Van-der-Waals forces have been generally suspected to be responsible for the sticking phenomena [52,193]. However, it has also been suggested by Waknis et al. that stronger forces resulting from polar interactions are responsible for the sticking mechanism [193]. Waknis et al. showed that an increased polarity of mefenamic acid crystals caused by different crystal morphologies may result in an increased sticking tendency. This assumption is

consistent with the findings of the present study, where the more polar IBU-Na shows a higher sticking tendency than IBU. Additional investigations – for instance the evaluation of the influence of humidity and temperature on the sticking tendency – are recommended to further explore the mechanisms leading to sticking of both APIs.

To evaluate the effect of the punch tip coating on the sticking tendencies, the interaction plots of the factors "compaction force" and "punch tip coating" were chosen as an example to illustrate this relationship (Fig. 30). With both APIs the sticking to the FCG-CRN and FCG-TIN punches was least pronounced. Even at the lowest compaction force, the differences in the anti-sticking properties of the different coating materials were still observable with the IBU formulation. In contrast, IBU-Na showed such a pronounced sticking tendency at the lowest compaction force that no differentiation between the punch tip coatings was possible with the exception of FCG-U. Surprisingly, the ranking of the anti-sticking performance of the differently coated punches was similar with both APIs and sticking was lowest with the FCG-CRN and FCG-TIN punches, while it was highest with FCG-HCP and FCG-DLC punches.
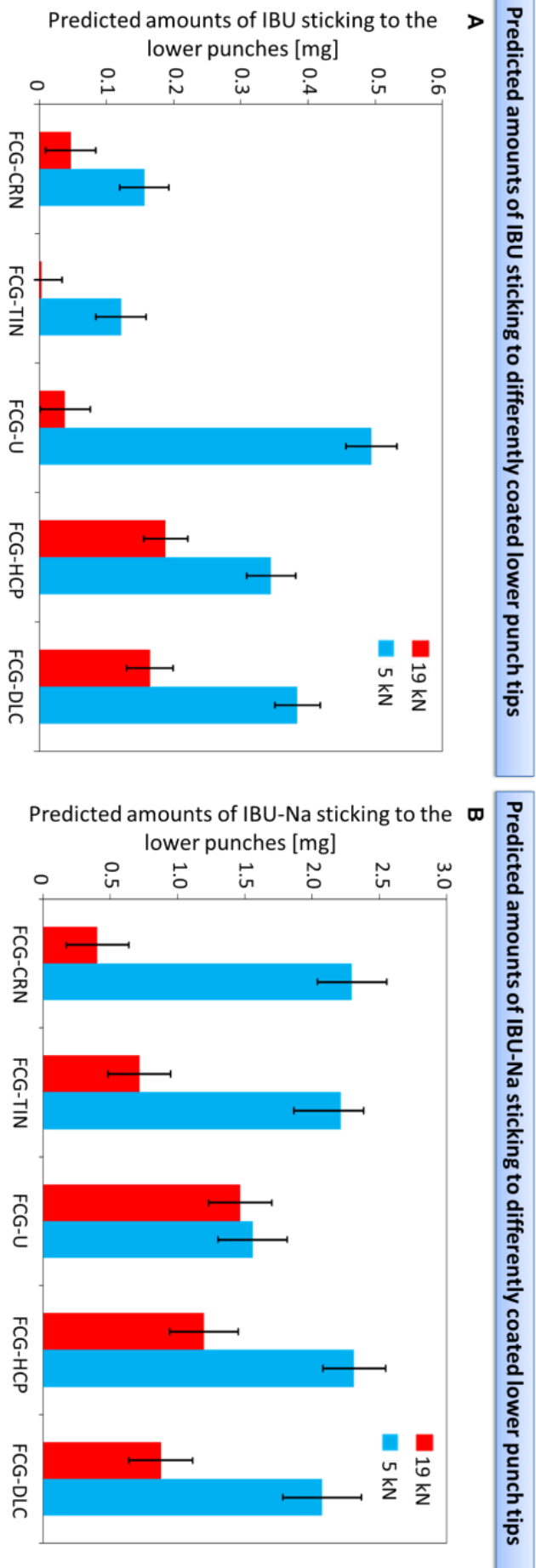
**Fig. 30:** Two-factor interaction plot of the factors "compaction force" and "punch tip coating" regarding the predicted sticking amounts of (A) IBU and (B) IBU-Na to the respective punches at a compaction speed of 55 rpm, displayed with LSD error bars.

## 4.3.2. *Investigation of the anti-sticking properties of the punch tip coatings*

The observation that the ranking of the anti-sticking performance of the coating materials was similar with the two differently polar APIs, which most probably exhibit different sticking mechanisms, was surprising. To further investigate the causes leading to the better anti-sticking performance of the FCG-CRN and FCG-TIN punches, several investigations were conducted.

### 4.3.2.1. *Results of the adhesive force analysis*

The results of the AFM adhesion force measurements of IBU and IBU-Na for each punch coating are shown in Fig. 31. The AFM adhesion force measurements revealed that adhesion between the IBU particle and the punch surfaces increased depending on the coating material in the following order: FCG-CRN ≈ FCG-U ≤ FCG-HCP < FCG-TIN ≈ FCG-DLC. This result was unexpected and was in contrast to the results acquired from the tableting experiments.

Furthermore, the adhesion force experiments with IBU-Na showed that the described AFM measurements may not be suitable for this API. They proved to be rather difficult to perform because IBU-Na adhered very strongly to all punch surfaces. Most of the prepared AFM tips were not usable with this API because the particles still adhered to the punch surfaces even after full z-range piezo retraction of the cantilever. To separate the particle from the surfaces, the cantilever had to be lifted with the motor drive instead of the z-range piezo, making adhesion force curve measurements impossible. The recording of such curves was only possible with one prepared AFM tip where the adhered IBU-Na particle was tiny enough and by chance turned to a position which allowed the contact area between it and the punch surface to be minimal. However, the measurements with the FCG-DLC punch could not be completed because the adhesion between the IBU-Na particle and the surface was still too large so that no usable data could be obtained. In the case of IBU-Na, a

differentiation between the adhesion forces to the differently coated punch surfaces was hardly possible although the tableting experiments revealed that sticking was lower with the FCG-CRN and FCG-TIN punches.
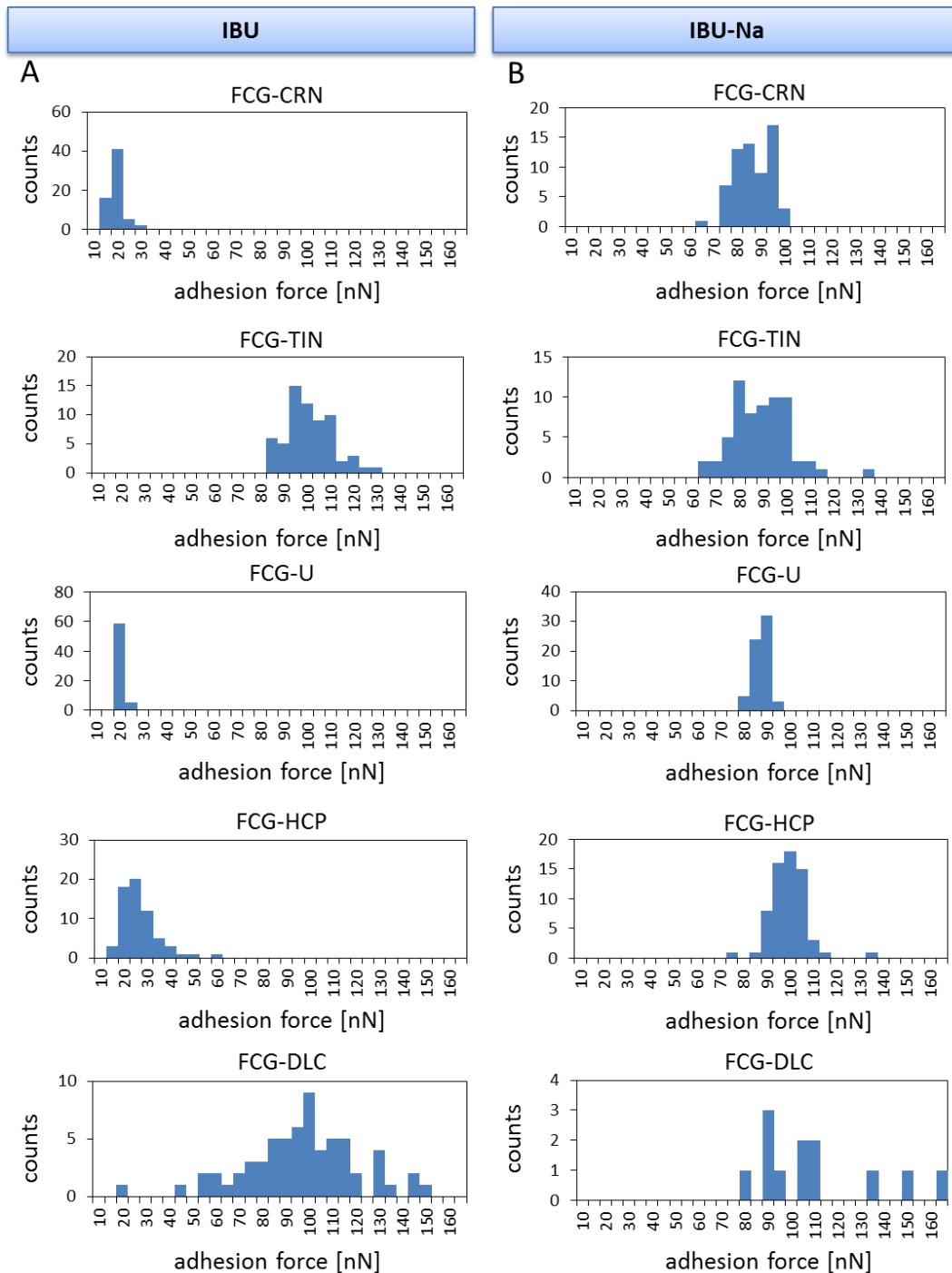


**Fig. 31:** Results of the AFM adhesion force measurements of (A) IBU and (B) IBU-Na with the FCG-CRN, FCG-TIN, FCG-U, FCG-HCP and FCG-DLC-coated cut punches.

Despite the mentioned complications with this method, the AFM adhesion force measurements clearly showed that IBU-Na exhibits a higher sticking tendency than IBU. It may therefore be assumed that AFM adhesion measurements do not sufficiently reflect the processes leading to sticking during tableting and are therefore not unsuitable to predict sticking. Furthermore, the preparation of the AFM tips and the measurements itself are very time-consuming. These limitations concerning this method have already been reported by other authors [72,193]. AFM adhesion force measurements may be used to estimate mainly pronounced differences between the sticking tendencies of different APIs. However, small differences between different surface coatings may not be detectable with AFM.

4.3.2.2. *Results of the contact angle analysis*

The results of the contact angle experiments with each punch tip coating are shown in Fig. 32. The measurements with the typically used liquids for contact angle investigations (Fig. 32 A) show that the hydrophilicity of the differently coated punches increases in the following order: FCG-CRN < FCG-HCP < FCG-U < FCG-TIN < FCG-DLC. These results correlated with the polar component of the calculated surface free energies (Fig. 32 B). However, the total surface free energies showed a slightly different order: FCG-CRN < FCG-U = FCG-HCP < FCG-TIN < FCG-DLC. The total surface free energies appeared to reflect the AFM adhesion data with IBU. This observation confirms the assumption that both methods may be used for the investigation of solid to solid adhesion but are not representative for sticking of IBU and IBU-Na to the punches during tableting.
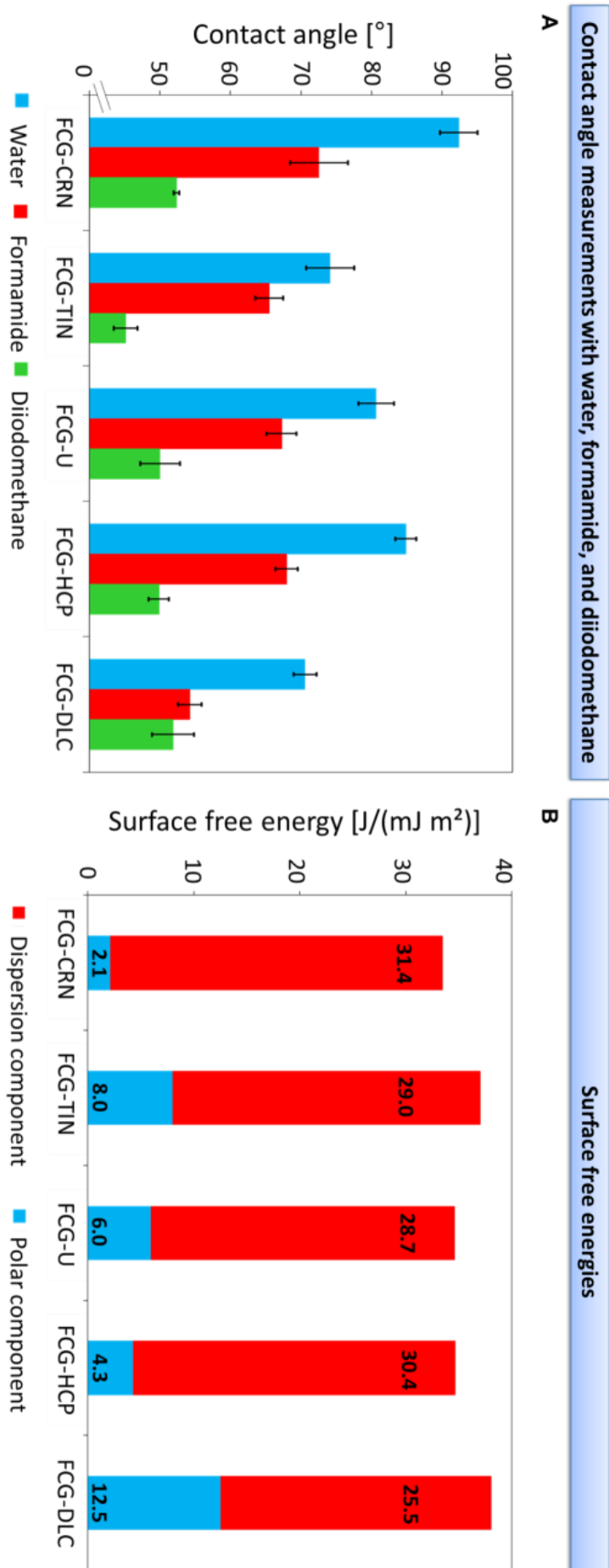
**Fig. 32:** (A) Contact angles of water, formamide, and diiodomethane on the differently coated cut punches at 20 °C (means ± SD, n = 4). (B) Surface free energies of the differently coated cut punches at 20 °C separated into the dispersion (red) and polar (blue) components.

In contrast to the measurements with the above mentioned liquids, the contact angle measurements with molten IBU revealed a better correlation with the anti-sticking properties of the different punch tip coatings (Fig. 33). The contact angles of FCG-CRN, FCG-TIN and FCG-U were significantly higher than the contact angles of FCG-HCP and FCG-DLC and thus less wettable with IBU. Again, these results were in good agreement with the tableting data where FCG-CRN and FCG-TIN showed the lowest sticking tendency followed by FCG-U, FCG-HCP and FCG-DLC (Fig. 30 A).   The contact angles of the FCG-U coating were high although its anti-sticking tendency during tableting was rather moderate. This result was not surprising because the cut punches used for the contact angle measurements were new and had never been used before in any tableting experiments. In contrast, the FCG-U punches in the tableting experiments had been used for several years during IBU tableting investigations. In a previous study, it has been shown that new FCG-U punches exhibited good anti-sticking properties, which were similar to the FCG-CRN and FCG-TIN punches [155]. However, the anti-sticking properties of the FCG-U punches decreased significantly over time because of corrosive wear. The observations of the present study may reflect these results, which provide an explanation for the similarly high contact angles of molten IBU on the new cut FCG-U punches. However, additional investigations should be conducted with corroded or worn cut FCG-U punches to confirm this hypothesis.
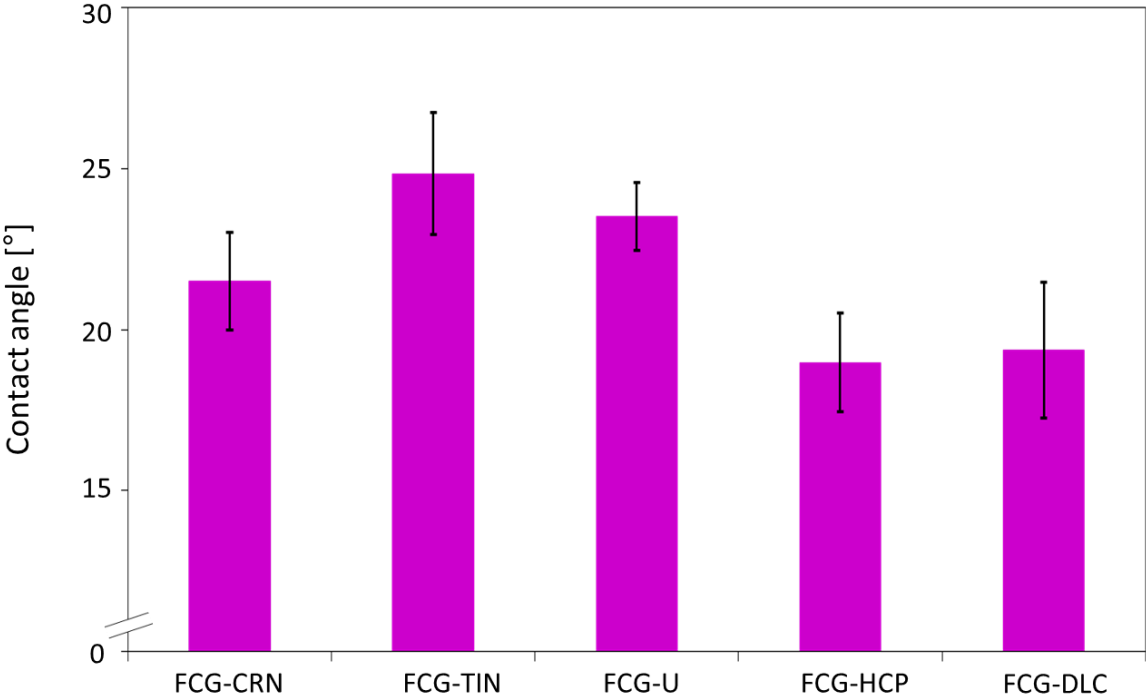
**Fig. 33:** Contact angles of molten IBU on the differently coated cut punches.

### 4.3.2.3. *Results of the surface texture analysis*

The results of the punch surface measurements are displayed in Fig. 34. It has to be emphasized that in contrast to the adhesion force and contact angle measurements, the surface data were not acquired from the unused cut punches but from those fully-sized punches, which were also used during the tableting experiments. While a distinction between the differently coated punch surfaces was possible with the PCA scores plot (Fig. 34 A), no common surface texture parameters between the less (FCG-CRN and FCG-TIN) and the more (FCG-U, FCG-DLC and FCG-HCP) adhesive punch surfaces were detectable by PCA or visual inspection (Fig. 34 B).
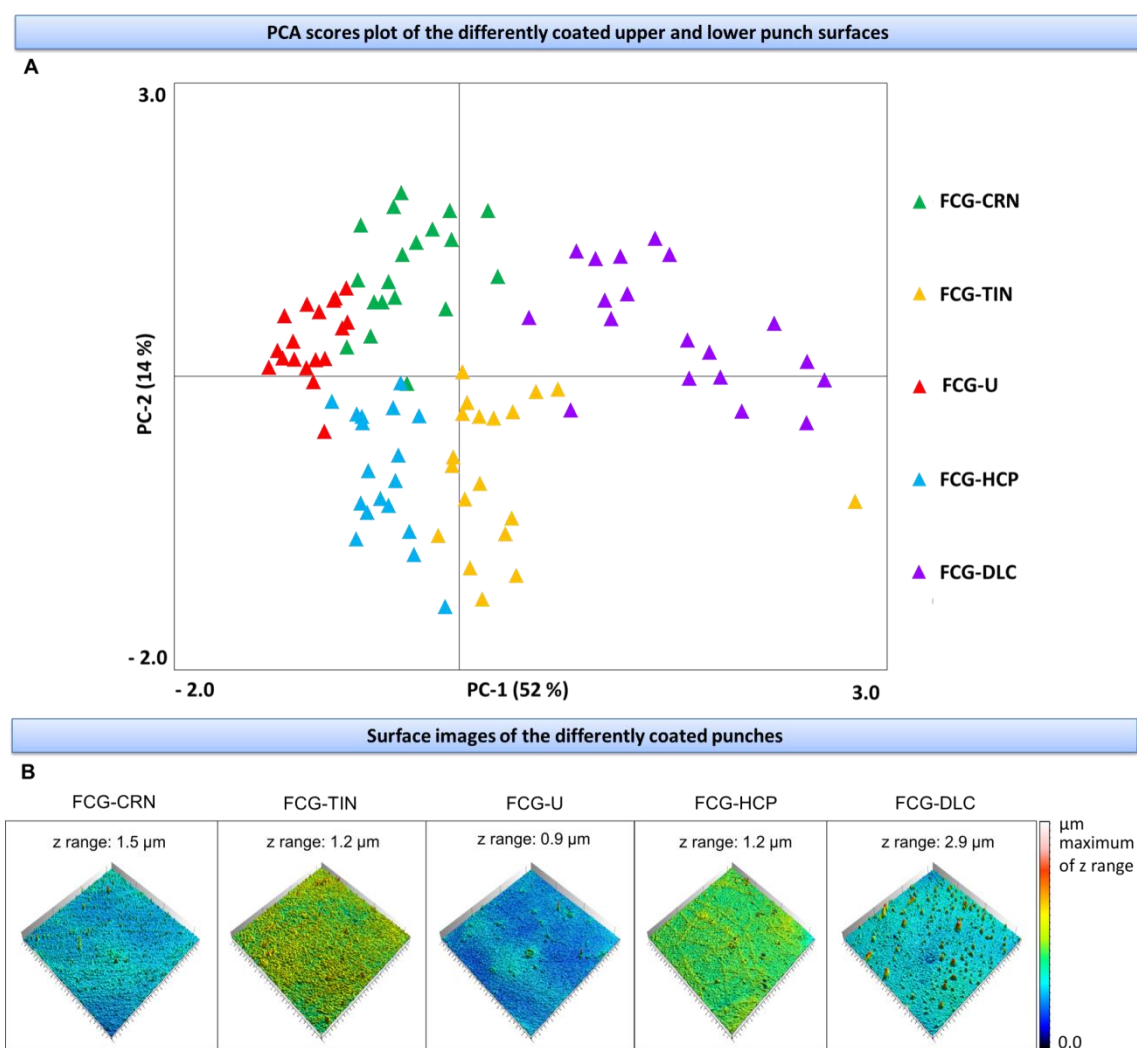


**Fig. 34:** (A) PCA scores plot and (B) exemplary surface images of the differently coated punch surfaces.

In a previous study, it was found that the rougher the surface of punches coated with the same coating material (FCG-CRN), the higher the sticking amount [170]. This relationship could not be found in the present study because the punch FCG-TIN with the low sticking tendency showed a rather rough but homogeneous punch surface. Considering the AFM adhesion data and the surface free energy data, it may be assumed that the FCG-TIN coating shows a high sticking tendency because of its high adhesive interaction with the APIs. Following a theory postulated by Podczeck et al. [89], it is hypothesized in the present study that the rough but fine surface texture leads to a lower contact area between the punch surface and IBU or IBU-Na particles: Some of the IBU and IBU-Na particles might be larger than the gap between the asperities and instead of becoming trapped inside the valleys with an increased contact area, they only come in contact with the pointed asperities of the surface. Further investigations should be conducted with smoothened FCG-TIN punches to verify this hypothesis. It is expected that smoother FCG-TIN punches lead to increased API sticking.

In comparison to the FCG-TIN punches, the FCG-DLC punch surfaces were highly sticky and rough but very inhomogeneous. In contrast, the also highly sticky FCG-HCP punches appeared to have a rather smooth but similarly inhomogeneous surface caused by the large summits and the small rifts on the surface, which may promote sticking. The FCG-CRN surfaces showed a low sticking tendency and were comparably smooth and homogeneous. These observations suggest that the more homogeneous the surface the less the sticking tendency.

However, the FCG-U punch surfaces were very smooth and homogeneous, yet they showed a moderate sticking tendency. According to the surface quality of these punches, it is expected that they are well suited for the prevention of sticking. Apparently, the chemical composition of these punches, especially after corrosive

wear, leads to more pronounced interactions with the APIs. This assumption may be supported by the results of previous work, where the FCG-U punches showed equally good anti-sticking properties as the FCG-CRN and FCG-TIN punches in their unworn state but worsened during the course of tableting acidic IBU formulations [155]. To confirm this hypothesis, additional contact angle and AFM adhesion force measurements with worn FCG-U punches should be conducted.

4.3.2.4. *Overall interpretation of the anti-sticking properties of punch coatings*

Overall, the presented results suggest that the surface texture – especially the homogeneity of the surface – as well as the chemical composition of the punch coatings affected the sticking tendency of both APIs. Considering both aspects, the following mechanisms are suggested for each individual punch tip coating: the FCG-CRN punches' excellent anti-sticking properties result from their low polarity, which reduces their surface interaction with the APIs. Their also very smooth and homogeneous surface texture supports this property. In contrast, FCG-TIN punches are sticky with regard to their chemical nature, which was demonstrated by the AFM and contact angle measurements. However, their rough surface texture with smaller gaps between the asperities than the API particle size compensates for this aspect by reducing the contact area between the API particles and the punch surface. New and unused FCG-U punches are – similar to FCG-CRN-coated punches – chemically less sensitive to sticking, which is also supported by their smooth and homogeneous surface. However, their chemical composition changes over time because of corrosive wear resulting in only moderate anti-sticking properties. FCG-HCP punches may be considered as moderate with regard to their chemical interactive potential and their surface texture, which results in a rather bad anti-sticking performance of these punches. FCG-DLC punches are chemically susceptible to sticking in both

aspects – the chemical interactive potential as well as their rough, inhomogeneous surface texture, which is reflected by their high sticking tendency during tableting.

However, additional investigations are necessary to confirm these hypotheses and to fully understand the underlying mechanisms. It is suggested that additional AFM adhesion and contact angle experiments should be conducted with corroded FCG-U punches. Furthermore, the sticking tendency of smoothened FCG-TIN punches should be evaluated in the future. The same applies to FCG-DLC punches, which have a similar the same roughness as the FCG-TIN punches investigated in this study.

### 4.3.3. Conclusion

The sticking tendency of IBU and IBU-Na as model substances for a lipophilic and a hydrophilic sticky API, respectively, to differently coated punches was investigated in the present study. It was shown that more pronounced sticking was observed with the more polar substance IBU-Na than with the less polar substance IBU. Interestingly, the anti-sticking performance of the different punch tip coatings proved to be independent of the APIs' polarity. Both the FCG-CRN and FCG-TIN punches showed the lowest extent of sticking with both APIs, followed by FCG-U, FCG-HCP and FCG-DLC punches. To understand the reason for this observation, AFM adhesion forces with both API particles, contact angles with different liquids and the surface texture of the differently coated punches were measured. The AFM adhesion results did not reflect the anti-sticking performance of the applied punch coatings but showed that the stickiness of IBU-Na was higher than that of IBU. Furthermore, contact angle measurements with molten IBU revealed a good correlation with the sticking data acquired from the tableting experiments. Both the AFM and the contact angle measurements indicated a more pronounced chemical interaction and thus a higher sticking tendency between the APIs and the punch coatings. However, the surface texture of the punches should also be considered because it may either amplify or limit these tendencies. Punches showing a low chemical interaction with the API combined with a homogeneous and smooth surface, exhibited superior anti-sticking properties which were observed with FCG-CRN punches. However, in cases such as FCG-TIN-coated punches, a homogeneous but rough surface with small gaps between the asperities can compensate for a high adhesive interaction between punch surface and API by reducing the effective contact area between both. Further studies are recommended to obtain a more comprehensive insight into these complex relationships.

## 4.4. Production-scale tableting of an optimized ibuprofen grade to decrease its sticking tendency (study 4)

### 4.4.1. Evaluation of the tableting behavior of Ibuprofen DC 85 W

An I-optimal design was used to analyze the effect of the three compaction forces on the tableting behavior of Ibuprofen DC 85 W tablets. The tablet disintegration and crushing strength are typical quality attributes for tablets and were therefore selected as responses. The results of the I-optimal design are shown in Table 13. One disintegration time value (the crossed out value in Table 13) was identified as an outlier because this sample was inadvertently mixed-up and was therefore not included in any of the following calculations.

**Table 13:** The I-optimal design including the responses. All runs were conducted in random order. The crossed-out value was identified as an outlier.

| Design point | Block # | Factor: Pre-compaction [kN] | Factor: Intermediate Compaction [kN] | Factor: Main compaction [kN] | Response: Disintegration time [min] | Response: Crushing strength [N] |
|---|---|---|---|---|---|---|
| **Vertex** | 1 | 0 | 0 | 5 | 0.37 | 39 |
| | 1 | 11 | 0 | 5 | 1.00 | 86 |
| | 1 | 0 | 11 | 5 | 1.12 | 86 |
| | 1 | 11 | 11 | 5 | 1.08 | 90 |
| | 1 | 0 | 0 | 11 | 0.95 | 81 |
| | 1 | 11 | 0 | 11 | 1.17 | 85 |
| | 1 | 0 | 11 | 11 | 1.10 | 86 |
| | 1 | 11 | 11 | 11 | 1.18 | 89 |
| **Central Edge** | 2 | 11 | 0 | 8 | 0.93 | 91 |
| | 2 | 0 | 11 | 8 | 0.95 | 86 |
| | 1 | 5.5 | 0 | 11 | 0.90 | 89 |
| | 2 | 0 | 5.5 | 11 | 0.93 | 89 |
| | 2 | 11 | 5.5 | 11 | 1.00 | 91 |
| | 2 | 5.5 | 11 | 11 | 1.02 | 92 |
| | 2 | 5.5 | 0 | 11 | 0.90 | 90 |
| **Plane Central** | 1 | 0 | 5.5 | 8 | 0.62 | 64 |
| | 1 | 11 | 5.5 | 8 | 1.03 | 89 |
| | 1 | 5.5 | 0 | 8 | 0.58 | 60 |
| | 1 | 5.5 | 11 | 8 | 1.10 | 88 |
| | 1 | 5.5 | 5.5 | 5 | 0.47 | 51 |
| | 1 | 5.5 | 5.5 | 11 | 0.98 | 88 |
| | 1 | 5.5 | 11 | 8 | 0.97 | 91 |
| **Axial** | 1 | 2.75 | 2.75 | 6.5 | 0.47 | 51 |
| | 1 | 8.25 | 2.75 | 6.5 | 0.75 | 71 |
| | 1 | 2.75 | 8.25 | 6.5 | 0.77 | 75 |
| | 1 | 8.25 | 8.25 | 6.5 | 0.78 | 74 |
| | 1 | 2.75 | 2.75 | 9.5 | ~~0.93~~ | 62 |
| | 1 | 8.25 | 2.75 | 9.5 | 0.83 | 75 |
| | 1 | 2.75 | 8.25 | 9.5 | 0.73 | 79 |
| | 1 | 8.25 | 8.25 | 9.5 | 0.80 | 76 |
| **Center Points** | 1 | 5.5 | 5.5 | 8 | 0.60 | 65 |
| | 1 | 5.5 | 5.5 | 8 | 0.62 | 56 |
| | 1 | 5.5 | 5.5 | 8 | 0.63 | 61 |
| | 1 | 5.5 | 5.5 | 8 | 0.67 | 65 |
| | 1 | 5.5 | 5.5 | 8 | 0.60 | 63 |

Significant models were detected by the ANOVA for both responses "disintegration time" and "crushing strength" (Table 14). Both models fitted the original data well, as the lack of fit was non-significant. Additionally, high $R^2$, adjusted $R^2$ and predicted $R^2$ values as well as high adequate precision values indicated good models for correlation and prediction.

**Table 14:** ANOVA results of the DoE models.

| Model | Disintegration time p-value | Crushing strength p-value |
|---|---|---|
| Data transformation | ---- | ---- |
| Model significance | < 0.0001 | < 0.0001 |
| Pre-compaction force (A) | < 0.0001 | < 0.0001 |
| Intermediate compaction force (B) | Non-significant | < 0.0001 |
| Main compaction force (C) | Non-significant | Non-significant |
| Interaction AB | < 0.0001 | 0.0010 |
| Interaction AC | 0.0162 | 0.0013 |
| Interaction BC | < 0.0001 | 0.0012 |
| $A^2$ | < 0.0001 | 0.0007 |
| $B^2$ | < 0.0001 | 0.0298 |
| $C^2$ | 0.0076 | Non-significant |
| ABC | 0.0014 | 0.0048 |
| $A^2C$ | Non-significant | 0.0018 |
| $AC^2$ | 0.0074 | 0.0466 |
| $B^2C$ | 0.0025 | Non-significant |
| $BC^2$ | 0.0106 | 0.0229 |
| $B^3$ | 0.0386 | Non-significant |
| $C^3$ | 0.0062 | 0.0349 |
| | | |
| Lack of fit | Non-significant | Non-significant |
| $R^2$ | 0.9707 | 0.9278 |
| Adjusted $R^2$ | 0.9448 | 0.8745 |
| Predicted $R^2$ | 0.8332 | 0.6902 |
| Adequate precision | 23.054 | 17.575 |

The resulting response surfaces (Fig. 35) were used to interpret the influence of the three compaction forces on the disintegration time and the crushing strength. As expected, the disintegration time and the crushing strength increased at higher compaction forces, independent of the position of the respective compaction roll. The influence of the pre-compaction force may be observed in Fig. 35 A and B, where a "classical" tableting setup is displayed without the influence of the intermediate

compaction roll (= 0 kN). With regard to the effect of factor interactions, it was observed that each factor amplified one another for both responses.

A slight prolongation of the tablet disintegration time (Fig. 35 A) was observed with the introduction of a pre-compaction force: for example, at a main compaction force of 8 kN and a pre-compaction force of 0 kN the predicted disintegration time was 0.37 min (dark blue area) whereas with a pre-compaction force of 5.5 kN and the same main compaction force of 8 kN, the predicted disintegration time extended to 0.55 min (light blue area). Additionally, if both compaction forces were set to the maximum of 11 kN, the maximum disintegration time of 1.2 min was achieved. At an intermediate compaction force of 5.5 kN (Fig. 35 C) the disintegration time was slightly prolonged at the center point, which manifested itself as a slight shift from the light blue color to the green color in the center of the response surface. However, no further effect resulting from an increase of the intermediate compaction force could be observed. When the intermediate compaction force was set to the maximum of 11 kN (Fig. 35 E), the disintegration time often reached approximately its maximum of 1.2 min at almost any point on the response surface. If all three compaction rolls were set to 11 kN compaction force, this disintegration time of 1.2 min was not exceeded. It may therefore be deduced that a pre-compaction force prolonged the tablet disintegration time of Ibuprofen DC 85 W while an intermediate compaction force did not have a pronounced influence on the tablet disintegration time. The maximum disintegration time was achieved, if two of the three compaction forces were set to 11 kN. A similar effect was observed in the study by Gamlen et al. [154], where a multiple compaction of Avicel® PH101 prolonged the disintegration time only slightly. Furthermore, it should be noted that all the disintegration times in the present study were very short and in an uncritical range with regard to tablet disintegration criteria of the Ph. Eur. for uncoated tablets, which requires a disintegration time of

less than 15 min. In comparison, the crushing strength showed an even lower dependency on the pre-compaction force (Fig. 35 B). For example, at a main compaction force of 8 kN and an increase of the pre-compaction force to 5.5 kN the crushing strength slightly improved from 50 N (light blue area) to 60 N (green area). In the study by Ruegger and Çelik [152], it was also shown that a pre-compaction force may significantly increase the crushing strength of tablets made of a directly compressible ibuprofen grade (63 % ibuprofen, wet granulated with MCC, pregelatinized starch, and polyvinylpyrrolidone). However, if in the present study just one of the two compaction rolls was set to the highest compaction force of 11 kN the highest crushing strength of about 90 N (red area) was already achieved. The crushing strengths of the resulting tablets were also independent of whether the pre-compaction force was higher than the main compaction force or vice versa. These results were in contrast to the findings in the study by Ruegger and Çelik, where higher main compaction forces than pre-compaction forces resulted in significantly harder ibuprofen tablets than those compacted at pre-compaction forces exceeding the main compaction forces. These differences might be caused by the different pre-processing of the ibuprofen grades performed in the study of Ruegger and Çelik in comparison to the Ibuprofen DC 85 W grade used in the present study. As stated above, Ibuprofen DC 85 W was produced by roller compaction. Roller compaction of materials may cause a loss of their compactibility [194], which manifested itself in the results of the present study. The introduction of an intermediate compaction force confirmed the observation that the crushing strengths of the resulting tablets were mainly dependent on the maximum compaction force applied from any of the compaction rolls. With an intermediate compaction force of 5.5 kN (Fig. 35 D) the minimum crushing strength increased up to about 60 N (green area) because at any point in the response surface at least two compaction rolls

exerted a force of at least 5 kN. The addition of a third compaction roll showed only a slight improvement of the tablet crushing strength, which becomes especially apparent when comparing the center points of the response surfaces of Fig. 35 B and Fig. 35 D, which both lay in the green area. Pre-compaction usually improves tablet properties because it may reduce the porosity of the tablet formulation by venting the powder bed [19]. Because roller compacted granules exhibit lower porosities and a better flowability than the respective powder [195], it was assumed that any additional compaction of the roller compacted Ibuprofen DC 85 W granules besides the main compaction caused only little further improvements in the resulting tablet properties. An increase of the intermediate compaction force to 11 kN (Fig. 35 B) confirmed this observation even further. The crushing strength reached its maximum of about 90 N (red area) at any point in the design space because at least one compaction roll exerted the maximum compaction force of 11 kN. Even if all three compaction rolls were set to a force of 11 kN no increase in the crushing strength was observed. This behavior was also described for materials with plastic deformation properties in previous studies [154,196,197], where the properties of Avicel[®] tablets were barely affected by multiple compactions in contrast to tablets made of brittle excipients. Although the above mentioned factors reduced the influence of a third compaction force, at low pre-compaction (5.5 kN) and main compaction forces (5 kN), the introduction of an intermediate compaction force (5.5 kN) increased the crushing strength of Ibuprofen DC 85 W from 59 N (dark blue area) to 68 N (light blue area). This observation indicates that with more challenging tableting formulations than Ibuprofen DC 85 W, the intermediate compaction force may improve the tablet properties. The improvement of the crushing strength at low compaction forces may be advantageous for tablet formulations, which are pressure-

and temperature-sensitive. Further investigations with such formulations should be conducted in future studies.
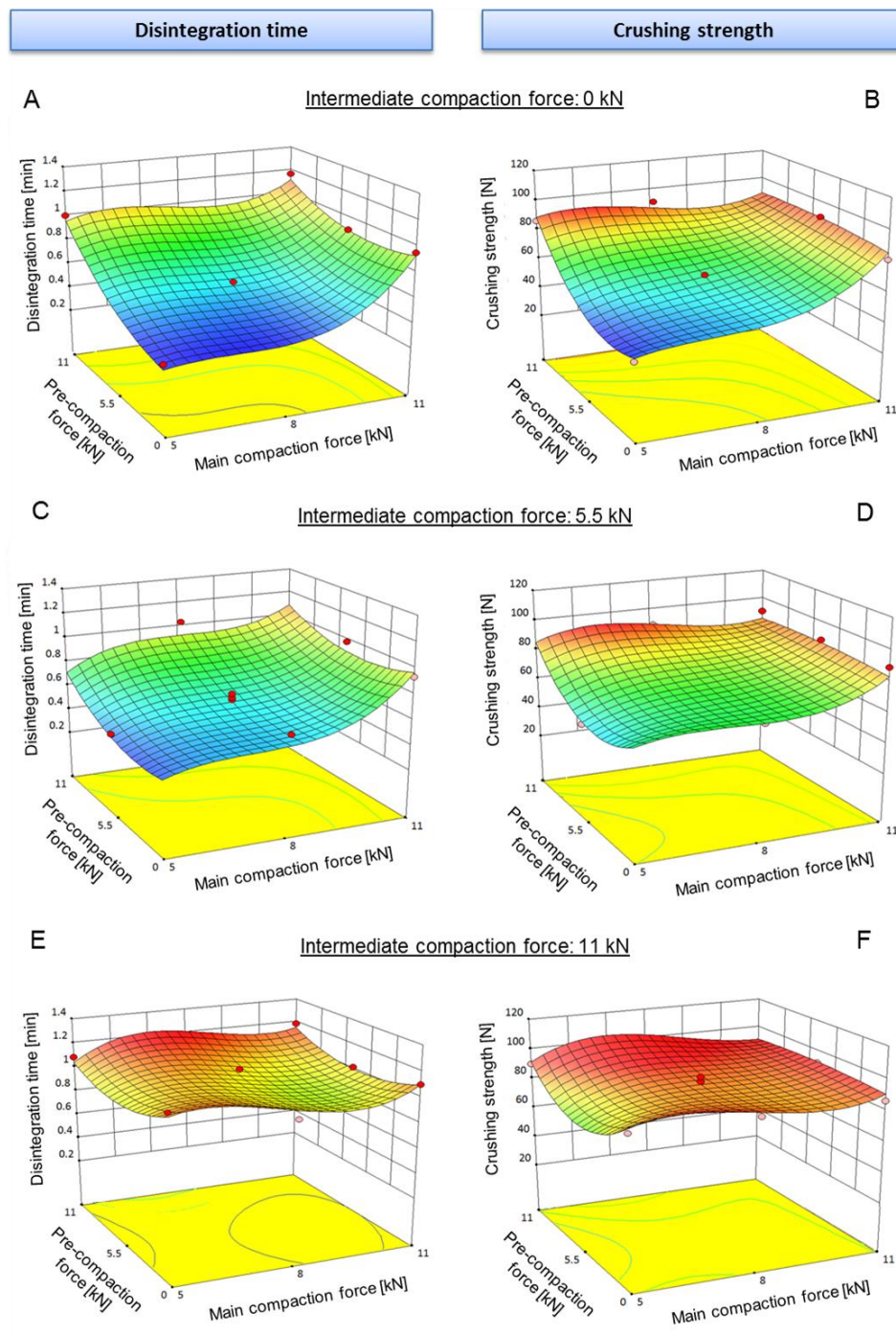


**Fig. 35:** Response surfaces obtained by plotting the disintegration time (A C, E) as well as the crushing strength (B, D, F) versus the pre-compaction force and the main compaction force displayed at 0 kN intermediate compaction force (A, B), at 5.5 kN intermediate compaction force (C, D), and at 11 kN intermediate compaction force (E, F). The red dots symbolize the recorded data points.

It is well known that the tablet disintegration time and the crushing strength typically correlate with each other, as both factors are influenced by the compaction force [33,174,198,199]. As expected, in the present study the disintegration time directly correlated with the crushing strength (Fig. 36). This behavior has already been described for Ibuprofen DC 85 W tablets [200] and was attributed among others to the increasing consolidation of the granules with increasing compaction force, which simultaneously leads to higher crushing forces and disintegration times.
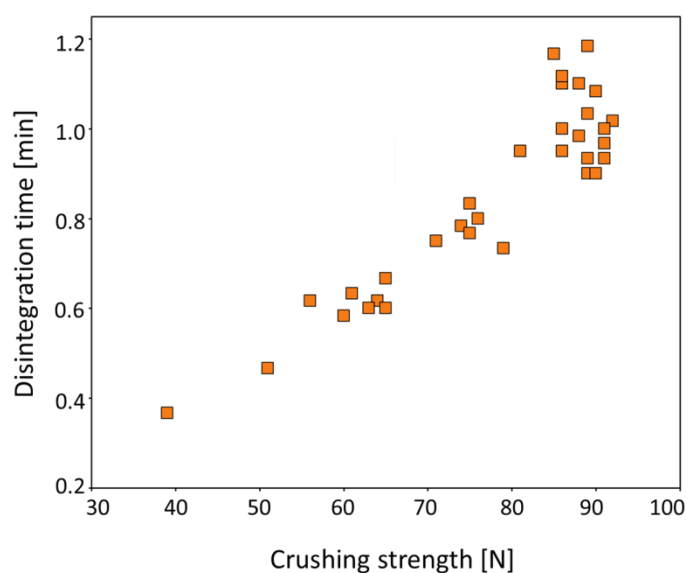


**Fig. 36:** Tablet disintegration time versus tablet crushing strength.

To validate the DoE models additional tableting runs selected at different factor levels than used to calculate the models were conducted. Subsequently, the resulting actual and predicted values for the disintegration time and crushing strength were compared (Table 15). Overall, a good prediction was achieved for most validation points with matching degrees between 95 % and 118 %. However, the models for both -the disintegration time and the crushing strength- underestimated all validation points if the main compaction force was set to the center level and the preceding compaction forces were lower than the center level. At these settings, the matching degrees of the predicted values and the actual values were between 59 % and 91 %.

It was concluded that additional design points were needed to improve the prediction in this particular area of the design space. The addition of at least one of these validation points with a bad prediction to the DoE improved the prediction of the remaining validation points up to 85 % - 93 %. However, the models already sufficiently described the tableting behavior of ibuprofen DC 85 W, no further tableting runs were conducted to improve the model.

**Table 15:** Validation of the DoE models.

| | | | predicted | | actual | | 100 x predicted/actual | |
|---|---|---|---|---|---|---|---|---|
| Pre-compaction [kN] | Intermediate compaction [kN] | Main compaction [kN] | Disintegration time [min] | Crushing strength [N] | Disintegration time [min] | Crushing strength [N] | Disintegration time [%] | Crushing strength [%] |
| 4.4 | 6.6 | 8 | 0.60 | 68.73 | 0.57 | 68 | 105.35 | 101.07 |
| 6.6 | 6.6 | 9.3 | 0.70 | 75.31 | 0.72 | 76 | 97.07 | 99.09 |
| 4.4 | 2.2 | 6.4 | 0.51 | 53.46 | 0.45 | 54 | 113.69 | 98.99 |
| 5.5 | 5.5 | 8 | 0.60 | 67.77 | 0.63 | 71 | 95.01 | 95.45 |
| 0 | 0 | 8 | 0.38 | 49.42 | 0.63 | 67 | 59.53 | 73.76 |
| 2.5 | 2.5 | 8 | 0.48 | 55.78 | 0.62 | 70 | 78.04 | 79.69 |
| 0 | 2.5 | 8 | 0.45 | 54.88 | 0.62 | 69 | 73.65 | 79.53 |
| 2.5 | 5 | 8 | 0.52 | 62.02 | 0.63 | 68 | 82.03 | 91.21 |
| 5.5 | 5.5 | 6.5 | 0.57 | 64.20 | 0.48 | 58 | 118.92 | 110.69 |
| 9 | 9 | 11.5 | 0.98 | 89.19 | 0.93 | 93 | 105.14 | 95.90 |
| 11 | 11 | 11 | 1.15 | 92.29 | 1.15 | 90 | 100.09 | 102.55 |
| 0 | 0 | 11 | 0.94 | 84.90 | 0.93 | 83 | 100.56 | 102.29 |

*4.4.2. Evaluation of the sticking behavior of Ibuprofen DC 85 W*

One of the most problematic properties of ibuprofen is its pronounced sticking to the tablet tooling such as the punch surfaces, which becomes worse over the tableting run time because of the consequent temperature increase and the temperature dependent sticking mechanism of ibuprofen. Therefore, an investigation on the sticking tendency of Ibuprofen DC 85 W was carried out with tableting settings as similar as possible to production conditions. In addition, to investigate the effect of

different punch tip coatings, a modified "compression toolbox" approach as suggested by Reed et al. [86] was applied, meaning that the tablet press was equipped with a set of differently coated punches. The resulting mean tablet mass of the produced tablets was 472.0 mg with a relative SD of 1.92 %, indicating an acceptable mass variation even though the process had not been optimized regarding mass variation and good powder flow. The produced tablets showed no signs of sticking after visual inspection. However, the visual inspection of the punch surfaces revealed a very small amount of material sticking to the punches but the sticking amount appeared to be independent of the punch tip coating. In contrast, the HPLC analysis of the Ibuprofen DC 85 W amount that stuck to the punches (Fig. 37) showed significant differences between the various punch tip coatings. On most punches, less than 100 µg of ibuprofen were detected, except for the FCG-HCP upper and lower punches and the FCG-CR+ upper punches, showing higher ibuprofen sticking amounts. In general, a good agreement between the results of the upper and lower punches with all investigated coatings except for FCG-CR+ punches was found, indicating a good reproducibility for this quantification method. The ranking of the punch tip coatings from "high" to "low" sticking tendency was conducted by considering primarily the means of the sticking amount and subsequently the respective standard deviations (SD), which resulted in the following order:

FCG TAN > FCG HCP > FCG CR+ ≈ FCG TIN ≈ FCG CRN ≈ FCG-PCR > FCG-U
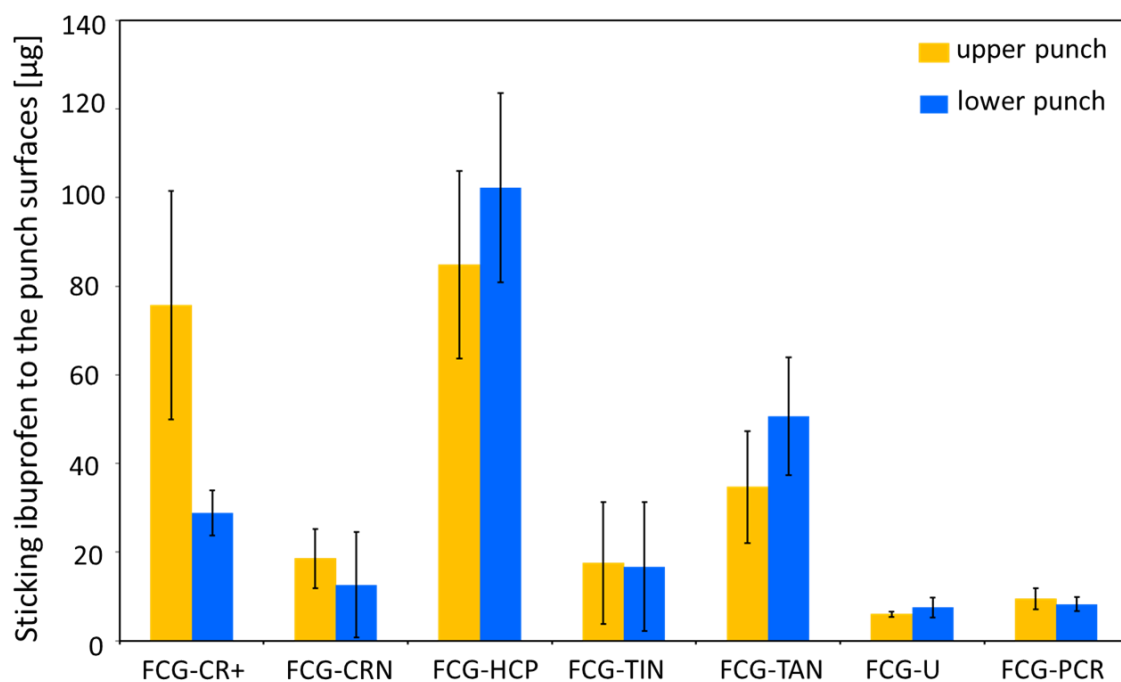
**Fig. 37:** Sticking amount of Ibuprofen DC 85 W to differently coated punches determined by HPLC after pre-compaction at 3 kN and main compaction at 8 kN. Tableting was carried out at a compaction speed of 120,000 tablets/h for 2 h without additional cooling of the tablet press (means ± SD, n = 4).

The ibuprofen formulation A, optimized for direct compaction, was tableted under the same conditions as Ibuprofen DC 85 W. However, because the tableting of only 500 tablets already caused pronounced sticking, the compaction speed had to be reduced and the die table had to be cooled. The resulting mean tablet mass was 571.3 mg with a relative SD of 1.40 %, showing that the mass variation and the powder flow were in an acceptable range. Although these adjustments reduced sticking and allowed an experimental run time of 2 h, the visual inspection of the punches revealed a distinctly higher amount of residue sticking to the punches than observed after tableting of Ibuprofen DC 85 W. Moreover, sticking was visually more pronounced with the FCG-HCP and the FCG-TAN coated punches. The HPLC quantification of the sticking ibuprofen to the differently coated punches confirmed these observations (Fig. 38). Because the previous HPLC results (Fig. 37) revealed

that sticking was similar with both upper and lower punches with the exception of FCG-CR+ upper punches, which showed an even higher sticking tendency, only the upper punches were used for all following ibuprofen quantifications by HPLC. Sticking to the differently coated punches decreased in the following order: FCG-HCP > FCG-TAN > FCG-CR+ ≈ FCG-TIN ≈ FCG-CRN ≈ FCG-PCR > FCG-U. The high SD observed with the FCG-HCP punches resulted from the varying amount of adhering residue on the punch surfaces. Compared to the results from the Ibuprofen DC 85 W experiments, with ibuprofen formulation A distinctly higher amounts of ibuprofen sticking to the FCG-HCP and FCG-TAN punches were found with maximum ibuprofen sticking amounts of up to about 850 µg. The sticking amounts on all other coated punches were approximately in the same range. Comparing the results from the Ibuprofen DC 85 W investigations with those of ibuprofen formulation A, the FCG-PCR punch coating showed a slightly higher sticking tendency, while the FCG-U punches again showed the least amount of sticking. A previous study showed that the sticking tendency of ibuprofen to the FCG-U punches was indeed very low followed by the FCG-CRN punches, if the punches were new [155]. However, after several years of usage, the anti-sticking performance of the FCG-U punches decreased while that of the FCG-CRN coated punches remained unchanged. Therefore, punch wear has to be considered before selecting a punch tip coating, especially with the FCG-U punches which are particularly susceptible to punch wear.

Overall, when comparing the above mentioned ranking orders, the results are very similar between the Ibuprofen DC 85 W and ibuprofen formulation A experiments with only FCG-CR+ and FCG-TAN as well as FCG-PCR and FCG-U having switched in order. These differences may result from the entirely different range of the amount of

Ibuprofen DC 85 W sticking to the punches, which is very low compared to that of ibuprofen formulation A.
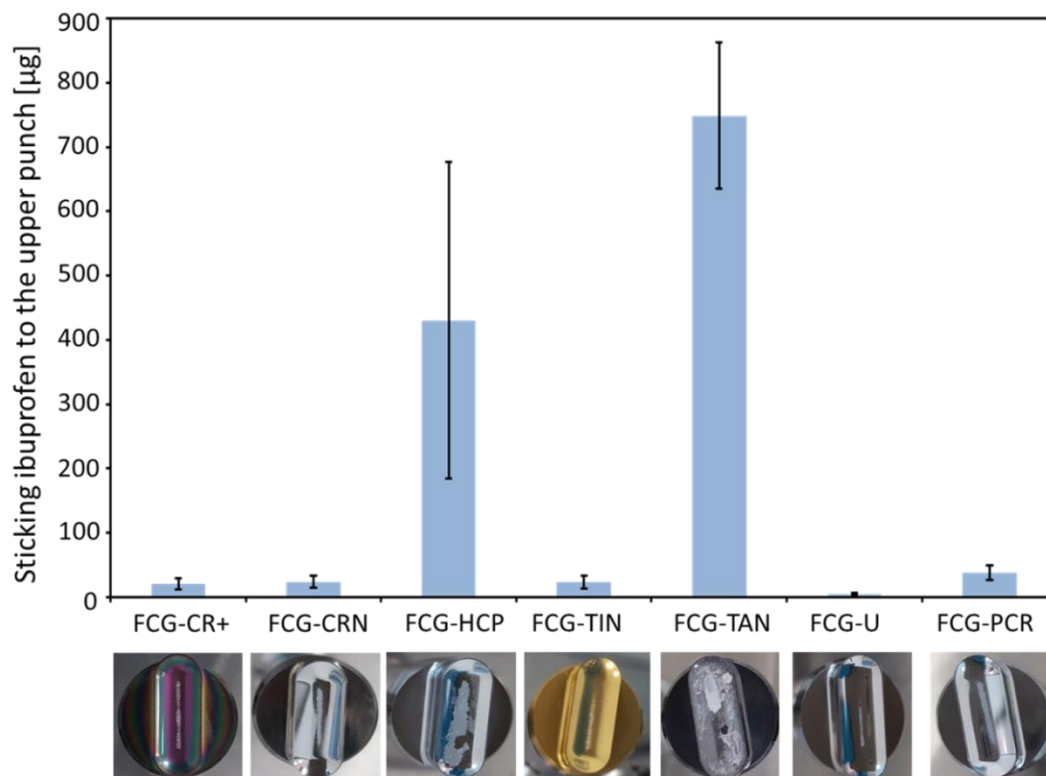


**Fig. 38:** Sticking amount of ibuprofen to differently coated upper punches determined by HPLC after tableting ibuprofen formulation A, optimized for direct compaction, at a main compaction force of 8 kN. Tableting was carried out at a compaction speed of 60,000 tablets/h for 2 h with additional vortex cooling of the tablet press (means ± SD, n = 4).

An additional investigation was conducted to assess the influence of a third (intermediate) compaction roll on the sticking tendency of ibuprofen to the tablet punches. Because of the very low sticking tendency of Ibuprofen DC 85 W, the influence on the sticking tendency was investigated with the strongly sticking ibuprofen formulation B. The mean tablet mass of the resulting tablets was 567.5 mg with a relative SD of 3.82 %, indicating that the lack of fumed silica and therefore the reduction of the flowability of formulation B caused a higher mass variation. However, no beneficial effect resulting from an additional intermediate compaction force could

be observed with regard to sticking (Fig. 39). Similar to the previous investigation with ibuprofen formulation A, the same ranking with regard to the anti-sticking performance of the punch tip coatings was found.
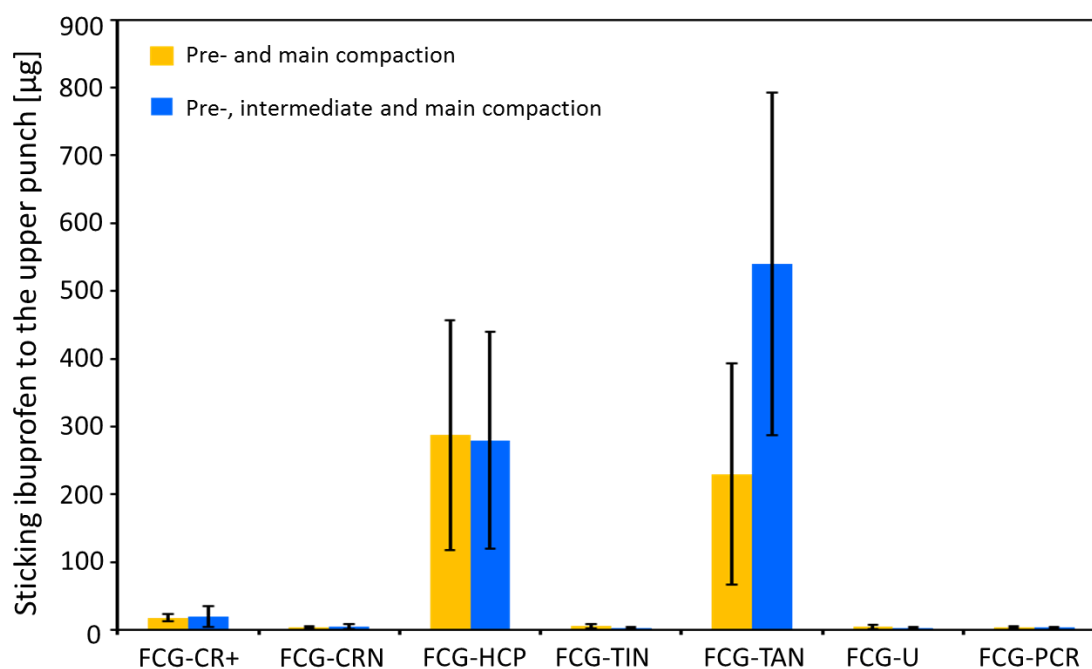


**Fig. 39:** Sticking amount of ibuprofen to differently coated upper punches after tableting ibuprofen formulation B, optimized for direct compaction, either at a pre-compaction force of 2 kN and a main compaction force of 8 kN or a pre-compaction force of 1kN, an intermediate compaction force of 3 kN and a main compaction force of 8 kN. Tableting was carried out at a compaction speed of 60,000 tablets/h over 30 - 50 min with additional vortex and external cooling of the rotary press (means ± SD, n = 4).

### 4.4.3. Conclusion

In the present study, the tableting behavior of Ibuprofen DC 85 W was investigated with regard to the tablet disintegration time, the tablet crushing strength, and the sticking tendency to punch surfaces as a function of the compaction force. With an I-optimal design of experiments, it was shown that the tablet disintegration was mainly prolonged if the highest compaction force level (11 kN) was applied. It was also dependent on the compaction forces preceding the main compaction such as the pre-compaction force and to a lower extent the intermediate compaction force. However, tablet disintegration was very fast in general and met the Ph. Eur. criteria of the tablet disintegration for uncoated tablets regardless of the applied compaction force, showing that with Ibuprofen DC 85 W tablets with fast disintegration could be obtained. In contrast to the disintegration time, the tablet crushing strength was mainly dependent on the highest compaction force level applied to Ibuprofen DC 85 W and was not influenced by additional pre-  or intermediate compactions. An acceptable hardness could be achieved with a compaction force of 11 kN. The results further indicate that an intermediate compaction force may be of benefit with more challenging tablet formulations than Ibuprofen DC 85 W. Tablet mass variation was in an acceptable range, showing a good flowability of this ibuprofen grade. Interestingly, the investigations regarding the sticking behavior showed that sticking was considerably less pronounced with Ibuprofen DC 85 W than with other ibuprofen powder formulations optimized for direct compaction. The punch tip coating had a high influence on sticking, and the application of either FCG-TIN, FCG-CRN or FCG-PCR-coated punches is recommended. With regard to a fast disintegration time, sufficient tablet hardness, good powder flowability, and a reduced sticking tendency, tablets meeting the Ph.Eur. criteria were produced in the present study. It can therefore be concluded that Ibuprofen DC 85 W is very well suited for long-term direct

compaction runs on a production scale without any additional powder processing. The choice of a suitable punch tip coating can further prolong tableting run time. Further investigations regarding the reasons for the reduced sticking tendency of Ibuprofen DC 85 W and the influence of the intermediate compaction force on challenging tablet formulations should be conducted in the future.

## References

[1] W. Brockedon, Shaping Pills, Lozenges and Black Lead by Pressure in Dies.

[2] M. Çelik, The past, Present, and Future of Tableting Technology, Drug Dev. Ind. Pharm. 22 (2008) 1–10.

[3] W.A. Ritschel, A. Bauer-Brandl, Die Tablette: Handbuch der Entwicklung, Herstellung und Qualitätssicherung, 2nd ed., ECV - Editio Cantor Verlag, Aulendorf, 2002.

[4] N. Ahmat, H. Ugail, G.G. Castro, Method of modelling the compaction behaviour of cylindrical pharmaceutical tablets, Int. J. Pharm. 405 (2011) 113–121.

[5] S.S. Bharate, S.B. Bharate, A.N. Bajaj, Incompatibilities of pharmaceutical excipients with active pharmaceutical ingredients: a comprehensive review, J. Excip. Food Chem. 1 (2010) 3–26.

[6] S. Patel, A.K. Bansal, Prediction of mechanical properties of compacted binary mixtures containing high-dose poorly compressible drug, Int. J. Pharm. 403 (2011) 109–114.

[7] C.-Y. Wu, S.M. Best, A.C. Bentham, B.C. Hancock, W. Bonfield, Predicting the tensile strength of compacted multi-component mixtures of pharmaceutical powders, Pharm. Res. 23 (2006) 1898–1905.

[8] M. Jivraj, L.G. Martini, C.M. Thomson, An overview of the different excipients useful for the direct compression of tablets, Pharm. Sci. Technol. Today 3 (2000) 58–63.

[9] G.K. Bolhuis, N.A. Armstrong, Excipients for direct compaction--an update, Pharm. Dev. Technol. 11 (2006) 111–124.

[10] M.C. Gohel, A review of co-processed directly compressible excipients, J. Pharm. Pharmaceut. Sci. 8 (2005) 76–93.

[11] H.G. Kristensen, T. Schaefer, Granulation: A Review on Pharmaceutical Wet-Granulation, Drug Dev. Ind. Pharm. 13 (1987) 803–872.

[12] J. Cooper, J.E. Rees, Tableting research and technology, J. Pharm. Sci. 61 (1972) 1511–1555.

[13] M.D. Tousey, The granulation process 101, Pharm. Technol. (2002) 8–13.

[14] A. Faure, P. York, R.C. Rowe, Process control and scale-up of pharmaceutical wet granulation processes: A review, Eur. J. Pharm. Biopharm. 52 (2001) 269–277.

[15] I. Saniocki, New insights into tablet sticking : characterization and quantification of sticking to punch surfaces during tablet manufacture by direct compaction. PhD thesis, Hamburg, Germany, 2014.

[16] M. Šantl, I. Ilić, F. Vrečer, S. Baumgartner, A compressibility and compactibility study of real tableting mixtures: The impact of wet and dry granulation versus a direct tableting mixture, Int. J. Pharm. 414 (2011) 131–139.

[17] S. Dhumal, P.A. Kulkarni, V.S. Kashikar, J. Baweja, M. Thottasseri, A review: Roller compaction for tablet dosage form development, Res. Rev. J. Pharm. Pharm. Sci. 2 (2013) 68–73.

[18] P. Ridgway-Watt, A. Chittey, H. Thacker, A. Ridgway-watt, Tablet and Capsule Machine Instrumentation, Pharmaceutical Press, 2008.

[19] I.C. Sinka, F. Motazedian, A. Cocks, K.G. Pitt, The effect of processing parameters on pharmaceutical tablet properties, Powder Technol. 189 (2009) 276–284.

[20] W.R. Vezin, H.M. Pang, K.A. Khan, S. Malkowska, The effect of precompression in a rotary machine on tablet strength, Drug Dev. Ind. Pharm. 9 (1983) 1465–1474.

[21] P.E. Wray, The physics of tablet compaction revisited, Drug Dev. Ind. Pharm. 18 (1992) 627–658.

[22] E.N. Hiestand, J.E. Wells, C.B. Peot, J.F. Ochs, Physical processes of tableting, J. Pharm. Sci. 66 (1977) 510–519.

[23] D. Zhou, Y. Qiu, Understanding material properties in pharmaceutical product development and manufacturing: Powder flow and mechanical properties, J. Validat. Technol. 16 (2010) 65–77.

[24] K. van der Voort Maarschalk, K. Zuurman, H. Vromans, G.K. Bolhuis, C.F. Lerk, Stress relaxation of compacts produced from viscoelastic materials, Int. J. Pharm. 151 (1997) 27–34.

[25] E. Nelson, S.M. Naqvi, L.W. Busse, T. Higuchi, The Physics of Tablet Compression, J. Am. Pharm. Assoc. 43 (1954) 596–602.

[26] A. Delacourte, J.C. Guyot, P. Colombo, P.L. Catellani, Effectiveness of Lubricants and Lubmcation Mechanism in Tablet Technology, Drug Dev. Ind. Pharm. 21 (2008) 2187–2199.

[27] S. Jain, Mechanical properties of powders for compaction and tableting: An overview, Pharm. Sci. Technol. Today 2 (1999) 20–31.

[28] Tabletting: the issues facing today's manufacturers, Pharm. Technol. Eur. 22 (2010).

[29] A.R. Fassihi, I. Kanfer, Effect of compressibility and powder flow properties on tablet weight variation, Drug Dev. Ind. Pharm. 12 (2008) 1947–1966.

[30] C.-Y. Wu, S.M. Best, A.C. Bentham, B.C. Hancock, W. Bonfield, A simple predictive model for the tensile strength of binary tablets, Eur. J. Pharm. Sci. 25 (2005) 331–336.

[31] J. Dressman, J. Krämer (Eds.), Pharmaceutical dissolution testing, Taylor & Francis, Boca Raton, FL, 2005.

[32] R.C. Moreton, Disintegrants in tableting, in: L.L. Augsburger, S.W. Hoag (Eds.), Pharmaceutical dosage forms. Tablets, 3rd ed., Informa Healthcare, New York, N.Y., 2008, pp. 217–249.

[33] E. Lahdenpää, M. Niskanen, J. Yliruusi, Crushing strength, disintegration time and weight variation of tablets compressed from three Avicel® PH grades and their mixtures, Eur. J. Pharm. Biopharm. 43 (1997) 315–322.

[34] I. Saniocki, A. Sakmann, C.S. Leopold, How suitable is the measurement of take-off forces for detection of sticking during direct compression of various ibuprofen tablet formulations?, Pharm. Dev. Technol. 18 (2013) 257–265.

[35] F. Waimer, M. Krumme, P. Danz, U. Tenter, P.C. Schmidt, A novel method for the detection of sticking of tablets, Pharm. Dev. Technol. 4 (1999) 359–367.

[36] Dale Natoli, Tooling for pharmaceutical processing, in: L.L. Augsburger, S.W. Hoag (Eds.), Pharmaceutical dosage forms. Tablets, 3rd ed., Informa Healthcare, New York, N.Y., 2008, pp. 1–48.

[37] E.E. Borzunov, V.M. Dekhtyarenko, S.A. Nosovitskaya, Quality control and use of the press tool of tableting machines, Pharm. Chem. J. 1 (1967) 231–233.

[38] M. Otz, H. Thoma, Effects of the metal type and the roughness of the die wall on the expended work for tablet ejection, Pharm. Dev. Technol. 5 (2000) 19–26.

[39] A.H. Gerhardt, Compression tooling surface treatments—options for resolving corrosion, wear, filming, and tablet defects, J. GXP Compliance 13 (2009) 68–74.

[40] Y.A. Alimov, An investigation of the matrix of the press tool in the tableting of drugs, Pharm. Chem. J. 9 (1975) 450–452.

[41] V. Hyvärinen, M. Sorjonen, K.-E. Peiponen, R. Silvennoinen, T. Niskanen, J. Kalliokoski, On all-optical laser cleaning and inspection of contaminated concave metal surfaces, Opt. Lasers Eng. 33 (2000) 311–315.

[42] C.J. Swartz, J. Cooper, S. Weinstein, J. Windheuser, A punch and die control program and its contribution to tableting technology, J. Pharm. Sci. 51 (1962) 1181–1187.

[43] V. Hyvärinen, K.-E. Peiponen, R. Silvennoinen, P. Raatikainen, P. Paronen, T. Niskanen, Optical inspection of punches: Flat surfaces, Eur. J. Pharm. Biopharm. 49 (2000) 87–90.

[44] V. Hyvärinen, Diffractive optical element based sensor for surface quality inspection of concave punches, Eur. J. Pharm. Biopharm. 49 (2000) 167–169.

[45] J.J. Wang, T. Li, S.D. Bateman, R. Erck, K.R. Morris, Modeling of adhesion in tablet compression-I. Atomic force microscopy and molecular simulation, J. Pharm. Sci. 92 (2003) 798–814.

[46] M. Roberts, J.L. Ford, G.S. MacLeod, J.T. Fell, G.W. Smith, P.H. Rowe, Effects of surface roughness and chrome plating of punch tips on the sticking tendencies of model ibuprofen formulations, J. Pharm. Pharmacol. 55 (2003) 1223–1228.

[47] S. Paul, L.J. Taylor, B. Murphy, J. Krzyzaniak, N. Dawson, M.P. Mullarney, P. Meenan, C.C. Sun, Mechanism and kinetics of punch sticking of pharmaceuticals, J. Pharm. Sci. 106 (2017) 151–158.

[48] S. Paul, L.J. Taylor, B. Murphy, J.F. Krzyzaniak, N. Dawson, M.P. Mullarney, P. Meenan, C.C. Sun, Powder properties and compaction parameters that influence punch sticking propensity of pharmaceuticals, Int. J. Pharm. 521 (2017) 374–383.

[49] T.S. McDermott, J. Farrenkopf, A. Hlinak, J.P. Neilly, D. Sauer, A material sparing method for quantitatively measuring tablet sticking, Powder Technol. 212 (2011) 240–252.

[50] H. Leuenberger, B.D. Rohera, Fundamentals of powder compression. I. The compactibility and compressibility of pharmaceutical powders, Pharm. Res. 3 (1986) 12–22.

[51] M. Bunker, J. Zhang, R. Blanchard, C.J. Roberts, Characterising the surface adhesive behavior of tablet tooling components by atomic force microscopy, Drug Dev. Ind. Pharm. 37 (2011) 875–885.

[52] S. Swaminathan, B. Ramey, J. Hilden, C. Wassgren, Characterizing the powder punch-face adhesive interaction during the unloading phase of powder compaction, Powder Technol. 315 (2017) 410–421.

[53] F. Podczeck, Particle-particle adhesion in pharmaceutical powder handling, Imperial College Press; Distributed by World Scientific Pub, London, River Edge, NJ, 1998.

[54] H.-J. Butt, K. Graf, M. Kappl, Physics and chemistry of interfaces, Wiley-VCH, Weinheim, 2003.

[55] E.M. Lifshitz, The theory of molecular attractive forces between solids., Soviet Physics 2 (1956) 73–83.

[56] C. Ahlneck, G. Alderborn, Moisture adsorption and tabletting. II. The effect on tensile strength and air permeability of the relative humidity during storage of tablets of 3 crystalline materials, Int. J. Pharm. 56 (1989) 143–150.

[57] S. Malamataris, P. Goidas, A. Dimitriou, Moisture sorption and tensile strength of some tableted direct compression excipients, Int. J. Pharm. 68 (1991) 51–60.

[58] K.K. Lam, J.M. Newton, Influence of particle size on the adhesion behaviour of powders, after application of an initial press-on force, Powder Technol. 73 (1992) 117–125.

[59] J.N. Israelachvili, Intermolecular and surface forces, 3rd ed., Elsevier, Amsterdam [etc.], op. 2011.

[60] L. Samiei, K. Kelly, L. Taylor, B. Forbes, E. Collins, M. Rowland, The influence of electrostatic properties on the punch sticking propensity of pharmaceutical blends, Powder Technol. 305 (2017) 509–517.

[61] J. Visser, Particle adhesion and removal: A Review, Particul. Sci. Technol. 13 (1995) 169–196.

[62] N. Rasenack, B.W. Müller, Crystal habit and tableting behavior, Int. J. Pharm. 244 (2002) 45–57.

[63] P. Di Martino, M. Beccerica, E. Joiris, G.F. Palmieri, A. Gayot, S. Martelli, Influence of crystal habit on the compression and densification mechanism of ibuprofen, J. Cryst. Growth 243 (2002) 345–355.

[64] D. Kaul, N.T. Nguyen, S. Venkataram, Crystal habit modifications and altered tabletting characteristics, Int. J. Pharm. 88 (1992) 345–350.

[65] N. Rasenack, B.W. Müller, Properties of ibuprofen crystallized under various conditions: a comparative study, Drug Dev. Ind. Pharm. 28 (2002) 1077–1089.

[66] N. Rasenack, B.W. Müller, Ibuprofen crystals with optimized properties, Int. J. Pharm. 245 (2002) 9–24.

[67] K. Zuurman, K. van der Voort Maarschalk, G.K. Bolhuis, Effect of magnesium stearate on bonding and porosity expansion of tablets produced from materials with different consolidation properties, Int. J. Pharm. 179 (1999) 107–115.

[68] T.A. Miller, P. York, Pharmaceutical tablet lubrication, Int. J. Pharm. 41 (1988) 1–19.

[69] S. Swaminathan, J. Hilden, B. Ramey, C. Wassgren, Modeling the formation of debossed features on a pharmaceutical tablet, J. Pharm. Innov. 11 (2016) 214–230.

[70] S.R. Bechard, G.R.B. Down, Infrared imaging of pharmaceutical materials undergoing compaction, Pharm. Res. 9 (1992) 521–528.

[71] P. Schleier, A. Prochnau, A.M. Schmidt-Westhausen, H. Peters, J. Becker, T. Latz, J. Jackowski, E.U. Peters, G.E. Romanos, B. Zahn, J. Ludemann, J. Maares, B. Petersen, Ibuprofen sodium dihydrate, an ibuprofen formulation with improved absorption characteristics, provides faster and greater pain relief than ibuprofen acid, Int. J. Clin. Pharmacol. Ther. 45 (2007) 89–97.

[72] J. Lee, Intrinsic adhesion force of lubricants to steel surface, J. Pharm. Sci. 93 (2004) 2310–2318.

[73] D. Weber, Y. Pu, C.L. Cooney, Quantification of Lubricant Activity of Magnesium Stearate by Atomic Force Microscopy, Drug Dev. Ind. Pharm. 34 (2008) 1097–1099.

[74] J.-I. Kikuta, N. Kitamori, Effect of mixing time on the lubricating properties of magnesium stearate and the final characteristics of the compressed tablets, Drug Dev. Ind. Pharm. 20 (2008) 343–355.

[75] R.E. Gordon, C.L. VanKoevering, D.J. Reits, Utilization of differential scanning calorimetry in the compatibility screening of ibuprofen with the stearate lubricants and construction of phase diagrams, Int. J. Pharm. 21 (1984) 99–105.

[76] M. Roberts, J.L. Ford, G.S. MacLeod, J.T. Fell, G.W. Smith, P.H. Rowe, A.M. Dyas, Effect of lubricant type and concentration on the punch tip adherence of model ibuprofen formulations, J. Pharm. Pharmacol. 56 (2004) 299–305.

[77] J. Li, Y. Wu, Lubricants in pharmaceutical solid dosage forms, Lubricants 2 (2014) 21–43.

[78] J. Muzikova, S. Muchova, A study of a co-processed dry binder composed of microcrystalline cellulose and glycerol monostearate, Ceska Slov. Farm. 61 (2012) 229–233.

[79] S. Aoki, K. Danjo, Effect of tableting conditions on the sticking of tablet using ibuprofen, Yakugaku Zasshi 118 (1998) 511–518.

[80] K. Kakimi, T. Niwa, K. Danjo, Influence of compression pressure and velocity on tablet sticking, Chem. Pharm. Bull. 58 (2010) 1565–1568.

[81] K. Danjo, K. Kamiya, A. Otsuka, Effect of temperature on the sticking of low melting point materials, Chem. Pharm. Bull. 41 (1993) 1423–1427.

[82] L. Seton, M. Roberts, F. Ur-Rehman, Compaction of recrystallised ibuprofen, Chem. Eng. J. 164 (2010) 449–452.

[83] B. Bhushan, Adhesion and stiction: Mechanisms, measurement techniques, and methods for reduction, J. Vac. Sci. Technol. B 21 (2003) 2262.

[84] E. Beach, G. Tormoen, J. Drelich, R. Han, Pull-off Force Measurements between Rough Surfaces by Atomic Force Microscopy, J. Colloid Interface Sci. 247 (2002) 84–99.

[85] M. Bunker, J. Zhang, R. Blanchard, C.J. Roberts, Characterising the surface adhesive behavior of tablet tooling components by atomic force microscopy, Drug Dev. Ind. Pharm. 37 (2011) 875–885.

[86] K. Reed, C. Davies, K. Kelly, Tablet sticking: Using a 'compression toolbox' to assess multiple tooling coatings options, Powder Technol. 285 (2015) 103–109.

[87] S. Schumann, G.D. Searle, The effects of chromium nitride ION bombardment treatment of tablet tooling on tablet adherence, Drug Dev. Ind. Pharm. 18 (1992) 1037–1061.

[88] T. Uchimoto, Y. Iwao, T. Yamamoto, K. Sawaguchi, T. Moriuchi, S. Noguchi, S. Itai, Newly developed surface modification punches treated with alloying techniques reduce sticking during the manufacture of ibuprofen tablets, Int. J. Pharm. 441 (2013) 128–134.

[89] F. Podczeck, J.M. Newton, M.B. James, The influence of physical properties of the materials in contact on the adhesion strength of particles of salmeterol base

and salmeterol salts to various substrate materials, J. Adhes. Sci. Technol. 10 (1996) 257–268.

[90] S.C. Colbeck, Capillary bonding of wet surfaces - the effects of contact angle and surface roughness, J. Adhes. Sci. Technol. 11 (1997) 359–371.

[91] J. Neilly, A. Vogt, W. Dziki, Characterization of Sticking Residue on Tablet Punch Faces by Scanning Electron Microscopy and X-Ray Mapping, Microsc. Microanal. 15 (2009) 18–19.

[92] J.V. Thomas, Evaluation and study on the adhesion of powder onto punch faces during tablet compaction. M.S. thesis, Materials Science & Engineering, Drexel University, 2015.

[93] D.J. Whitehouse, Handbook of surface and nanometrology, 2nd ed., CRC press, Boca Raton, 2011.

[94] L. Blunt, X. Jiang, Advanced techniques for assessment surface topography: Development of a basis for 3D surface texture standards "Surfstand", Kogan Page Science, Sterling, 2007.

[95] L. de Chiffre, P. Lonardo, H. Trumpold, D.A. Lucca, G. Goch, C.A. Brown, J. Raja, H.N. Hansen, Quantitative characterisation of surface texture, CIRP Annals - Manufacturing Technology 49 (2000) 635–652.

[96] ASME B46.1, Surface texture (surface roughness, waviness and lay), American Society of Mechanical Engineers, New York, N.Y.

[97] ISO 12781, Geometrical product specifications (GPS) - flatness - part 1: Vocabulary and parameters of flatness (ISO 12781-1:2011), International Organization for Standardization.

[98] ISO 25178, Geometrical product specifications (GPS) - surface texture: Areal - part 1: Indication of surface texture (ISO 25178-1:2016), International Organization for Standardization.

[99] EUR 15178N, The development of methods for the characterisation of roughness in three dimensions, Ken Stout Liam Blunt W. Dong E. Mainsah N. Luo T. Mathia P. Sullivan H. Zahouani; Commission of the European Communities.

[100]  R. Deltombe, K.J. Kubiak, M. Bigerelle, How to select the most relevant 3D roughness parameters of a surface, Scanning 36 (2014) 150–160.

[101]  W. Grzesik, Prediction of the functional performance of machined components based on surface topography: State of the Art, J. Mater. Eng. Perform. 25 (2016) 4460–4468.

[102]  S.G. Prolongo, G. Rosario, A. Ure?a, Study of the effect of substrate roughness on adhesive joints by SEM image analysis, J. Adhes. Sci. Technol. 20 (2006) 457–470.

[103]  E. Dekempeneer, K. van Acker, K. Vercammen, J. Meneve, D. Neerinck, S. Eufinger, W. Pappaert, M. Sercu, J. Smeets, Abrasion resistant low friction diamond-like multilayers, Surf. Coat. Technol. 142 (2001) 669–673.

[104]  C.-C. Sun, S.-C. Lee, W.-C. Hwang, J.-S. Hwang, I.-T. Tang, Y.-S. Fu, Surface free energy of alloy nitride coatings deposited using closed field unbalanced magnetron sputter ion plating, Mater. Trans. 47 (2006) 2533–2539.

[105]  T. Hoornaert, Z.K. Hua, J.H. Zhang, Hard Wear-Resistant Coatings: A Review, in: J. Luo (Ed.), Advanced Tribology, Springer, Berlin, London, 2009, pp. 774–779.

[106]  W. König, R. Fritsch, D. Kammermeier, Physically vapor deposited coatings on tools: Performance and wear phenomena, Surf. Coat. Technol. 49 (1991) 316–324.

[107]  B. Navinšek, P. Panjan, I. Milošev, PVD coatings as an environmentally clean alternative to electroplating and electroless processes, Surf. Coat. Technol. 116 (1999) 476–487.

[108]  P. Hones, R. Consiglio, N. Randall, F. Leacutevy, Mechanical properties of hard chromium tungsten nitride coatings, Surf. Coat. Technol. 125 (2000) 179–184.

[109]  F. Meng, N. Chen, Z. Chen, Hard chromium coating effects on tribological performances for nonlubricated and lubricated spindle of cotton picker, P. I. Mech. Eng. 230 (2016) 446–453.

[110]  M. Costa, M. Cioffi, H. Voorwald, V.A. Guimarães, An investigation on sliding wear behavior of PVD coatings, Tribol. Int. 43 (2010) 2196–2202.

[111]  G.G. Fuentes, R. Rodriguez, J.C. Avelar-Batista, J. Housden, F. Montalá, L.J. Carreras, A.B. Cristóbal, J.J. Damborenea, T.J. Tate, Recent advances in the chromium nitride PVD process for forming and machining surface protection, J. Mater. Process. Technol. 167 (2005) 415–421.

[112]  P. Hedenqvist, S. Jacobson, S. Hogmark, Tribological PVD coatings — characterisation of mechanical properties, Surf. Coat. Technol. 97 (1997) 212–217.

[113]  B. Navinšek, P. Panjan, I. Milošev, Industrial applications of CrN (PVD) coatings, deposited at high and low temperatures, Surf. Coat. Technol. 97 (1997) 182–191.

[114]  E.J. Bienk, H. Reitz, N.J. Mikkelsen, Wear and friction properties of hard PVD coatings, Surf. Coat. Technol. 76-77 (1995) 475–480.

[115]  Y.C. Chim, X.Z. Ding, X.T. Zeng, S. Zhang, Oxidation resistance of TiN, CrN, TiAlN and CrAlN coatings deposited by lateral rotating cathode arc, Thin Solid Films 517 (2009) 4845–4849.

[116] W. Brandl, C. Gendig, Corrosion behaviour of hybrid coatings, Thin Solid Films 290-291 (1996) 343–347.

[117] R. González, A. Hernández Battez, D. Blanco, J.L. Viesca, A. Fernández-González, Lubrication of TiN, CrN and DLC PVD Coatings with 1-Butyl-1-Methylpyrrolidinium tris(pentafluoroethyl)trifluorophosphate, Tribol. Lett. 40 (2010) 269–277.

[118] R.K. Roy, K.-R. Lee, Biomedical applications of diamond-like carbon coatings: A review, J. Biomed. Mater. Res. Part B Appl. Biomater. 83 (2007) 72–84.

[119] G. Habenicht, Kleben: Grundlagen, Technologien, Anwendungen, 6th ed., Springer, Berlin, 2009.

[120] A. Dupré, P. Dupré, Théorie mécanique de la chaleur, Gauthier-Villars, 1869.

[121] F. Podczeck, J.M. Newton, M.B. James, The adhesion force of micronized Salmeterol Xinafoate particles to pharmaceutically relevant surface materials, J. Phys. D: Appl. Phys. 29 (1996) 1878–1884.

[122] J.C. Hooton, C.S. German, S. Allen, M.C. Davies, C.J. Roberts, S.J.B. Tendler, P.M. Williams, Characterization of particle-interactions by atomic force microscopy: effect of contact area, Pharm. Res. 20 (2003) 508–514.

[123] F.M. Fowkes, Attractive forces at interfaces, Ind. Eng. Chem. 56 (1964) 40–52.

[124] B. Janczuk, A. Zdziennicka, A study on the components of surface free energy of quartz from contact angle measurements, J. Mater. Sci. 29 (1994) 3559–3564.

[125] D.K. Owens, R.C. Wendt, Estimation of the surface free energy of polymers, J. Appl. Polym. Sci. 13 (1969) 1741–1747.

[126] D.H. Kaelble, Dispersion-polar surface tension properties of organic solids, J. Adhes. 2 (1970) 66–81.

[127]   W. Rabel, Einige Aspekte der Benetzungstheorie und ihre Anwendung auf die Untersuchung und Veränderung der Oberflächeneigenschaften von Polymeren, Farbe Lack 77 (1971) 997–1005.

[128]   G. Cappelletti, S. Ardizzone, D. Meroni, G. Soliveri, M. Ceotto, C. Biaggi, M. Benaglia, L. Raimondi, Wettability of bare and fluorinated silanes: A combined approach based on surface free energy evaluations and dipole moment calculations, J. Colloid Interface Sci. 389 (2013) 284–291.

[129]   M.J. Anderson, P.J. Whitcomb, DOE simplified: Practical tools for effective experimentation, Productivity Press, New York, 2015.

[130]   N. Bolourtchian, N. Hadidi, S.M. Foroutan, B. Shafaghi, Formulation and optimization of captopril sublingual tablet using D-optimal design sublingual tablet using D-optimal design., Iran. J. Pharm. Res. 7 (2010) 259-267.

[131]   M.J. Anderson, P.J. Whitcomb, RSM simplified: Optimizing processes using response surface methods for design of experiments, Productivity Press, New York, 2005.

[132]   N. Kettaneh-Wold, Use of experimental design in the pharmaceutical industry, J. Pharm. Biomed. Anal. 9 (1991) 605–610.

[133]   B. Jones, P. Goos, I-optimal versus D-optimal split-plot response surface designs., J. Qual. Technol. 44 (2012) 85–101.

[134]   E. Kuram, B. Ozcelik, M. Bayramoglu, E. Demirbas, B.T. Simsek, Optimization of cutting fluids and cutting parameters during end milling by using D-optimal design of experiments, J. Clean. Prod. 42 (2013) 159–166.

[135]   R.H. Hardin, N. Sloane, A new approach to the construction of optimal designs, J. Stat. Plan. Inference 37 (1993) 339–369.

[136]   D.P. Mays, Optimal central composite designs in the presence of dispersion effects, J. Qual. Technol. 31 (1999) 398–407.

[137]  C.M. Anderson-Cook, C.M. Borror, D.C. Montgomery, Response surface design evaluation and comparison, J. Stat. Plan. Inference 139 (2009) 629–641.

[138]  R.K. Meyer, C.J. Nachtsheim, The Coordinate-Exchange Algorithm for Constructing Exact Optimal Experimental Designs, Technometrics 37 (1995) 60–69.

[139]  A. Heredia-Langner, W.M. Carlyle, D.C. Montogomery, C.M. Borror, G.C. Runger, Genetic algorithms for the construction of D-optimal designs., J. Qual. Technol. 35 (2003) 28–46.

[140]  L.X. Yu, Pharmaceutical quality by design: Product and process development, understanding, and control, Pharm. Res. 25 (2008) 781–791.

[141]  I. Saniocki, A. Sakmann, C.S. Leopold, Direct compression of ibuprofen-containing powder blends: Influence of the ibuprofen grade on the flow and compaction properties of an ibuprofen tablet formulation, Pharm. Ind. 74 (2012) 1842–1852.

[142]  A. Nokhodchi, A. Homayouni, R. Araya, W. Kaialy, W. Obeidat, K. Asare-Addo, Crystal engineering of ibuprofen using starch derivatives in crystallization medium to produce promising ibuprofen with improved pharmaceutical performance, RSC Adv. 5 (2015) 46119–46131.

[143]  M. Jbilou, A. Ettabia, A.M. Guyot-Hermann, J.C. Guyot, Ibuprofen agglomerates preparation by phase separation, Drug Dev. Ind. Pharm. 25 (1999) 297–305.

[144]  M. Roberts, J.L. Ford, G.S. MacLeod, J.T. Fell, G.W. Smith, P.H. Rowe, A.M. Dyas, Effect of punch tip geometry and embossment on the punch tip adherence of a model ibuprofen formulation, J. Pharm. Pharmacol. 56 (2004) 947–950.

[145]  A. Hutchins, B.C. MacDonald, M.P. Mullarney, Assessing tablet-sticking propensity, Pharm. Technol. 36 (2012) 57–62.

[146]  R. Bushra, M.H. Shoaib, N. Aslam, D. Hashmat, M. Rehman, Formulation development and optimization of ibuprofen tablets by direct compression method., Pak. J. Pharm. Sci. 21 (2008) 113–120.

[147]  A. Nokhodchi, M.H. Rubinstein, H. Larhrib, J.C. Guyot, The effect of moisture on the properties of ibuprofen tablets, Int. J. Pharm. 118 (1995) 191–197.

[148]  L. Qu, Q.T. Zhou, T. Gengenbach, J.A. Denman, P.J. Stewart, K.P. Hapgood, M. Gamlen, D.A.V. Morton, Investigation of the potential for direct compaction of a fine ibuprofen powder dry-coated with magnesium stearate, Drug Dev. Ind. Pharm. 41 (2015) 825–837.

[149]  Q. Zhou, L. Shi, W. Marinaro, Q. Lu, C.C. Sun, Improving manufacturability of an ibuprofen powder blend by surface coating with silica nanoparticles, Powder Technol. 249 (2013) 290–296.

[150]  K. Meyer-Boehm, K. Kolter, A. Quadir, Method for production of directly compressible ibuprofen formulations, 2014.

[151]  K. Meyer-Boehm, H. Einig, New ibuprofen direct compression formula, ExAct (2006) 2–4.

[152]  C.E. Ruegger, M. Celik, The influence of varying precompaction and main compaction profile parameters on the mechanical strength of compacts, Pharm. Dev. Technol. 5 (2000) 495–505.

[153]  O.F. Akande, M.H. Rubinstein, P.H. Rowe, J.L. Ford, Effect of compression speeds on the compaction properties of a 1: 1 paracetamol–microcrystalline cellulose mixture prepared by single compression and by combinations of precompression and main compression, Int. J. Pharm. 157 (1997) 127–136.

[154]  M.J.D. Gamlen, L.G. Martini, K.G. Al Obaidy, Effect of repeated compaction of tablets on tablet properties and work of compaction using an instrumented laboratory tablet press, Drug Dev. Ind. Pharm. 41 (2015) 163–169.

[155]  C. Al-Karawi, I. Lukášová, A. Sakmann, C.S. Leopold, Novel aspects on the direct compaction of ibuprofen with special focus on sticking, Powder Technol. 317 (2017) 370–380.

[156]  T.J. Legg, A.L. Laurent, R. Leyva, D. Kellstein, Ibuprofen sodium is absorbed faster than standard Ibuprofen tablets: Results of two open-label, randomized, crossover pharmacokinetic studies, Drugs R. D. 14 (2014) 283–290.

[157]  L.N. Boudoin, G.H. Lambeth, E.W. Llimatta, P.C. Hu, High content sodium ibuprofen granules, their preparation and their use in preparing non-effervescent solid dosage forms, 2012.

[158]  P. Gruber, M. Reher, Dosage form of sodium ibuprofen, 2003.

[159]  D. Hooper, F.C. Clarke, A modern approach to the Heckel equation: The effect of compaction pressure on the yield pressure of ibuprofen and its sodium salt, J. Nanomed. Nanotechnol. 7 (2016).

[160]  P.V. Marshall, P. York, J.Q. Maclaine, An investigation of the effect of the punch velocity on the compaction properties of ibuprofen, Powder Technol. 74 (1993) 171–177.

[161]  BTC Europe GmbH (Ed.), Sicherheitsdatenblatt Ibuprofen 50: ID Nr. 56929882/SDS_GEN_DE/DE, 2015.

[162]  BTC Europe GmbH (Ed.), Sicherheitsdatenblatt Ibuprofen Sodium Dihydrate: ID Nr. 51217385/SDS_GEN_DE/DE, 2015.

[163]  R.C. Rowe, P.J. Sheskey, M.E. Quinn (Eds.), Handbook of pharmaceutical excipients, 6th ed., The Pharmaceutical Press, London, 2010.

[164]  K.G. Pitt, J.M. Newton, P. Stanley, Tensile fracture of doubly-convex cylindrical discs under diametral loading, J. Mater. Sci. 23 (1988) 2723–2728.

[165]  H.-J. Butt, B. Cappella, M. Kappl, Force measurements with the atomic force

microscope: Technique, interpretation and applications, Surf. Sci. 59 (2005) 1–

152.

[166]  M. Kappl, H. Butt, The colloidal probe technique and its application to

adhesion force measurements, Part. Part. Syst. Charact. 19 (2002) 129–143.

[167]  T.H. Ibrahim, T.R. Burk, F.M. Etzler, R.D. Neuman, Direct adhesion

measurements of pharmaceutical particles to gelatin capsule surfaces, J. Adhes.

Sci. Technol. 14 (2000) 1225–1242.

[168]  J.L. Hutter, J. Bechhoefer, Calibration of atomic-force microscope tips, Rev.

Sci. Instrum. 64 (1993) 1868.

[169]  S. Jonat, S. Hasenzahl, A. Gray, P.C. Schmidt, Mechanism of glidants:

Investigation of the effect of different colloidal silicon dioxide types on powder

flow by atomic force and scanning electron microscopy, J. Pharm. Sci. 93 (2004)

2635–2644.

[170]  C. Al-Karawi, T. Kaiser, C.S. Leopold, A novel technique for the visualization

of tablet punch surfaces: Characterization of surface modification, wear and

sticking, Int. J. Pharm. (2017).

[171]  S. Lerdkanchanaporn, D. Dollimore, A thermal analysis study of ibuprofen, J.

Therm. Anal. 49 (1997) 879–886.

[172]  M. Cespi, G. Bonacucina, L. Casettari, S. Ronchi, G.F. Palmieri, Influence of

temperature on the compaction and strength of some pharmaceutical excipients.

// effect of temperature increase during the tableting of pharmaceutical materials,

Int. J. Pharm. 448 (2013) 320–326.

[173]  N. Pilpel, J.R. Britten, A.O. Onyekweli, S. Esezobo, Compression and tableting

of pharmaceutical powders at elevated temperatures, Int. J. Pharm. 70 (1991)

241–249.

[174]  W. Lowenthal, Disintegration of tablets, J. Pharm. Sci. 61 (1972) 1695–1711.

[175]  P.M. Desai, C.V. Liew, P.W.S. Heng, Review of disintegrants and the disintegration phenomena, J. Pharm. Sci. 105 (2016) 2545–2555.

[176]  A.C. Shah, A.R. Mlodozeniec, Mechanism of surface lubrication: Influence of duration of lubricant-excipient mixing on processing characteristics of powders properties of compressed tablets, J. Pharm. Sci. 66 (1977) 1377–1382.

[177]  Z.T. Chowhan, L.-H. Chi, Drug-excipient interactions resulting from powder mixing IV: Role of lubricants and their effect on in vitro dissolution, J. Pharm. Sci. 75 (1986) 542–545.

[178]  A.W. Hölzer, J. Sjögren, Evaluation of sodium stearyl fumarate as a tablet lubricant, Int. J. Pharm. 2 (1979) 145–153.

[179]  I. Saniocki, A. Sakmann, L. Claudia S., Evaluation of the suitability of various lubricants for direct compaction of sorbitol tablet formulations., J. Excip. Food Chem. 4 (2013) 169–182.

[180]  K.D. Rainsford, Ibuprofen: A critical bibliographic review, Taylor & Francis, London, Philadelphia, 1999.

[181]  K. Bobzin, E. Lugscheider, R. Nickel, P. Immich, (Cr1-x,Alx)N a review about a multi-purpose coating system, Materwiss. Werksttech. 37 (2006) 833–841.

[182]  D. Sixsmith, Punch tip geometry effects on powder compression, J. Pharm. Pharmacol. 32 (1980) 854–855.

[183]  D. Sixsmith, D. McCluskey, The effect of punch tip geometry on powder movement during the tableting process, J. Pharm. Pharmacol. 33 (1981) 79–81.

[184]  B. Eiliazadeh, K. Pitt, B. Briscoe, Effects of punch geometry on powder movement during pharmaceutical tabletting processes, Int. J. Solids Struct. 41 (2004) 5967–5977.

[185]  A. Djemai, I.C. Sinka, NMR imaging of density distributions in tablets, Int. J. Pharm. 319 (2006) 55–62.

[186]  T.G. Mathia, P. Pawlus, M. Wieczorowski, Recent trends in surface metrology, Wear 271 (2011) 494–508.

[187]  C. Sinka, Modelling Powder Compaction, KONA Powder Part. J. 25 (2007) 4–22.

[188]  S. Nakamura, N. Otsuka, Y. Yoshino, T. Sakamoto, H. Yuasa, Predicting the occurrence of sticking during tablet production by shear testing of a pharmaceutical powder, Chem. Pharm. Bull. 64 (2016) 512–516.

[189]  S.D. Bateman, The effect of speed of compression on the properties of compacts. Dissertation, Liverpool, 1988.

[190]  A.J. Romero, L. Savastano, C.T. Rhodes, Monitoring crystal modifications in systems containing ibuprofen, Int. J. Pharm. 99 (1993) 125–134.

[191]  R. Saleh, D. Parichkov, A. Kane, V. Sant, Preventing filming, sticking of cohesive compounds: Inline cooling to reduce temperatures at tablet compression offers relief from this sticky issue, Pharm. Manuf. (2014).

[192]  J.J. Wang, M.A. Guillot, S.D. Bateman, K.R. Morris, Modeling of adhesion in tablet compression- II. Compaction studies using a compaction simulator and an instrumented tablet press, J. Pharm. Sci. 93 (2004) 407–417.

[193]  V. Waknis, E. Chu, R. Schlam, A. Sidorenko, S. Badawy, S. Yin, A.S. Narang, Molecular basis of crystal morphology-dependent adhesion behavior of mefenamic acid during tableting, Pharm. Res. 31 (2014) 160–172.

[194]  X. He, P.J. Secreast, G.E. Amidon, Mechanistic study of the effect of roller compaction and lubricant on tablet mechanical strength, J. Pharm. Sci. 96 (2007) 1342–1355.

[195]  F. Freitag, P. Kleinebudde, How do roll compaction/dry granulation affect the tableting behaviour of inorganic materials?: Comparison of four magnesium carbonates, Eur. J. Pharm. Sci. 19 (2003) 281–289.

[196]  N.A. Armstrong, N.M.A.H. Abourida, L. Krijgsman, Multiple compression of powders in a tablet press, J. Pharm. Pharmacol. 34 (1982) 9–13.

[197]  M.R.A.K. Al-Aghbar, N.A. Armstrong, The repeated compression of powders, Eur. J. Pharm. Biopharm. 44 (1997) 283–288.

[198]  M.M. Rawas-Qalaji, F.E.R. Simons, K.J. Simons, Fast-disintegrating sublingual tablets: Effect of epinephrine load on tablet characteristics, AAPS PharmSciTech 7 (2006) E41.

[199]  K. Kachrimanis, I. Nikolakakis, S. Malamataris, Tensile strength and disintegration of tableted silicified microcrystalline cellulose: Influences of interparticle bonding, J. Pharm. Sci. 92 (2003) 1489–1501.

[200]  F. Bang, T. Cech, W. Schlindwein, Evaluating critical quality attributes of direct compressible ibuprofen in a QbD approach: 10th world meeting on pharmaceutics, biopharmaceutics and pharmaceutical technology, Glasgow, UK, 2016.

# Appendix

## A Hazardous materials

| Substance | Supplier | Danger symbol | Hazard statements | Precautionary statements |
|---|---|---|---|---|
| Acetonitrile | VWR, USA |  | H225, H302 + H312 + H332, H319 | P210, P240, P302 + P352, P305 + P351, P403 + P233 |
| Diiodomethane | Alfa Aesar, USA |  | H302 + H332, H315, H319, H335 | P261, P280, P305+P351+P338, P304 + P340, P405, P501 |
| Formamide | Alfa Aesar, USA |  | H360 | P201, P281, P202, P308 + P313, P405, P501 |
| Ibuprofen | BASF, Germany |  | H319, H302, H335 | P271, P280, P260, P270, P264, P312, P305 + P351 + P338, P304 + P340, P301+ P330, P337 + P311, P403 + P233, P405, P501 |

| Ibuprofen sodium dihydrate | BASF, Germany | ⚠ | H319, H302, H335 | P271, P280,P261, P273, P270, P264, P312, P305 + P351 + P338, P304 + P340, P330, P337 + P311, P403 + P233, P405, P501 |
|---|---|---|---|---|
| Methanol | VWR, USA | 🔥 ☠ ⚠ | H225, H301, H311, H331 H370 | P210, P233, P280 P302+P352, P304+P340, P308+P310, P403+P235 |
| Phosphoric acid 85 % | Carl Roth, Germany | ⚗ | H290, H314 | P280, P301 + P330 + P331, P303 + P361 + P353, P305 + P351 + P338, P310 |

## B  Curriculum vitae

The CV is not published for reasons of data protection.
.

## C Acknowledgments

This thesis was prepared at the University of Hamburg, in the Department of Chemistry in the division of Pharmaceutical Technology under supervision of Professor Dr. Claudia S. Leopold.

First of all, I would like to thank Prof. Dr. Leopold for entrusting me with this highly interesting research topic and for giving me the opportunity to be a member of her research group. I am especially grateful for her provided freedom in my research and her guidance.

My special thanks go to Prof. Dr. Micheal Steiger for evaluating of this thesis. Moreover, I thank Prof. Dr. Sebastian Wicha and Prof. Dr. Christian B. W. Stark for being members of the examination committee.

I also thank Dr. Albrecht Sakmann for his support in this work and mainly for his help with student's supervision as well as for enabling my attendance to every conference or training even during student's supervision. In addition, I would like to thank Petra Borbe and Kai Braunschweig for the experimental assistance, especially in conducting the HPLC analysis.

I am deeply grateful to Thomas Heinrich, Martin Schoeler, Janis Herrmann and Marten Klukkert from Fette Compacting for all the valuable discussions, for their assistance in the joint research projects and the provision of the tablet presses and the tablet tooling.

I am also thankful to Thorsten Cech and Florian Bang from BASF for the fruitful discussions, the provision of the ibuprofen used in this work and for their effort in the joint research projects.

Furthermore, I would like to thank my colleagues from the working group of pharmaceutical technology for the great working atmosphere and all memorable moments together. I would like to thank Alexander Kalies, Anna Novikova, Heike

**Declaration on oath (affirmation in lieu of oath) / Eidesstattliche Versicherung**

Hiermit versichere ich an Eides statt, die vorliegende Dissertation selbst verfasst und keine anderen als die angegebenen Hilfsmittel benutzt zu haben. Die eingereichte schriftliche Fassung entspricht der auf dem elektronischen Speichermedium. Ich versichere, dass diese Dissertation nicht in einem früheren Promotionsverfahren eingereicht wurde.

Datum, Unterschrift